UNIVERSITY OF SAO PAULO
Faculty of Pharmaceutical Sciences
Graduate Program in Drugs and Medicines
Pharmaceuticals Production and Control

Polymorph screening and solubility characterization of lercanidipine hydrochloride

Ilia Alekseevich Repin

A thesis submitted in fulfillment of the requirements
for the degree of Master of Science
Supervisor: Dr. Gabriel Lima Barros de Araujo

São Paulo
2019

UNIVERSITY OF SAO PAULO
Faculty of Pharmaceutical Sciences
Graduate Program in Drugs and Medicines
Pharmaceuticals Production and Control

Polymorph screening and solubility characterization of lercanidipine hydrochloride

Ilia Alekseevich Repin

Corrected version

A thesis submitted in fulfillment of the requirements
for the degree of Master of Science
Supervisor: Dr. Gabriel Lima Barros de Araujo

São Paulo
2019

Ficha Catalográfica elaborada eletronicamente pelo autor, utilizando o programa desenvolvido pela Seção Técnica de Informática do ICMC/USP e adaptado para a Divisão de Biblioteca e Documentação do Conjunto das Químicas da USP

Bibliotecária responsável pela orientação de catalogação da publicação:
Marlene Aparecida Vieira - CRB - 8/5562

R425p

Repin, Ilia Alekseevich
Polymorph screening and solubility characterization of lercanidipine hydrochloride / Ilia Alekseevich Repin. - São Paulo, 2019.
113 p.

Dissertação (mestrado) - Faculdade de Ciências Farmacêuticas da Universidade de São Paulo. Departamento de Farmácia.
Orientador: de Araujo, Gabriel Lima Barros

1. Tecnologia farmacêutica. 2. Polimorfismo. 3. Solubilidade. I. T. II. de Araujo, Gabriel Lima Barros , orientador.

Ilia Alekseevich Repin

Polymorph screening and solubility characterization of lercanidipine hydrochloride

Referee Commission of the thesis submitted in fulfillment of
the requirements for the degree of Master of Science

Dr. Gabriel Lima Barros de Araujo
Supervisor/Chairman

_____
1st Examiner

_____
2nd Examiner

_____
3rd Examiner

São Paulo, _____de _____de 2019.

ACKNOWLEDGMENT

First of all, I would like to thank Dr. Humberto Gomes Ferraz, who generously invited me to try my forces in the academic field and become part of his research group DEINFAR (Laboratório de Desenvolvimento e Inovação Farmacotécnica), for his guidance during my initial steps at the beginning of a master degree course.

Secondly, I would like to acknowledge my supervisor, Dr. Gabriel Lima Barros de Araujo, without his faith in me, his patient and dedicated accompaniment this work would not find its conclusion. I greatly thank Drs. Flávio Machado de Souza Carvalho and Selma Gutierrez Antonio for their contribution with X-ray powder diffraction analysis. The Raman spectroscopy part would not have been accomplished without the aid of Dr. Dalva Lucia Araujo de Faria. The crystallographic structure determination became possible only because of the participation of Dr. Alexandre Cuin and our colleagues from Portugal Drs M. Fátima M. Piedade and Carlos E.S. Bernardes, and Prof. Manuel E. Minas da Piedade. I also gratefully acknowledge Simulation Plus for providing the software license.

The research succeeds with the constant support of the DEINFAR group of researchers. I would like to thank each and all of them; I believe it was not easy for them to find a common tongue with a "wild Russian, almost Siberian boy" with deep communication problems in Portuguese. I want to thank Eremita Souza Santos for her motherlike care, sorry mom.

The group of amazing scientist which include: Dr. Michele Georges Issa cannot stay unnotable for sharing of experience in academic writing; Lucas, Rosemary, Franklin, Fabiana, Catharine whom contributed in parts of study related to thermal analysis, HPLC, intrinsic dissolution and physiologically based pharmacokinetic modeling studies. Edilson whom, I believe, became my friend and helped me a lot with his critical view, knowledge of ABNT norms, and long academic conversation.

This conquest would not occur without my patient and loving family and husband Luiz who supported me through this journey. My special thanks to CNPq and FipFarma, the scholarship provided by them allowed to maintain me in Brazil through this period and complete the work.

RESUMO

REPIN, I. A. **Triagem polimórfica e caracterização da solubilidade do cloridrato de lercanidipino.** 2019. 113p. Dissertação (Mestrado) – Faculdade de Ciências Farmacêuticas, Universidade de São Paulo, São Paulo, 2019.

A investigação do polimorfismo do cloridrato de lercanidipina (LRC) revelou um impacto significativo na solubilidade com forte dependência do tipo de tampão, pH e força iônica. Pela primeira vez, mudanças inesperadas na relação de solubilidade entre duas formas polimórficas de LRC (formas I e II), dependendo da composição do meio, foram identificadas e suas conseqüências potenciais para o desempenho farmacocinético foram avaliadas através de modelagem farmacocinética (PBPK) usando GastroPlus™; os resultados sugerem que, em casos de baixa acidez estomacal, a forma II é potencialmente menos biodisponível que a forma I. O tampão fosfato mostrou promover menor variação de solubilidade na faixa de concentração de 0.01-0.1 $mol \cdot L^{-1}$ e aumento de solubilidade favorecido para ambas as formas em pH 2-3,5 quando comparado com um tampão de ácido cítrico. A caracterização em estado sólido de ambos os polimorfos e experimentos politermais de solubilidade realizados em etanol e acetonitrila permitiram estabelecer a relação termodinâmica de estabilidade entre os dois polimorfos como monotrópica. Além disso, a degradação forçada foi aplicada para determinar as propriedades térmicas e fotoestáveis de cada forma, determinando a forma I como menos quimicamente estável. A determinação da estrutura cristalina da forma II de LRC foi realizada com base na obtenção de seu monocristal, enquanto os dados estruturais da forma I de LRC foram estimados aplicando uma abordagem de decomposição de valor único para suas varreduras de difração de raios X.

Keywords: Polymorphism; Lercanidipine Hydrochloride; Solid State Characterization; Thermodynamic Properties; Solubility.

ABSTRACT

REPIN, I. A. **Polymorph screening and solubility characterization of lercanidipine hydrochloride.** 2019. 113p. Thesis (MS) – Faculty of Pharmaceutical Sciences, University of Sao Paulo, Sao Paulo, 2019.

The study of the polymorphism of lercanidipine hydrochloride (LRC) has revealed a significative impact on solubility with a strong dependence on buffer type, pH, and ionic strength. For the first time, unexpected changes in the solubility ratio between two polymorphic forms of LRC (forms I and II) depending on the media composition were identified, and its potential consequences to the pharmacokinetic performance were evaluated through physiologically based pharmacokinetic (PBPK) modeling using GastroPlus™; the results suggest that in cases of low stomach acidity, form II is potentially less bioavailable than form I. Phosphate buffer showed to promote less solubility variation in the concentration range of 0.01–0.1 $mol \cdot L^{-1}$ and favored solubility increase for both forms in the 2–3.5 pH range when compared to a citric acid buffer.

Solid-state characterization of both polymorphs accompanied by polythermal solubility experiments carried out in ethanol and acetonitrile permitted to establish the thermodynamic relationship between the two polymorphs as monotropic. Furthermore, forced degradation was applied to determine thermal and photostability of each form, determining form I as the less chemically stable. Determination LRC form II crystalline structure was accomplished based on the successful obtainment of its single crystal, while structural data of LRC form I was estimated by applying single-value decomposition approach to its X-ray powder diffraction scans.

Keywords: Polymorphism; Lercanidipine Hydrochloride; Solid State Characterization; Thermodynamic Properties; Solubility.

LIST OF FIGURES

LIST OF TABLES

LIST OF SYMBOLS

A – the area of the measured curve in microcalorimetric studies, mV·s;

AUC_t – the area under the concentration-time curve from zero up to a definite time t, ng·h·mL^{-1};

C – the molar concentration, M or mol·mL^{-1};

$C_{constant}$ – the BET constant;

C_{max}– the maximum (or peak) serum concentration, ng·mL^{-1};

ΔC_p – the change of heat capacity, J·g^{-1}·K;

D – the diameter of the particles, m;

ε – the calibration constant in microcalorimetric studies, V·W^{-1};

F – the absolute bioavailability, %;

F_a – the fraction of the extravascularly administered dose to absorbed, %;

ΔG_d – the free Gibbs energy of dissolution kJ·mol^{-1};

ΔG_t – the free Gibbs energy of transition, J·g^{-1}·K;

ΔH_d – the enthalpy of dissolution, kJ·mol^{-1};

ΔH_f – the enthalpy of fusion, J·g^{-1};

i – the ionic strength, M or mol·mL^{-1};

I – the current, A;

k – the heat capacity correction constant, K^{-1};

m – the mass, g;

M – the molar mass g·mol^{-1};

ρ – the density, g·cm^{-3};

P – the pressure, bar;

Q – the heat, J;

R – the ideal gas constant equals 8.314 J·mol^{-1}·K;

$Span$ – the span factor of particle size distribution;

ΔS_d – the entropy of dissolution, J·mol^{-1}·K;

ΔS_t – the entropy of transition, J·g·K^{-1};

t – the time, s;

t_{max} – the time to reach C_{max}, h;

T_m – the temperature, K or (°C);

T_m – the peak melting temperature, K or (°C);

$T_{onset\ d}$ – the extrapolated onset-temperature of decomposition, K or (°C);

$T_{onset\ m}$ – the extrapolated onset-temperature of melting, K or (°C);

T_t – the temperature of transition, K or (°C);

V – the potential difference, V;

x – the mole fraction solubility;

Z – the ion charge.

LIST OF ABBREVIATIONS

API – active pharmaceutical ingredient;

BCS – Biopharmaceutics Classification System;

BET – Brunauer, Emmett, and Teller method;

DSC – differential scanning calorimetry;

FDA – Food and Drug Administration;

HPLC – high-performance liquid chromatography;

HPMC – hydroxypropyl methylcellulose;

HTE – high-throughput experimentation method;

IR – infrared spectroscopy;

LRC – lercanidipine hydrochloride;

MEK – methyl ethyl ketone;

Mid-IR – mid infrared spectroscopy;

Near-IR – near infrared spectroscopy;

PBPK – physiologically based pharmacokinetic;

SCXRD – X-ray single crystal diffraction;

SMT – solvent-mediated phase transition;

SSNMR – solid-state nuclear magnetic resonance;

TG – thermogravimetric analysis;

THF – tetrahydrofuran;

XRPD – X-ray powder diffraction.

SUMMARY

1 INTRODUCTION

Drug solubility is one of the most critical molecular physicochemical parameters to be considered in the development of tablet and capsules that affect gastrointestinal absorption and, consequently, bioavailability (SOUZA *et al*., 2019). The predominance of oral solid dosage forms among other routes of administration together with a continually increasing amount of challenging active pharmaceutical ingredient (API) belonging to Class II or IV (according to Biopharmaceutics Classification System, BCS) makes solubility enhancement one of the most common issues for the pharmaceutical industry (CENSI; DI MARTINO, 2015; THABET; KLINGMANN; BREITKREUTZ, 2018). For those poorly soluble drugs, regulatory agencies recommend special attention to structural modifications that could affect solubility, in particular, the presence of polymorphic forms (FOOD AND DRUG ADMINISTRATION, 2007; DOMINGOS *et al*., 2015).

Pudipeddi and Serajuddin (PUDIPEDDI; SERAJUDDIN, 2005) work based on the evaluation of enthalpy of fusion and melting temperature of the broad range polymorphs concludes that in the most of cases the impact of polymorphism results as the difference in the solubility in about two-fold. Nevertheless, despite being useful to postulate a general tendency, calculations should be accompanied by proper experimental confirmation. Among *in-vitro* measurement, the classical shake-flask method (FOOD AND DRUG ADMINISTRATION, 2015) remains the standard and the most commonly used one to determine equilibrium solubility even despite being a time-consuming task. Moreover, the number of experimental parameters may lead to variation in obtained results; the most important of them is the temperature, stirring rate and composition of buffer medium (BRITTAIN, 2014).

The primary purpose of usage of aqueous buffers is to maintain certain pH as the solubility of ionizable drugs is profoundly affected by the level of acidity or basicity, which should be selected according to pKa of the solute. However, solubility may also be affected by buffer capacity, ionic strength, and common ion effect, which may affect the solubility of a salt form of the API (MAUGER, 2017).

A brief review of solubility studies associated with polymorphism, summarized in **Table 1**, reveals that inappropriate comparisons between salt and free base forms or even solvate, hydrates and amorphous forms, may not permit to rate the impact of

polymorphism on solubility adequately. Moreover, some studies do not go beyond measurements accomplished in purified water, at only one pH medium or even organic solvent (BANNIGAN *et al*., 2016; GE; LI; CHENG, 2016). Finally, in the case of polymorphism, the importance of differences in obtained results as a function of experimental conditions remain almost untouched in related researches. Thus, from a wide variety of applied solubility evaluation methods together with its strong dependence on analytical parameters may emerge misleading conclusions.

Table 1 – Examples of the impact of experimental conditions on solubility studies on polymorphism

Drug	Methodology and observations	Year
Celecoxib	Dissolution measured by paddle method performed in 0.04 M tribasic sodium phosphate buffer with 1% sodium lauryl sulfate at 37 °C showed faster dissolution of form A with the total amount of dissolved API achieved by it 97.3% and 82.2% for form III (JIN; SOHN, 2018).	2018
Nateglinide	Solubility by shake-flask method and intrinsic dissolution rate were measured in pH 7.4 phosphate buffer at 37 °C showed higher solubility of Form MS and B with 89.7 $mg \cdot mL^{-1}$ (0.496 $mg \cdot cm^{-2} \cdot min^{-1}$)and 87.1 $mg \cdot mL^{-1}$ (0.479 $mg \cdot cm^{-2} \cdot min^{-1}$). Consequently, while less soluble forms achieved solubility 71.3 $mg \cdot mL^{-1}$ (0.263 $mg \cdot cm^{-2} \cdot min^{-1}$) for form S and 86.5 $mg \cdot 100\ mL^{-1}$ (0.317 $mg \cdot cm^{-2} \cdot min^{-1}$ for form H (GOYAL; RANI; CHADHA, 2017).	2017
Amlodipine Besylate	The basket dissolution test was performed in pH 1.2 buffer at 37 °C with capsules containing 4 obtained forms of amlodipine besylate revealed the following total amount of dissolved solute after 60 min of testing: form 1 89.3%, form 2 97.6%, form 3 91.7%, form 4 98.1% (SUBRAMANIAN *et al*., 2017).	2017
Bisoprolol fumarate	The solubility of bisoprolol fumarate form I, II and hydrate were determined by shake-flask method; obtained solubility showed insignificant divergence about 1% between three of them in 0.1 M HCl solution, pH 4.5 phosphate buffer and pH 6.8 phosphate buffer at 37 °C (DETRICH *et al*., 2019).	2019
Brexpiprazole and aripiprazole	Brexpiprazole and aripiprazole hydrated forms solubility were evaluated by the shake-flask method in the pH range from 2 to 8 at 37 °C. While brexpiprazole form I and dihydrate have not shown a significant difference in solubility in the pH range studied, aripiprazole form III and monohydrate presented a variation of about 20 $mg \cdot mL^{-1}$ for solubility at the interval 2-5 pH, what promotes solubility (ZEIDAN *et al*., 2018).	2018
Ambrisentan	Shake-flask equilibrium study performed in 0.1 M HCl (pH 1.2) at 37 °C appointed improvement of solubility by 1.5 for metastable form II of ambrisentan in comparison with the stable form I (HANEEF *et al*., 2018).	2018
Azithromycin	Dissolution measured by paddle method in distilled water at 37 °C revealed that both amorphous forms of azithromycin were able to achieve approximately 40% of total dissolution amount, while dihydrate resulted with 15% (NEGLUR *et al*., 2018).	2018

continue next page

continue

Drug	Methodology and observations	Year
Praziquantel	Novel praziquantel form B was compared with the form A by shake-flask and intrinsic dissolution in distilled water at 20 °C and 37 °C consequently. It has been found two times more soluble by both of them (140.3 and 281.3 $mg \cdot mL^{-1}$ by shake-flask and 31.2 and 62.2 by $mg \cdot cm^{-2} \cdot min^{-1}$ by IDR) (ZANOLLA *et al*., 2018).	2018
Daidzein	The paddle dissolution experiments were performed for daidzein form I, II and III in water, and pH 2.0 and 6.8 buffer medium at 37 °C. Form III was considered less soluble in all three mediums with 5% of the total dissolved amount; form II showed the highest solubility (75–80% dissolved) and form I was less soluble (38–60% dissolved) depending on the medium (JIA *et al*., 2017).	2017
Ciprofloxacin saccharinate	The intrinsic dissolution rate was compared between ciprofloxacin and ciprofloxacin saccharinate salt, which tend to be four times more soluble. The difference in solubility between form I of ciprofloxacin saccharinate and form III, however, turned up to be only 1.2 better (SINGH; CHADHA, 2017).	2017
Nifuroxazide	The new obtained forms II and III were found to be 1.4 and 1.2 times, respectively, more soluble than the stable form I in pure water 37 °C at the initial 10 min of the experiment. Due to recrystallization of form I, at the experimental conditions solubility measured after 24 hours showed the 1.2 increase for form II and 1.15 for form III. (COVACI *et al*., 2017).	2017
Amisulpride	Form II equilibrium solubility obtained by powder dissolution method in pure water and 25 °C turned up to be 1.3 times higher than one of form I (0.91 $mg \cdot mL^{-1}$ compared to 0.70 $mg \cdot mL^{-1}$ of form I) (ZHANG; CHEN, 2017).	2017
Rebamipide	Despite transition into a more stable form I both new rebamipide forms III and IV showed significant improvement in solubility, which depended on the composition of the medium. Form III turned out to be the most soluble form in pure water, with 1.4 fold improvement when compared to form I; form IV was the most soluble form in pH 6.8, is 1.7 times more soluble than form I (XIONG *et al*., 2017).	2017
Glibenclamide	Measured in pure water and pH 7.0 buffer are ordered in following sequence glibenclamide potassium form I > glibenclamide potassium form II > glibenclamide sodium form III > glibenclamide sodium form I > glibenclamide free acid form. However, comparing the polymorphic form of each salt between each other, the difference in solubility is insignificantly small (SURESH *et al*., 2017).	2017
Clevudine	Solubility data obtained after 72 h in pure water at 25 °C showed that clevudine form II is slightly 1.1 times higher soluble than form I, form III presented better improvement approximately 1.2; however, transition into form II and I was observed (NOONAN *et al*., 2016).	2016
Loratadine	Dissolution study performed at apparatus II in pure water at 37 °C showed slower and lower dissolution of form A with equilibrium concentration of 3.14 $\mu g \cdot mL^{-1}$, form B was capable achieve solubility of 5.01 $\mu g \cdot mL^{-1}$ (1.6 times improvement) (CHANG *et al*., 2016).	2016
Olopatadine hydrochloride	Solubility measured after 5 h stirring in pure water at 25 and 35 °C showed that form II is 1.5 and 1.4 times more soluble than form I, respectively (ŁASZCZ *et al*., 2016).	2016

continue next page

continue

Drug	Methodology and observations	Year
Glipizide	Glipizide form III showed significant improvement of solubility in both water and pH 6.8 at 25, and 37 °C in comparison with form I. Improvement made up 2–3 times depending on experimental conditions. The total amount of dissolved solute in dissolution studies showed a 30% improvement in pH 6.8 and 20% improvement in pure water (XU *et al*., 2016).	2016
Hydrochlorothiazide	Hydrochlorothiazide metastable form IA appeared to be 1.2 times more soluble than form I in pure water at 37 °C; however, the only stable form I was determined in residual excess of solid (SAINI *et al*., 2016).	2016
Metoprolol succinate	Metoprolol succinate metastable form II was demonstrated to have 1.1 times higher equilibrium solubility in water at ambient temperature than stable form I (ZHOU *et al*., 2017).	2017
Baicalein	Powder dissolution revealed that form γ of baicalein is approximately 2.5 times more soluble in pH 2.0 and 4.5 buffers containing 0.5% of Tween 80 at 37 ºC (ZHU; WANG; MEI, 2015).	2015
Nimodipine	Nimodipine polymorphic form I turned up to be 1.05–1.18 times more soluble than form II based on intrinsic dissolution studies performed in a water-ethanol mixture at 37 ºC depending on disk's rotation speed (RIEKES *et al*., 2014).	2014
Benznidazole	Benznidazole forms I, II and III showed almost similar solubility obtained by paddle dissolution method in pH 1.2 buffer at 37 ºC, which are equal 0.22 $mg \cdot mL^{-1}$, 0.24 $mg \cdot mL^{-1}$ and 0.25 $mg \cdot mL^{-1}$, respectively (HONORATO *et al*., 2014).	2014
Lornoxicam	Lornoxicam form II exhibited approximately three times higher solubility in pure water at 25 ºC than form I. Best paddle dissolution test results were obtained in pH 7.4 buffer at 37 ºC with 45% and 15% total amount of solute dissolved for form II and I, respectively (ZHANG *et al*., 2013).	2013
Flucloxacillin sodium	Flucloxacillin sodium form I is 3.5 more soluble in water at 20 °C in phosphate pH 6.8 than form II, however difference in solubility decrease with the increase of temperature and become insignificant at 38 °C (ZHOU *et al*., 2011).	2011
Indiplon	New form A of indiplon turned up to be approximately 1.1 times more soluble in the temperature range 27 to 67 °C in pure water (XU *et al*., 2012).	2012
Glimepiride	Tablets containing form II of glimepiride achieved 90% of dissolution by the paddle dissolution testing in pH 6.8 medium with 0.1% SDS at 37 °C, while form I approached only 50% (BONFILIO *et al*., 2012).	2012
Isoxyl	Form's II solubility of isoxyl achieved its maximum value at within 12 hours in pure water at 25 ºC and became 1.6 times higher than form I; however, after 12 hours, it starts to convert into form I and at 24 hours solubility became equal due to complete polymorphic transition (LI *et al*., 2011).	2011

conclusion

In this context, lercanidipine hydrochloride (LRC; **Figure 1**), a highly lipophilic BCS class II dihydropyridine calcium antagonist, has demonstrated the solubility ratio variation between polymorphs I and II according to changes in the pH range. In order to explore this peculiar behavior, the common ion effect hypothesis was taken to amplify the range of dissolution media and explore the interaction between LRC crystal forms and ion composition of the solutions.

Figure 1 – The structural formula of lercanidipine hydrochloride

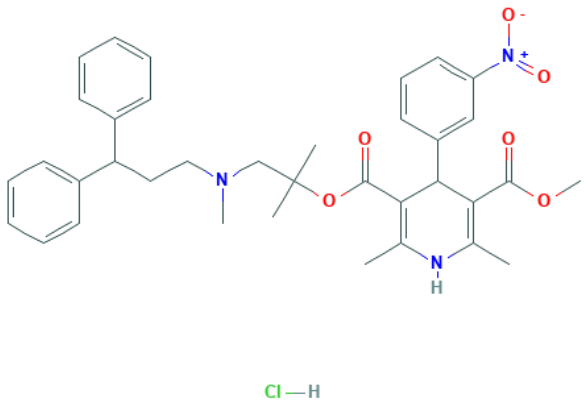

Source: Reproduced with permission from NATIONAL CENTER FOR BIOTECHNOLOGY INFORMATION, 2019

Further detailed crystallographic and thermodynamic characterization of polymorphs, their relation, and stability coupled with solvent-mediated phase transition (SMT) experiments were performed (BOBROVS; SETON; ACTIŅŠ, 2014) were addressed and investigated in this research work.

2 LITERATURE REVIEW

2.1 Phenomenon of polymorphism

Back in 1965, McCrone defined polymorphism by following quote “a solid crystalline phase of a given compound resulting from the possibility of at least two different arrangements of the molecules of that compound in the solid state” (MCCRONE, 1965). Modern definition accepted by Food and Drug Administration (FDA) describes it as the ability of a drug substance to exist as two or more crystalline phases that have a different arrangement and/or conformations of the molecules in the crystal lattice (FOOD AND DRUG ADMINISTRATION, 2007). Impact of the interest to the phenomenon of polymorphism in pharmacological compounds both in academic and industrial circles occurred at the end of the twentieth century due to the factors described below in the following section of the thesis.

Pharmaceutical solids can be divided into two classes, the first one is crystalline that have the regular repeating three-dimensional arrangement of species, which is known as the crystalline lattice, and the second one is amorphous that does not have the particular order in their structure. The amorphous form is the most soluble form and may be as well obtained during polymorph screening, but without specific techniques and addition of stabilizing polymers it has the lowest chemical and physical stability, tendency to crystallize that negates solubility advantages and makes this form challenging to be used desirable in the pharmaceutical industry (KAVANAGH *et al*., 2012; SUN *et al*., 2012).

According to crystal engineering, the difference in crystalline structure between polymorphs is caused by the complexity of inter and intramolecular interactions. Geometry of molecule, presence of both strong hydrogen bonds, such as O-H · · · O, N-H · · · O, or O-H· · ·N, and weak hydrogen bonds, for example, C-H · · · O, C-H · · · N, and N-H···π, as well as forming supramolecular synthons play crucial role in variety of crystalline forms (NANGIA, 2008; MUKHERJEE, 2015).

Based on these structural and geometric properties emerged two possible types of polymorphism: packing and conformational. The packing polymorphism occurs wherein rigid molecules form a crystalline lattice; in case of large and flexible molecules, the conformational type takes place (**Figure 2**). Most of the organic compounds exhibit both types of polymorphism, and this division may be considered speculative, but still frequently used to describe predominant factors of the phenomenon (YU; REUTZEL-EDENS; MITCHELL, 2000; RODRÍGUEZ-SPONG *et al*., 2004).

Figure 2 – Schematic representation of conformational and packing polymorphism

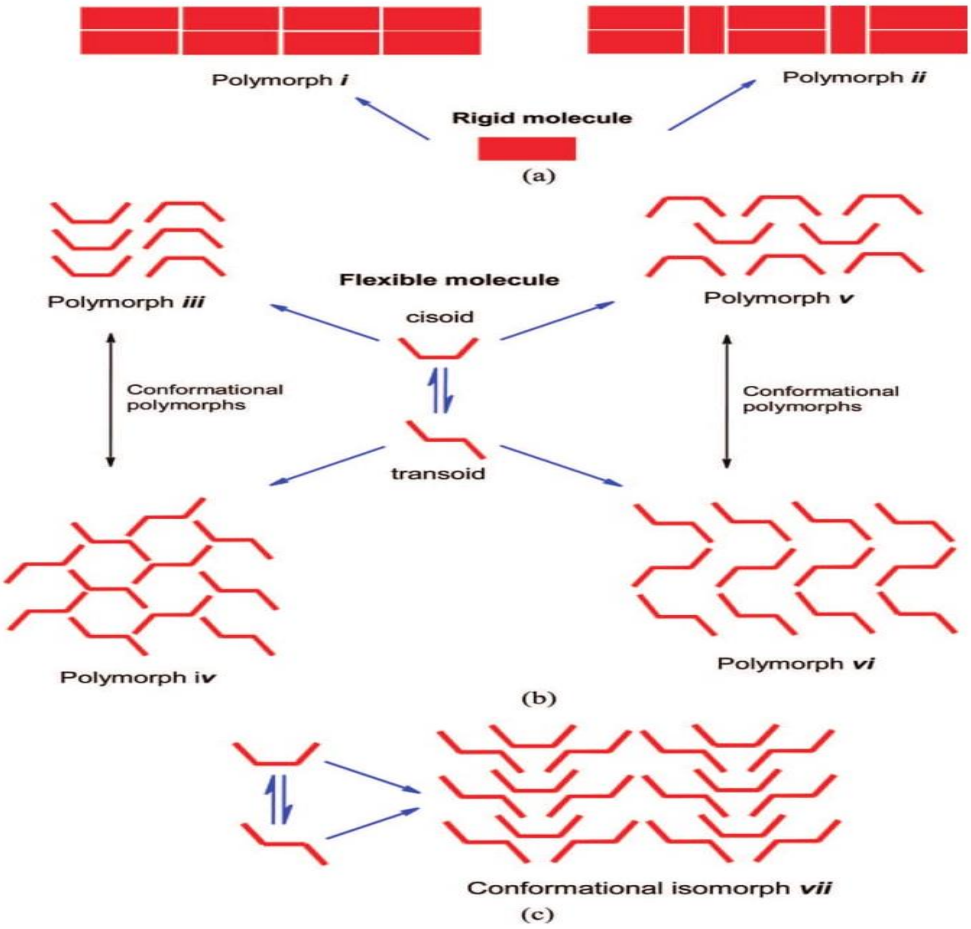

* (a) polymorphs i and ii for a rigid molecule, (b) a conformationally flexible molecule has a greater number of packing arrangements, iii-vi, and (c) two symmetry-independent molecules in conformational isomorph vii.

Source: Reproduced with permission from NANGIA, 2008.

The nomenclature of described solid forms of a substance is often confusing as it may of consists of both single and multicomponent systems, and besides it, each of these systems may exhibit polymorphism phenomenon. Multicomponent systems, in addition to API, contain inclusion of the other molecules or ions and classified by the type of “guest molecules”. The variety of possible forms is shown in **Figure 3**, components forming a crystal lattice can be presented by neutral (free forms, solvates/hydrates and co-crystals) or charged (salts, salts solvates and hydrates and salts of co-crystals) species. As salts by themselves can also form solvates or co-crystals the first desirable step of the solid form screening is the selection of exact salt or free form of the drug; this work was focused on lercanidipine hydrochloride salt as it is the commercially used one (HILFIKER; MARKUS, 2006; VISHWESHWAR *et al*., 2006).

Figure 3 – The variety of mono and multicomponent solid form systems

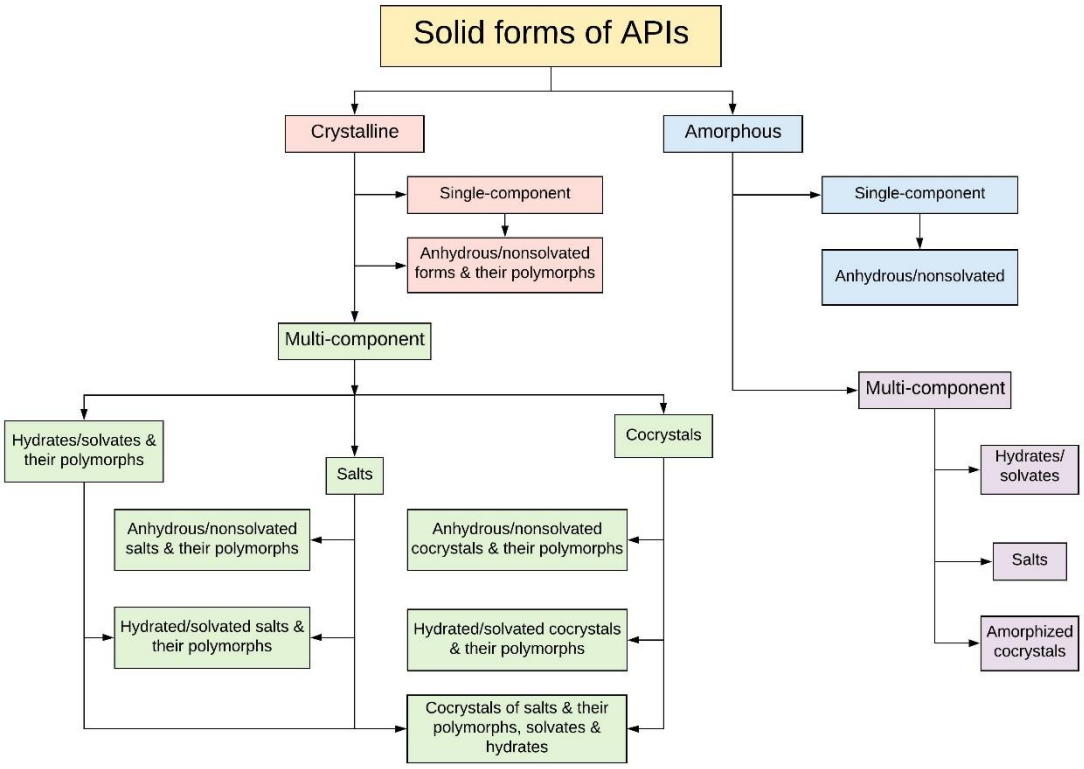

Source: Reproduced with permission from AITIPAMULA *et al*., 2012.

2.2 Impact of polymorphism on physicochemical properties

The difference in the crystal structure of polymorph may provide considerable variation in a wide range of physicochemical properties, which is shown in **Table 2**. For pharmaceutical industrial practice, the most significant of them are solubility, dissolution rate, physical and chemical stability, and hygroscopicity *(*AALTONEN *et al*., 2009; LEE, 2014).

Table 2 – The properties of solid form impactable by polymorphism

Physical/packing	**Thermodynamical**
Molar volume and density; refractive index; electrical and thermal conductivity; hygroscopicity; participle morphology; color.	Melting and sublimation point; vapor pressure; solubility; free energy and chemical potential; heat capacity; thermal stability, enthalpy, and entropy.
Kinetic	**Surface**
Rate dissolution; the rate of solid state reactions; physical (chemical) stability; the rate of crystal growth.	Surface free energy; crystal habit; surface area; particle size distribution; interfacial tensions.
Mechanical	**Spectroscopic**
Hardness; compression; powder flow; tableting and compatibility; tensile strength; cleavage; handing filtration flow and bending.	Electronic (UV-spectra); vibrational (IR and Raman spectra); rotational (far-IR and microwave spectra); nuclear spin transition (NMR spectra).

Source: Reproduced with permission and modification from Aaltonen *et al.*, 2009.

Nevertheless, the difference in solubility is not the only one interest of pharmacists; an example is the anticonvulsant carbamazepine. Despite the best dissolution profile shown by carbamazepine form III, the United States Pharmacopeia (USP) recommends using a form I, as form III is very hygroscopic and quickly transforms into dehydrated form with the worst solubility characteristics. Temperature control during manufacture of form I is crucial as the transition into form III may occur at higher temperatures (CHIENG; RADES; AALTONEN, 2011). However, recently, a generic carbamazepine form III tablet was approved by the FDA, taking into account strict control for the avoidance of water contact. Another example is sulfamerazine, its two discovered forms expose similar solubility and stability, but the form I has smaller

crystals and provide better compression and tableting (OMAR; MAKARY; WLODARSKI, 2015).

Chloramphenicol palmitate, with its three forms A, B, and C is a historical case of the difference between polymorphs that lead to insufficient pharmaceutical activity. Form A despite its stability have not found its use due to its almost complete pharmaceutical inactivity, from the other hand, form C is a highly unstable one, challenging to obtain and maintain. Only metastable form B with better in comparison with form A bioavailability should be employed in the drug formulation process (AGUIAR *et al*., 1967).

2.3 Screening Methods

The key to successful polymorph screening lies in the application of broad range crystallization methods. Diversity of them can be divided into two groups: solid-state such as cooling from the melt, sublimation or grinding, and solvent-based. From the variety of methods displayed in **Figure 4,** cooling crystallization, evaporation, and antisolvent addition were selected to be performed in this work.

Figure 4 – The variety of crystallization methods

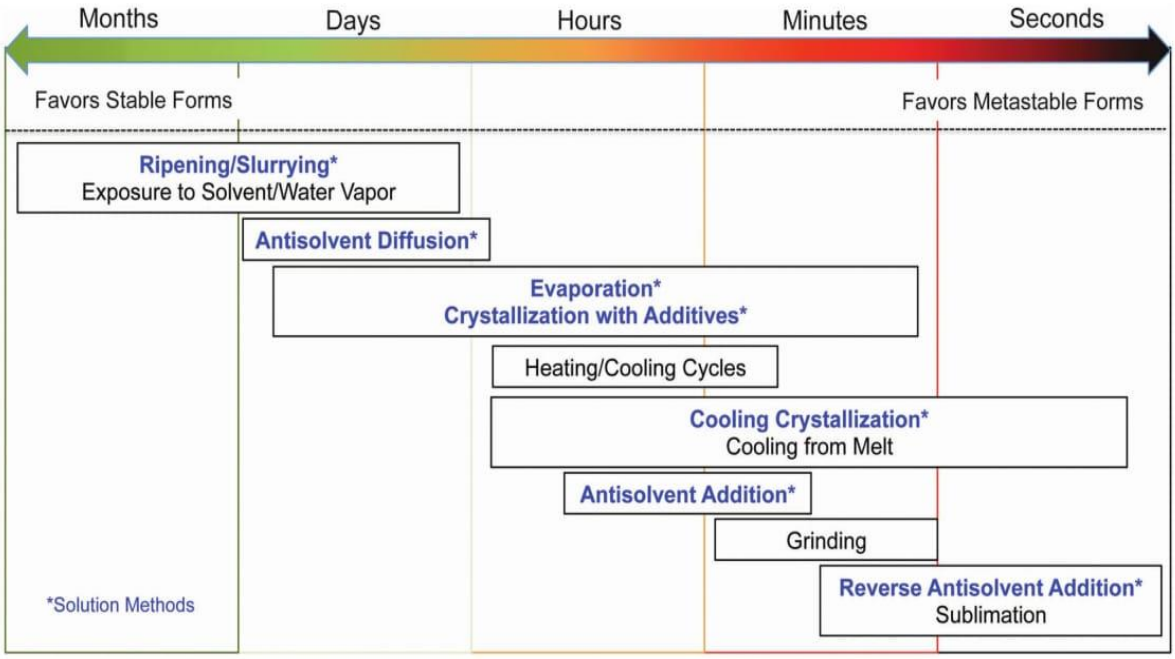

Source: Reproduced with permission from CRUZ-CABEZA; REUTZEL-EDENS; BERNSTEIN, 2015.

The methods of crystallization from solution were selected for this work as they make a standard part of the technological process and regularly used in the chemical and pharmaceutical industry and allow utilizing a variety of solvents and experimental conditions. The supersaturation is the fundamental driving force for these techniques of screening as it induces nucleation with following crystal growth occurs. It may be achieved by increasing of concentration of solute, which happens during evaporation process or due decreasing of solubility of solute by cooling or addition of antisolvent (ALVAREZ; SINGH; MYERSON, 2009; LEE; ERDEMIR; MYERSON, 2011).

Unfortunately, our understanding of the nucleation and crystal growth processes is not enough to predict the formation of the solid form, which leads to an enormous amount of carried out experiments required for the successful acquirement of polymorphic forms. Since crystal form achieved from solution depends from the domination of thermodynamic or kinetic factors by varying operational parameters described in **Table 3**, it may be possible to discover different polymorphs (GARDNER *et al*., 2004; AALTONEN *et al*., 2009).

Table 3 – Solvent-based crystallization methods

Method	**Variable parameters**
Cooling crystallization	Solvent/solvent mixture, cooling profile (rate), stirring, concentration.
Evaporation	Solvent/solvent mixture, initial concentration, evaporation rate, humidity.
Antisolvent crystallization	Solvent/solvent mixture, antisolvent, rate of antisolvent addition, stirring, temperature of addition (cooling profile).
SMT (slurry conversion)	Solvent/solvent mixture, incubation temperature and time, thermal cycling and gradient.

Source: Reproduced and compiled with permission from MORISSETTE *et al*., 2004; AALTONEN *et al*., 2009.

According to Ostwald's rule of stages in enantiotropic systems, metastable form occurs first, and then it transforms into the stable one, in case of monotropic relationship only stable form crystallizes from solution (**Figure 5**). Under the specific condition, polymorphic transformation can be ceased, and metastable form can be achieved from solution (ALLESØ *et al*., 2010; CHEN *et al*., 2011; LEE, 2014).

Figure 5 – The thermodynamic and kinetic control of crystallization processes

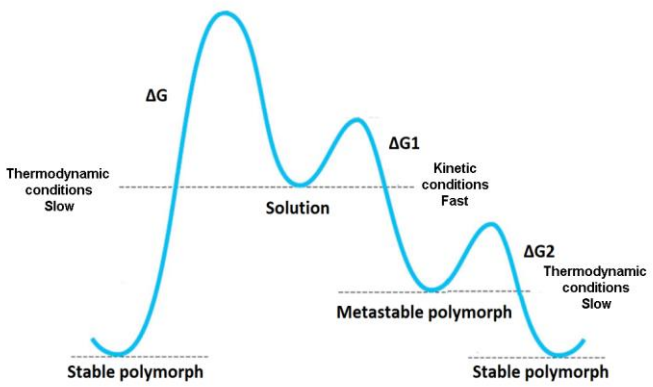

Source: Reproduced with permission and modification from CHEN *et al*., 2011.

Cooling crystallization is based on the phenomenon of the high dependence of solubility from the temperature of a solvent-solute system; first heating step allows us to obtain a high concentration of solute, which is insoluble at ambient temperature, by following cooling we reduce solubility and our system enter the metastable zone. Crash cooling with high cooling rates tends to provide a crystallization of metastable or even amorphous form. Cooling crystallization is widely used in manufacturing practice, as it is easy to establish initial conditions and control process by maintaining determining cooling rate. Crystallized solid should be separated from the solution as soon as it is possible to ensure that polymorphic transition from one form to another is excluded. Recent examples of screening performed by cooling include the study of metformin hydrochloride and isonicotinamide (STOREY, 2011).

The antisolvent method rests on the addition to the prepared solution a second solvent, which called antisolvent in this case, as the solubility of solute is immensely low in it, solvent/antisolvent miscibility should be verified as well. The solubility of the

API in the mixed solvent system is lower in comparison to it in the initial solution, and in this way, a driving force for crystallization or supersaturation can be created. Antisolvent crystallization is especially useful for crystallization of heat-sensitive compounds when initial heating is undesirable; however, control of polymorph formation is more complicated in comparison with the cooling method. This method can be combined with cooling; in order to do so, antisolvent should be added into the initially heated solution, followed by cooling (RENUKA *et al*., 2016).

Evaporation method relies on gradually raising the concentration of API in the sample to achieve supersaturation and to increase its degree in order to induce crystallization. Unfortunately, in evaporative methods, differential rates of solvent loss from mixtures result in the unknown composition of the crystallization medium at the time of crystallization. Besides, the degree of supersaturation changes throughout the experiment often results in the appearance of multiple crystal forms. Fast evaporation induced by vacuum may lead to obtaining the kinetic forms that crystallize first and do not get an opportunity to transform to the more stable thermodynamic polymorphs as the solvent is removed very fast (BAG; REDDY, 2012).

2.4 Classical approach and high-throughput experimentation

Classical manual approach of solid form screening does not require high-tech equipped laboratory and allow executing several types of sequential experiments with the same sample. Solvent and solid-based screening can be carried out. Manually, it is possible to perform the broadest range of experimental methods with the widest variety of work parameters. As a disadvantage of the classical procedure, high demand of time required for a decent amount of experiments and significant consumption of investigated compound as well as solvents should be mentioned. The typical amount of API requisite for this type of studies lay in the range 20 to 100 and even more milligrams (NEWMAN, 2012).

High-throughput experimentation method (HTE) enables to design, execute, analyze, and interpret from hundreds to thousands of individual experiments at the same time. This method found various application in drug discovery and development; it is relevant to the fields of chemistry and biology. In case of solid form screening initially it was applied in the field of biocrystallization for the obtaining of protein crystals, but it was spread to the area of small molecules. The method should be designed to

perform a large number of experiments by a single workflow. Additionally, for the high cost of required equipment and high-specialized personnel to operate another one disadvantage of this method is its limitedness by solvent-based crystallizations (VARIANKAVAL *et al*., 2014).

Generally, the HTE approach does not put purpose in the high rate of positive outcomes as well as little attention is paid to figure out what exactly causes of the positive or negative result. The classical solid screening, on the contrary, should be designed to achieve, as crystallization to occur, as well as each crystallization result, have to be carefully analyzed (GARDNER *et al*., 2004).

Crystal16 (Avantum/Technobis, The Netherlands), which was utilized in this study, is considered as a medium-throughput screening system since it contains only 16 wells to carry out experiments. Ideally, crystallization occurs during cooling ramp and leads to obtaining different polymorphic forms, provide us information about metastable zone width and induction time in less successful experiments solubility curve still can be determined (BIRCH *et al*., 2005).

2.5 Single crystal growth

Growing a single crystal suitable for X-Ray crystallography is far more challenging in comparison with a multicrystal crystallization. Same methods as in common solid form screening can be applied to obtain single crystal, but specific conditions should be used. The tendency to crystallize as mono or multi-crystalline structure depend on experimental conditions. Single crystals tend to grow when rates of supersaturation are not high, so diluted solutions with a concentration of solute about several mg in mL are recommended to use. The prolonged way of carrying out of experiments is considered better, as rapid processes lead to crystal growth at multiple points (HULLIGER, 1994; SPINGLER *et al*., 2012).

Vapor diffusion method is carried out by dissolving a small amount of the sample in a tiny vial, then placing this inner vial inside a larger vessel that contains a second solvent (antisolvent) in which the API is insoluble. The outer vessel is then sealed. In order to perform experiment solvent in the inner vial should be less volatile than the second one and miscible with it. This technique allows working with a tiny amount of compound but is limited by effective solvent/antisolvent combinations (JONES, 1981; BOYLE *et al*., 2007).

Slow evaporation allows the material to crystallize out as the solvent evaporates this method is good then a relatively large amount of substance is available and can be performed with solutions obtained after solubility tests. To decrease evaporation rate the limited open area or cooling the solution generally used less volatile solvents preferable in this case. It is necessary to protect the system from the dust during the whole process (VAN DER SLUIS; HEZEMANS; KROON, 1989; TATUM, 2012).

Layer diffusion method is performed by putting concentrated sample of compound to the bottom of a container, with following addition of antisolvent down the side of the container such that the two solvents for distinct layers and do not mix, prepared system should be sealed and left for several days to allow occurrence of slow mixing of solvents. Solvents must be miscible and better results achieved in case of least dense antisolvent, for its layering is recommended to utilize a syringe and needle to add the solvent down the side of the container. Slow cooling crystallization should be executed with a cooling rate among 0.1 ºC per minute to avoid multiple spontaneous growths, selection of the solvent or solvent mixture is essential as well (JIANG; KLOC, 2013).

Same crystallization methods as mentioned above apply to gel media instead of solution can provide better results as gel structure allows to obtain larger crystals as it reduces convection in the growth medium, prevent sedimentation, suppress foreign nucleation, and reduce twinning, that imitates under microgravity conditions experiments (CHOQUESILLO-LAZARTE; GARCÍA-RUIZ, 2011; MORENO; MENDOZA, 2015).

2.6 Solid state characterization techniques

Wide variety of methods can be applied to analyze and characterize solid state properties of the polymorphs, among them are: mid-infrared (Mid-IR), Raman, and near-infrared (Near-IR) spectroscopies and solid-state nuclear magnetic resonance (SSNMR) on the molecular level; X-Ray powder and single crystal diffraction (XRPD and SCXRD), differential scanning calorimetry and thermogravimetric analysis (DSC and TGA), and microscopy on the participle level. Generally, at least two or even more techniques are used to characterize the polymorphs. In **Table 4** below the short review of each method of analysis is represented (CHIENG; RADES; AALTONEN, 2011; NEWMAN; BYRN, 2003).

Table 4 – The analytical techniques applied for solid state characterization

Analytical technique	**Advantages and disadvantages**
XRPD	Gives “fingerprint” diffraction peaks for each polymorph; for amorphous form halo, instead peaks are represented. Sensitive in a long-range order. Nondestructive. Difficult to differentiate the mixtures. Describes crystallographic properties.
SCXRD	Provides the same information as PXRD. It is challenging to prepare a single crystal, which is required to perform the technique. Nondestructive.
DSC	Provides information about thermal events such as transition, fusion, and crystallization. Easy to detect the drug/drug and drug/recipient mixtures; Does not provide information about the nature of the events. Destructive.
TGA	Quantitative information about the change of mass applicable for solvates/hydrates study. Destructive.
Raman	Provides information about chemical structure based on unique vibrational spectra fingerprint. Sensitive in short-range order. Nondestructive, preparation of the sample is not required. Local heating of sample and photodegradation may occur.
Polarized microscopy	Information on crystal morphology and size, qualitative information on crystallinity. Quantitative information not available, interference from excipient occurs.
Mid-IR	Provides information about chemical structure and H-bonding based on unique vibrational spectra fingerprint. Sensitive in short-range order. Interference from moisture and excipient occurs; the difference between polymorphs may be minimal. Phase transformation may occur during sample preparation.
Near-IR	Provides information about chemical structure based on unique overtones and combinations of IR vibrations spectra fingerprint. Sensitive in short-range order. Very low sensitivity and selectivity. Nondestructive.
SSNMR	Provides information about nuclei and chemical environment within a molecule, molecular dynamics and drug/drug and drug/recipient interactions. Relatively expensive and long data acquisition time. Requires excellent understanding of underlying physics to avoid incorrect interpretation.

Source: Compiled with permission NEWMAN; BYRN, 2003; CHIENG; RADES; AALTONEN, 2011.

3 OBJECTIVE

3.1 General objectives

The main objectives were to investigate the polymorphism of the lercanidipine hydrochloride by solvent-based crystallization methods, to characterize through solid state analytical techniques, and to evaluate its impact on the solubility.

3.2 Specific objectives

- Obtaining of the single crystal with the further determination of crystalline structure;
- Determination of the thermodynamic relationship between obtained polymorphic forms;
- Estimation of the transition temperature, enthalpy, entropy and free Gibbs energy of transition;
- Perform complementary studies to investigate the impact of polymorphism on surface area and particle size distribution;
- Investigate photo and isothermal stability of obtained forms;
- Evaluate the influence of ionic strength of buffer media and its composition on the solubility of both forms;
- Execute comparative intrinsic dissolution rate studies;
- Carry out physiologically based pharmacokinetic (PBPK) modeling and simulation to evaluate bioequivalence between polymorphs.

4 MATERIALS AND METHODS

4.1 Materials

Lercanidipine HCl raw material was generously provided by Medley Pharmaceuticals Ltd. HPMC K15M was supplied by Colorcon, Inc. High purity crystallization solvents were obtained from Labsynth Produtos para laboratorios Ltda, Lichrosolv and Sigma-Aldrich Merck KGaA. Citric acid, hydrochloric acid, sodium dihydrogen phosphate, and sodium hydroxide were purchased from Labsynth produtos; trisodium citrate was obtained from Casa Americana. All reagents were used without further purification.

4.2 Methods

4.2.1 Polymorph screening

4.2.1.1 Apparatus Crystal16

Crystal16 (Avantum/Technobis, The Netherlands) consists of 16 wells that can carry standard HPLC vials as mini-reactors for crystallization, each with its turbidity sensor using light transmission, which allows performing experiments within volume range from 0.5 to 1.5 mL. The wells are divided into four groups; each group can be heated and cooled separately by utilizing a combined Peltier heating and water bath cooling system accompanied by magnetic stirring.

4.2.1.2 Solvent selection and preparation of solutions

Performing successful polymorphism screening requires the usage of a broad range of the solvents, which should be selected from the several groups or clusters with different properties such as polarity, dipole moment, dielectric constant, hydrogen-bond acceptor/donor, etc (GU *et al*., 2004; XU; REDMAN-FUREY, 2007; ALLESØ *et al*., 2008).

An initial step of every crystallization technique was the preparation of a highly saturated solution. Firstly, slurries were prepared by weighing into a 1mL HPLC amber

glass vial the precise amount of LRC in HPLC vials with the following addition of solvent. The weighing was carried out with an analytical balance Marte AUW220D (Santa Rita, Brazil).

Secondly, prepared slurries were placed into Crystal16 to follow temperature program: holding at 25 °C for 5 min, heating ramp to 55, 60, 65, 75, 80 or 100 °C, that depends on the boiling point of utilized solvent, with heating rate 1 °C·min^{-1}, holding for 20 min at peak temperature. Holding step is necessary to ensure the absence of undissolved LRC crystals. Stirring was kept at a constant rate of 700 rpm for every cycle and sample.

The list of solvents consists of methanol, toluene, ethyl acetate, acetone, THF, 2-propanol, ethanol, benzyl alcohol, isobutanol, diethyl ether, 1,4-dioxane, MEK, chloroform, dichloromethane, 1,2-dichloroethane, hexane, dimethylformamide, dimethylsulfoxide, acetonitrile, anisole, pyridine, n-butyl acetate.

4.2.1.3 Cooling crystallization

Crystallization experiments from a heated highly saturated solution of LRC were performed by following the cooling ramp to 20 °C with cooling rate 1 or 5 °C·min^{-1}, holding at 20 °C for 20 min. Samples that showed no evidence of crystal growth were placed into a freezer –18 ºC afterward.

4.2.1.4 Slow evaporation crystallization

A part of the heated saturated solutions of LRC after cooling to 20 °C with described above program was selected to perform evaporation. To perform slow evaporation closed cap of HPLC vials were changed to septum with a tiny aperture and were placed into fume hood and left there at room heat to perform slow evaporation of the solvents until dry.

4.2.1.5 Antisolvent crystallization

Initially, LRC form II was obtained based on solvent systems extracted from the US patent 0192323 A1 (BONIFACIO *et al*., 2005); three methods described in the patent were modified by scaling down and performed on Crystal16 medium-throughput

system; additional solvent/antisolvent pairs (not reported in LRC patents) were used to expand the reported methodologies. Briefly, 100 µL saturated solutions of each solvent were pipetted to new 1mL vessels. Afterward, 1 mL of antisolvent was gradually added with a 100 µL step and constantly stirring as to obtain 1:10 (v/v) ratio of solvent/antisolvent.

4.2.2 Single crystal growth

4.2.2.1 Vapor diffusion method

To perform vapor diffusion crystallization, 1 mL a prepared solution of LRC (concentration of solute was 100 $mg \cdot mL^{-1}$ in isobutanol and acetonitrile, 200 $mg \cdot mL^{-1}$ in 1,2-dichloroethane and methanol) was added into a test-tube and placed inside a larger vessel filled with the excess of antisolvent. Subsequently, the vessel was sealed and left at room temperature in a fume hood.

4.2.2.2 Gel-based crystallization

A diluted solution of 10 mg LRC was prepared in 1 mL solvent mixtures of water and organic solvent of choice in volume ratio 1:1. The HPMC K15M powder in an amount of 10 mg was added as a gelling agent. Consequently, solutions LRC with added HPMC were placed backward into Crystal16 for further gel preparation. These mixtures were heated and held up to 55 °C under stirring at 700 rpm during 2 hours to ensure homogeneity in gel formation. Cooled to the room temperature gels were placed into fume hood with a tiny aperture in the septum of HPLC vial as to perform slow evaporation of an organic part of the solvent mixture and precipitate crystals in a water-based gel.

4.2.2.3 Crystallization from acetone/water system

Single crystal of LRC was obtained by dissolving 300 mg of LRC in a 1 mL mixture of acetone-ultra purified water (80:20). The solution was heated up to 50 ºC with a heating rate of 0.5 $°C \cdot min^{-1}$ and held for 30 min, followed by cooling to room

temperature at 1 °C·min^{-1} using a Crystal16. The sample was stored in a refrigerator at 1-5 °C. The formation of single crystals was observed after 4 weeks of storage.

4.2.3 Structure determination

4.2.3.1 X-ray powder diffraction

XRPD measurements were performed using a Rigaku RINT2000 X-ray diffractometer (Tokyo, Japan) at an accelerating voltage of 40 kV and tube current of 50 mA, copper radiation by position sensitive detector D/teX Ultra in wavelengths Ka_1=1.55056 Å and Ka_2=1.5444 Å and Ia_2/Ia_1 at 0.5. The measurements were carried out at room temperature in continuous mode over the angular range of 4° = 2Theta = 40° with a step size of 0.02° approximately, by using the following optical slit system: divergence slit set at 1/6°; with 5 mm horizontal opening of the divergence slit; soller 2.5° and receiving slit at 0.3 mm.

4.2.3.2 Crystal structure determination

The crystal structure of LRC (form II) at 296 ± 2 K, was solved from the results of single crystal X-ray diffraction analysis. The experiments were carried out on a Bruker D8 QUEST area detector diffractometer, equipped with a diffracted beam a graphite monochromator. The crystals were coated with Paratone-N oil and mounted on a Kaptan loop. All data was collected with Mo Kα radiation (λ = 0.71073 Å) and generator operating settings at 50 kV and 30 mA. The temperature scale of the apparatus had been previously calibrated against a standard platinum resistance thermometer placed at the same position as the crystal (JOSEPH *et al*., 2019). Empirical absorption correction was applied by using Bruker SADABS (BRUKER, 2004), and the data reduction was performed with the Bruker SAINT program (SAINT, 2004). The structure was solved by direct methods with Bruker SHELXTL (SHELDRICK, 2008), and refined by full-matrix least-squares on F^2 using SHELXLv.2017 (SHELDRICK, 2015), included in WINGX version 1.80.05 (FARRUGIA, 1999).

Non-hydrogen atoms were refined with anisotropic thermal parameters, and the hydrogen atoms were introduced in calculated positions riding in the parent carbon,

except those attached to the nitrogen and chlorine atoms, which were found in the density map and refined freely. Structural representations were prepared with Mercury 3.1.1 (MACRAE *et al*., 2008) PLATON (SPEK, 2009) was used for the hydrogen bond interactions.

4.2.3.3 X-ray powder diffraction and indexation data of form I.

Since no suitable single crystal of form I was obtained, an attempt to solve the structure by powder diffraction was carried out. The diffraction data for LRC form I was collected by overnight scans in the 2θ range of 5-105° with step of 0.02° using a *Bruker AXS D8 Da Vinci* diffractometer, equipped with Ni-filtered CuKα radiation (λ=1.5418 Å), a Lynxeye linear position-sensitive detector was used and the following optics were set up: primary beam Soller slits (2.94°), fixed divergence slit (0.3°) and receiving slit 9.30mm. The generator was set up at 40 kV and 40 mA. The analysis was performed in the Laboratório de Difratometria de Raios X do NAP-Geoanalítica USP.

Approximate unit cell parameters were determined using about 21 low-angle peaks, followed by indexing through the single-value decomposition approach (COELHO, 2003) implemented in TOPAS (BRUKER, 2000). The space group suggested by TOPAS was P-1, and cell parameters and intensity or each reflection were eventually refined using diffraction data up to 55° (2θ) range by the Pawley method (PAWLEY, 1981). Since LCR has a high number of variables – 18 torsion angles associated with trivial variables as rotation, translation, background, and so on, the determination of its crystal structure took days of calculations. Even taking into account the single crystal model of LCR form II and hundred thousand trials on structure solution process, performed by the simulated annealing technique (COELHO, 2000).

4.2.3.4 Raman

Raman spectroscopic analyses of samples were carried out on a Bruker RFS100/S FT-Raman spectrometer was also used; such an instrument is fitted with liquid nitrogen cooled Ge detector and with a Nd^{3+}/YAG laser (1064 nm). Laser power

at the sample was 65 mW with 0.2 mm as the estimated laser footprint; the spectra ranged from 100 to 3500 cm^{-1} with 4 cm^{-1} spectral resolution.

4.2.4 Physicochemical characterization

4.2.4.1 Differential scanning calorimetry

DSC was performed with a DSC7020 system (SII NanoTechnology Inc., Japan) in a temperature range of 25 to 350 °C, at a heating rate of 10 °C·min^{-1} under a nitrogen gas flow of 50 mL·min^{-1}. Powders (~2 mg) were weighed into an aluminum pan, crimped, and placed in the thermal analysis chamber.

4.2.4.2 Thermogravimetric analysis

TGA was performed using a TG/DTA7200 system (SII NanoTechnology Inc., Japan). Samples we weighted (~10 mg) in an open aluminum pan and analyzed under the following conditions: temperature range of 25 to 600 °C, the heating rate of 10 °C·min^{-1} under a nitrogen gas flow of 100 mL·min^{-1}.

4.2.4.3 Pycnometric density

Pycnometric density measurements of LRC form I and II were performed using a helium-pycnometer Quantachrome Ultrapycnometer 1000 (Odelzhausen, Germany) at 25 °C. Samples were weighed with an analytical balance Marte AUW220D (Santa Rita, Brazil), transferred into an of a 20 cm^3 sample chamber and flushed with helium.

4.2.4.4 Particle size distribution

Measurement of particles size of LRC form I and II was carried out on a Cilas 1090 particle-size analyzer (Orleans, France) equipped with a 5 mW He/Ne (635 nm) laser beam. Analyses were carried out using aqueous dispersions of samples; in order to induce the formation of suspension 2 drops of diluted detergent solutions were added. Following experimental parameters were used: Franhoufer operational principle, stirring at the sample tank was set at 320 rpm before during and after each measurement circulation in sampling line were equal 120 rpm for 20 sec., ultrasound

was activated before each measurement to ensure the absence of agglomerated particles obscuration was in a range of 10-20 %. The measurements were repeated five times for each of the forms.

4.2.4.5 Surface area

Nitrogen sorption studies were performed at liquid nitrogen temperature (77 K) using Quantachrome Nova 2200e and contained 20 adsorption and 19 desorption points. Before the adsorption experiments, the samples of LRC form I and II were outgassed under the nitrogen atmosphere at 423 K during 20 min. All calculations were performed using the NovaWin Version 11.03 the surface area analyzer own software.

4.2.5 Solubility by temperature variation (polythermal) method

LRC solubility in ethanol and acetonitrile were obtained using Crystal16 (Avantum/Technobis, The Netherlands). A certain amount (in range 20 to 70 mg in ethanol and 15 to 40 mg in case of acetonitrile) of LRC was placed in a standard HPLC vial and weighed with an analytical balance Marte AUW220D (Santa Rita, Brazil). The solvent of choice was then added (1 mL), and the flask was weighted. Solubility was measured by the last crystal disappearance method, which is considered as one of the synthetic methods of measurement. (KRIVANKOVA; MARCISINOVA; SOHNEL, 1992) The samples proceeded through following experimental program: initial cooling down to 10 °C and holding during 5 min without agitation followed by heating up to 78 °C with heating rate 0.3 $°C \cdot min^{-1}$ with 700 rpm stirring and final shock cooling to 15 °C, slow heating rate was chosen to maximize the precision of obtained data. Similar solubility studies are generally performed in the large scale of operational volume (50–100 mL), while Crystal16 operational volume is limited by 1 mL, leading to a higher impact of mass measurement error; however, the obtained data can be used for the qualitative compilation of dissolution thermodynamic properties (SUN *et al*., 2014; ZHANG *et al*., 2018a).

The experimental molar concentration of LRC was calculated by the following **Equation (1)**:

$$x = \frac{m_1/M_1}{m_1/M_1 + m_2/M_2} \quad (1)$$

, where m_1 and m_2 represent the masses of LRC and solvent, respectively; M_1 and M_2 are the molar masses of LRC and solvent, respectively.

4.2.6 Isothermal Solution Microcalorimetry

Enthalpy of solution measurements were carried out at 298.15 K on a LKB 2277 Thermal Activity Monitor (TAM). An in-house designed stainless-steel dissolution cell was used. It consisted of a 23 cm^3 cylindrical vessel closed by a lid that supported the stirring, electrical calibration, and sample drop systems. The whole apparatus was inside an air-conditioned room whose temperature was regulated to 295 ± 1 K. Instrument control and data acquisition were performed with the CBCAL 3.0 program (BERNARDES, 2016).

In a typical experiment, a stainless-steel crucible (diameter = 6.5 mm; height 2 mm) was weighed with a precision of ± 0.1 µg on a Mettler XP2U ultra-micro balance. It was then charged with ~ 9 mg of LRC (forms I or II) and weighed again to obtain the mass of the sample. The crucible+sample ensemble was transferred to the drop chamber in the cell lid. The lid was adjusted to the cell body, which contained ~ 12 g of methanol, previously weighted to ± 10 µg in a Mettler XS 205 balance. The assembled cell was inserted in the measurement well of the calorimeter unit and left to equilibrate. After recording an appropriate baseline, the crucible was dropped into methanol by opening the trapdoor at the bottom of the drop chamber. This started the sample dissolution as reflected by a shift of the calorimetric signal from the baseline. The end of the dissolution process was marked by the return of the signal to the baseline.

4.2.7 Solvent-mediated phase transition

The SMT not only determines the most stable phase but also can serve as evaluating criteria, which provide the information about how long does it take for such transformation to occur (VEGA *et al*., 2016). Its dependence from specific solute-solvent interaction was reported (BOBROVS; SETON; ACTIŅŠ, 2014; BOBROVS; SETON; DEMPSTER, 2015) and to ensure broad coverage of solvent properties water, toluene, ethanol, and hexane were selected as work solvents. As the crystal surface of one form may induce transition and even determine the occurrence of the transition to another one (MUNROE *et al*., 2014), it was considered appropriate instead of pure metastable form I to perform slurring experiments containing a physical mixture in proportion by mass 1:1 of both forms. The physical mixture in amount 500 mg was placed in 4 mL amber glass vial with the further addition of 4 mL of toluene and water, due to the higher solubility of LRC in ethanol amount of solvent was decreased to 1 mL to evade complete dissolution of the polymorphic mixture.

The transition was explored at ambient temperature and at 50 °C maintained by putting vials in a water bath and accompanied by stirring with a magnetic bar with 700 rpm. Samples were taken by single-channel 100 µL pipette BRAND® in the amount of 200 µL for toluene, water, hexane and 100 µL in case of ethanol after 1, 2, 3, 6, 7 days from the beginning of the study. Collected samples were placed on clock glasses, which were placed into the fume hood to evaporate the solvent from slurries.

4.2.8 High-performance liquid chromatography

The HPLC analyses related to the determination of solubility by the shake-flask method and degradation studies were carried out on a Shimadzu Prominence (Shimadzu, Japan). It consists of LC 20AT pumps (for organic and aqueous part of a mobile phase) accompanied with DGU-20A5 degasser; absorbance was measured by SPD-M20A diode array detector, connection with the laptop was provided by CBM-20A communication bus module. Experimental data were acquired and processed by LabSolutions v 5.81 software as the chromatographic column was used Shim-pack GVP-ODS C18 (250 × 4.6 mm I.D., Shimadzu, Japan) with an addition pre-column GVP-ODS 10L × 4.6. Manual injections were performed by syringe in volume 20 µL with acetonitrile-water-triethylamine 55:44.8:0.2 (v/v/v) adjusted with o-phosphoric acid

to pH 3.0 as mobile phase. The flow rate of mobile phase was 1 mL·min^{-1}; detector wavelength was set at 240 nm. Experiment time was set to 15 min with an observed retention time of LRC of about 7 min (MIHALJICA; RADULOVIĆ; TRBOJEVIĆ, 2005).

The mobile phase was prepared by adding 2 mL of triethylamine in 448 mL of ultra-purified water (Milli-Q), and pH was adjusted to 3.0 with o-phosphoric acid. This solution was then mixed with 550 mL of acetonitrile in order to obtain acetonitrile-water-trimethylamine 55:44.8:0.2 (v/v/v) ratio. A stock drug solution (1 mg·mL^{-1}) was prepared with the mobile phase and diluted to construct the calibration curve using concentrations of 4 µg·mL^{-1}, 10 µg·mL^{-1}, 30 µg·mL^{-1}, 50 µg·mL^{-1}, 100 µg·mL^{-1}, 100 µg·mL^{-1}, 150 µg·mL^{-1}, 200 µg·mL^{-1} for curve corresponding to the lower limit of concentration. The Dilutions of more concentrated stock drug solution (2 mg·mL^{-1}) were used to form calibration curve with following concentrations 200 µg·mL^{-1}, 450 µg·mL^{-1}, 700 µg·mL^{-1}, 900 µg·mL^{-1}, 1100 µg·mL^{-1}, 1300 µg·mL^{-1} for upper concentration limit. All solutions were prepared using amber glass volumetric flasks and protected from light.

Due to the higher amount of samples related to IDR studies, assays were conducted on a LaChrom Elite ® (Hitachi, Tokyo, Japan). It consisting of L-2130 pump, L-2130 automatic sampler. Experimental data were acquired, and processed EZChrome Elite V. 3.3.2 SP software as the chromatographic column was used Shim-pack GVP-ODS C18 (250 × 4.6 mm I.D., Shimadzu, Japan) maintained at 25 °C. The mobile phase consisted of acetonitrile-water-triethylamine 55:44.8:0.2 (v/v/v) adjusted with o-phosphoric acid to pH 3.0 as the mobile phase. The injection volume was 60 µL; the flow rate of the mobile phase was 1 mL·min^{-1}; analyzed wavelength was set at 240 nm.

4.2.8.1 Photostability

Photostability in the solid-state of both polymorphs was performed on photostability chamber 424-CF (Nova Ética, Brazil) by exposure of samples to artificial white, visible and ultraviolet fluorescent light (Phillips Master TLS HE 14W/840 lamps and Philips Actinic BL 15W) with power 1800 W and controlled temperature 25 °C for 72 hours. Sample powders were spread on glass plates in order to increase of exposed area to the light and reduce layer thickness. Photo exposed powders were dissolved

in the mobile phase at a concentration of 500 μg·mL^{-1} and analyzed by Shimadzu Prominence HPLC system.

4.2.8.2 Isothermal stability

Stability of LRC form I and II under isothermal conditions was carried out in environmental chamber 420/CLD 300 (Nova Ética, Brazil). LRC polymorphs were exposed to 40 °C at 75% RH for one month. Further samples were dissolved in the mobile phase at a concentration of 500 μg·mL^{-1} and processed on Shimadzu Prominence HPLC system.

4.2.9 Solubility studies

4.2.9.1 Kinetic solubility determination

The 400 Series CCD array UV/vis spectrophotometer (S.I. Photonics, Inc., USA) permits to obtain real-time solubility data. Solubility for both polymorphs was determined at pH 1.2 in simulated gastric fluid without enzymes (BOU-CHACRA *et al*., 2017) at 37 ± 2 °C accompanied by stirring with a magnetic bar at 100 rpm. To perform the experiment, an amber glass flask containing 10 mL of media submerged in a water bath and equilibrated. Afterward, approximately 2 mg was added into the medium; this amount of solid sample guaranty the necessary saturation at these experimental conditions. Absorbance was measured in the wavelengths ranging from 200 to 900 nm every 5 min, during 24 hours.

4.2.9.2 Solubility by shake-flask

Equilibrium solubility of lercanidipine was determined by the shake-flask method (BOX *et al*., 2006) at isothermal conditions on shaker TE-420 (Technal, Piracicaba, Brazil) with experiment time 24 h, at 37 ± 1 °C, and under stirring (100 rpm). Solubility studies of LRC form I and II were expanded into a pH physiological range and were performed in triplicate with following buffers: pH 1.2 and 2.0 (chloride), pH 2.0, 2.5 and 3.0 (phosphate), pH 3.0, 3.5 and 4.0 (citrate) and pH 4.5 (acetate) (**Attachment A**). Additionally, to investigate the influence of the buffer ionic strength, data with 0.01 M

pH 3.0 citric and phosphate buffer were obtained. The ionic strength of the buffer medium was evaluated by the following **Equation (2)** (ELLIS; MORRISON, 1982):

$$i = \frac{1}{2}\sum_{i=1}^{n} C_i * Z_i^2 \qquad (2)$$

, where i is ionic strength, C_i is the molar concentration and Z_i charge of each type of ions in solution.

At the end of incubation, samples were collected and filtered through 0.45 µm nylon syringe filter into HPLC amber flasks. The concentration of LRC in filtered samples was measured by an HPLC Shimadzu Prominence system (Shimadzu, Japan); the method described in “High-performance liquid chromatography (HPLC)” section.

4.2.9.3 Intrinsic dissolution rate

Intrinsic dissolution measurements were carried out on a VK 7010 dissolution apparatus (Varian Inc., Palo Alto, CA, USA) equipped with rotating discs containing about 100 mg LRC form I and II compressed with 1000 and 2000 psi by a hydraulic press (American Lab, Charqueada, SP, Brazil). Due to the small solubility of LRC volume of the medium was established as 500 mL, each experiment was performed in triplicate. Samples were collected at 5, 30, 60, 90, 120, 150, 180, 210, and 240 min accompanied by HPLC on a LaChrom Elite (Hitachi, Tokyo, Japan).

4.2.9.4 Physiologically based pharmacokinetic modeling and simulation

GastroPlus™ 9.6 (Simulation Plus, Inc.) was used to simulate and predict the effect of both polymorphs and their solubility differences in the pharmacokinetic profile of LRC. The software was loaded with experimental solubility data, and clinical pharmacokinetic data obtained by Barchielli *et al*. (BARCHIELLI *et al*., 1997).

The values of permeability, particle size, renal clearance, the volume of distribution, and the physiology model were optimized to fit the curve plasma concentration x time to the one in the literature. The modeling was conducted by fitting clinical pharmacokinetic data and considering experimental solubility data of form II since this form is used in the commercial product; the simulation parameters are summarized in **Table 5**.

Table 5 – The PBPK input simulation parameters

Parameter	Value
Molecular weight, $g \cdot mol^{-1}$	611.74
Reference logP at neutral pH	7.23
pKa	9.36
Dosage form	IR: Tablet
Dose volume, mL	250
Mean precipitation time, sec	900
Particle size, µm	6.24
Effective permeability, $cm \cdot s^{-1} \cdot 10^{-4}$	6.84
ASF model	Opt logD Model SA/V 6.1
PK model	Compartmental
Volume of distribution	2.91
Clearance, $L \cdot h^{-1}$	31
Renal clearance, $L \cdot h^{-1}$	4

Source: Adopted and modified with data elaborated by the author from Barchielli *et al.*, 1997.

4.2.10 Thermodynamic calculation

4.2.10.1 Estimation of temperature of transition

Based on experimental data obtained from in this work, the temperature of transition was calculated by solubility extrapolation method and melting data method.

a) Melting data method. The Transition temperature can be calculated from the melting enthalpy and temperature obtained by DSC studies of the polymorphic pair (QI *et al.*, 2015). The change of heat capacity (ΔC_p) between the stable melt and highest melting point can be calculated based on the melting enthalpy (ΔH_{fII}) of the highest melting form using **Equation (3)**:

$$\Delta C_p = k \times \Delta H_{fII} \quad (3)$$

, where k is the heat capacity correction constant, which vary above 0.001–0.007 (K^{-1}) depending on the investigated compound; however, Yu (1995) in his work

suggested using $k = 0.003$ (K^{-1}) in general case (YU, 1995). Thus the transition enthalpy ΔH_t, the transition entropy ΔS_t and the transition Gibbs energy ΔG_t can be obtained from the following **Equations (4, 5, 6)**, considering that in case of LRC form II is highest and form I the lowest melting:

$$\Delta H_t = \Delta H_{fI} - \Delta H_{fII} + \Delta C_p \times (T_{mII} - T_{mI}) \tag{4}$$

$$\Delta St = \left(\frac{\Delta_{HfI}}{T_{mI}} - \frac{\Delta H_{fII}}{T_{mII}}\right) + \Delta C_p \times \ln\left(\frac{T_{mII}}{T_{mI}}\right) \tag{5}$$

$$\Delta G_t = \Delta H_t - T\Delta S_t = \Delta H_{fI}\left(\frac{T_{mI}}{T_{mII}} - 1\right) \tag{6}$$

, where ΔH_{fI} and ΔH_{fII} are the enthalpies of fusion of form I and II, T_{mI} and T_{mII} are their melting temperatures, consequently. As an equilibrium state is reached between polymorph pair ΔG_t is considered equal to zero, and the estimated transition temperature Tt can be calculated from **Equation (9)** by modifying the **Equation (7)** with **Equation (3-5)**:

$$T_t = \frac{\Delta H_t}{\Delta S_t} \tag{7}$$

$$T_t = \frac{\Delta H_{fI} - \Delta H_{fII} + \Delta C_p \times (T_{mII} - T_{mI})}{\left(\frac{\Delta H_{fI}}{T_{mI}} - \frac{\Delta H_{fII}}{T_{mII}}\right) + \Delta C_p \times \ln(\frac{T_{mII}}{T_{mI}})} \tag{8}$$

$$T_t = \frac{\Delta H_{fI} - \Delta H_{fII} + k \times \Delta H_{fII} \times (T_{mII} - T_{mI})}{\left(\frac{\Delta H_{fI}}{T_{mI}} - \frac{\Delta H_{fII}}{T_{mII}}\right) + k \times \Delta H_{fII} \times \ln(\frac{T_{mII}}{T_{mI}})} \tag{9}$$

b) Solubility extrapolation method. To fit experimental solubility data, several thermodynamic models can be applied; modified ideal solubility model can be expressed through thermodynamic parameters with further simplification to the equation of linear regression, **Equation (11)** and utilized to estimate transition temperature T_t (BENNEMA *et al.*, 2008; ZHANG *et al.*, 2018b):

$$Lnx = \frac{\Delta H_f}{R} \times \left(\frac{1}{T_m} + \frac{1}{T}\right) \tag{10}$$

$$Lnx = \frac{a}{T} + b \quad (11)$$

, where x is the ideal molar solubility, R is the ideal gas constant, ΔH_f is the heat of fusion, T_m is the onset melting temperature, and T is any temperature. Considering that ΔH_f is independent of T in a narrow temperature range the Lnx is linearly dependent from $1/T$. Thus, the transition temperature can be obtained as the extrapolation of solubility curves up to their intersection point, as their free Gibbs energies and solubility should be equal at this point.

4.2.10.2 Estimation of dissolution enthalpy, entropy, and the molar Gibbs free energy

Solubility data expressed by standard van't Hoff equation that represents the same linear regression as in case of modified ideal solubility model (WANG *et al*., 2015) and can be written as **Equations (12, 13)**:

$$Lnx = -\frac{\Delta H_d}{RT} + \frac{\Delta S_d}{R} \quad (12)$$

$$Lnx = \frac{a}{T} + b \quad (13)$$

, where ΔH_d is the enthalpy of dissolution, ΔS_d is the entropy of dissolution, R is the ideal gas constant equals 8.314 J·mol^{-1}·K, and T is the experimental temperature in K.

The enthalpy and entropy of dissolution can be calculated by using slope a and intercept b of linear regression from the curve fitting equation:

$$\Delta H_d = -R \times a \quad (14)$$

$$\Delta S_d = R \times b \quad (15)$$

Furthermore, the Gibbs energy of dissolution ΔGd at each experimental temperature can be calculated from the following **Equation (16)** (TAO *et al*., 2013):

$$\Delta G_d = \Delta H_d - \Delta S_d \times T \quad (16)$$

5 RESULTS AND DISCUSSION

5.1 Polymorph screening results

5.1.1 Solvent selection and preparation of solutions

This stage allowed us to establish methanol, acetone, THF, 2-propanol, ethanol, benzyl alcohol, isobutanol, MEK, chloroform, dichloromethane, 1,2-dichloroethane, dimethylformamide, dimethylsulfoxide, acetonitrile, pyridine as suitable solvents for further recrystallization experiments; work concentrations of LRC in each of them were also determined.

The following solvents were selected as antisolvents due to the very limited solubility of LRC in them: ethyl acetate, 1,4-dioxane, hexane, anisole, n-butyl acetate.

5.1.4 Cooling crystallization

Each of established as suitable for crystallization solvent was tested in the cooling crystallization method as it is considered the most used classical methods for inducing crystal growth. Nor the experimental conditions tested by Crystal16 neither the prolonged storage in the freezer did not promote crystal growth. However, the negative result permit to avoid usage of this technique in further researches involved crystallization of LRC.

5.1.3 Evaporation crystallization

Volatile solvents were selected for this method among them are methanol, acetone, ethanol, isobutanol, 1,2-dichloroethane, dichloromethane, acetonitrile. Successful crystallization occurred only in 1,2-dichloroethane, dichloromethane obtained crystals were further characterized as LRC form I. Other experiments led to the formation of highly viscous amorphous mass instead of an expected crystalline solid.

Studies of crystallization from undercooled melt and spray drying technique were widely used to classify drugs according to the glass formation tendency (BAIRD; VAN EERDENBRUGH; TAYLOR, 2010; MAHLIN; BERGSTRÖM, 2013). The high

viscosity of the melt may constrain diffusion of molecules together to form nuclei as well as the complexity of molecule can complicate occupation of specific orientation constrained by the lattice structure, which is required to crystal formation. Based on that information and extrapolating the concept to the observations in this study, it is possible to infer that lercanidipine belongs to the class of substances with high glass-forming ability and stability due to its high molecular weight and molecular complexity.

5.1.4 Antisolvent crystallization

Lercanidipine form II was successfully obtained by reproducing methods described in the US patent 0192323 A1 (BONIFACIO *et al*., 2005). Additionally, form II was also obtained from the following solvent/antisolvent mixtures: methanol/ethyl acetate, methanol/water, methanol/n-butyl acetate, dimethylacetamide/1,4-dioxane, dimethylacetamide/n-butyl acetate. The form II crystals obtained from methanol/water recrystallization experiment was selected to perform this study. The raw material was characterized as form I and used for characterization without further purification. This polymorph was also possible to be obtained from a wide range solvent/antisolvent combinations, among them: 1,2-dichloroethane/toluene, methanol/anisole, chloroform/anisole, chloroform/1,4-dioxane, chloroform/ethyl acetate, methanol/1,4-dioxane, benzyl alcohol/ diethyl ether, benzyl alcohol/1,4-dioxane, benzyl alcohol/ n-butyl acetate, dimethylformamide/1,4-dioxane, dimethylformamide/n-butyl acetate, pyridine/dioxane, dimethylacetamide/diethyl ether.

5.1.2 Single crystal growth results

The solvent/antisolvent pairs selected for vapor diffusion technique included isobutanol/hexane, 1,2-dichloroethane/hexane, acetonitrile/diethyl ether, methanol/diethyl ether. The systems mentioned above were able to promote crystallization, still instead of the expected growth of single crystals was observed formation of multi-crystalline solid. The obtained crystals were characterized as form I.

Similarly, despite the expectation obtaining single crystals of LRC in gels, multi-crystallization of small crystals were observed in the gel volume. Due to unsatisfying results and difficulties of gel retrieval from HPLC vials, the obtained samples were left without further characterization.

The successful obtainment of LRC single crystals occurred in acetone/water solvent mixture; the crystals collected were suitable for crystal structure determination of LRC form II.

5.2 Structure determination results

5.2.1 The XRPD results

The XRPD data of form I and II obtained in this work is concordant with the reported data from the patent US 0192323 A1 (BONIFACIO *et al*., 2005). The XRPD studies showed an evident difference between LRC form I and II shown in **Figure 6**.

Figure 6 – The X-ray powder diffractograms of lercanidipine hydrochloride form I and II

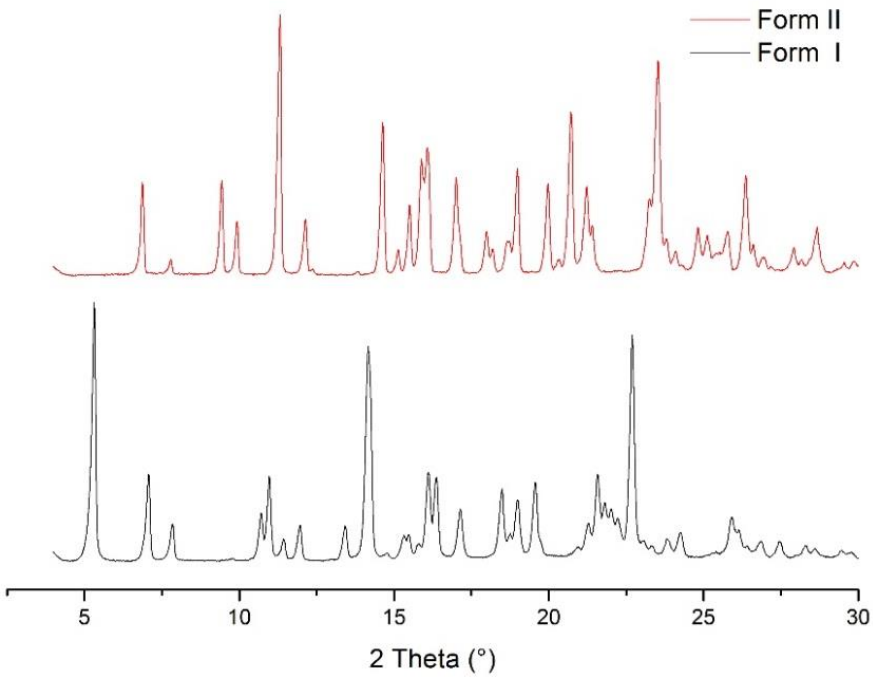

Source: Own authorship.

Form I exhibits the most characteristic peaks at 5.40°, 14.33°, 22.79° (2Theta). The peak at 5.40° (2Theta) is most intense of all, and it was used as a marker in solvent-mediated transition studies; form II presents characteristic peaks at 11.27°, 14.68°, 20.78° and 23.58° (2Theta). Experimental characteristic peaks are used to confirm successful two polymorphs with different arrangement and/or conformation in the crystal lattice.

5.2.2 Crystal structure determination

The molecular structure of lercanidipine hydrochloride (form II) and the corresponding atom-labeling scheme are shown in **Figure 7**.

Figure 7 – Molecular structure of lercanidipine hydrochloride with the atom-labeling scheme obtained by Mercury 3.1.1, ellipsoids are set at 50% probability

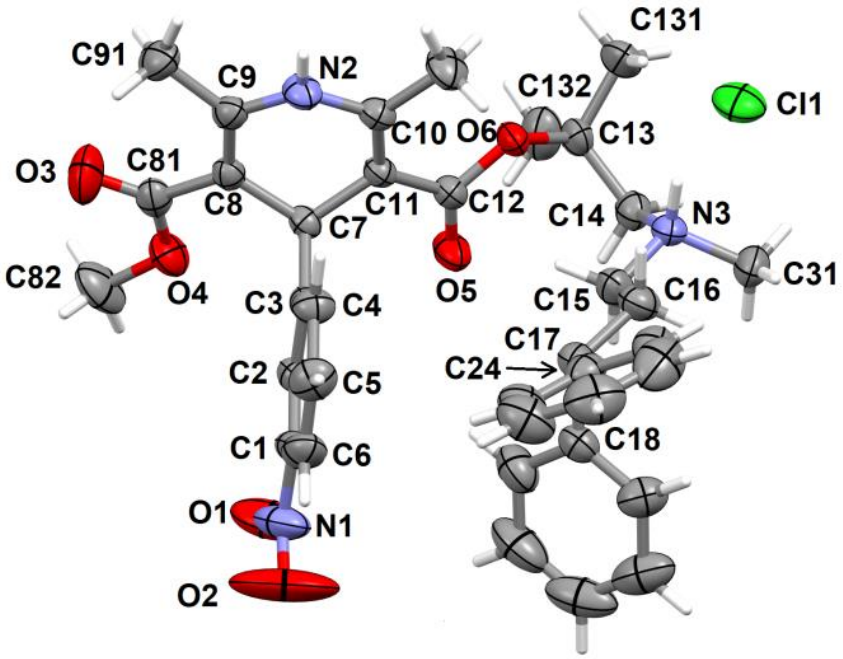

Source: Own authorship

Also, the summary of the crystal data, structure solution, and refinement parameters are given in **Table 6**. The data corresponding to LRC form I is not complete as it was obtained based on indexation of XRPD results.

Table 6 – Crystal data and structure refinement parameters for lercanidipine hydrochloride form I and II

Parameters	LRC·form I	LRC·form II
CCDC number	*n/a*[*]	1909799
T, K	296 ± 2 K	
Empirical formula	$C_{36}H_{42}ClN_3O_6$	
Formula weight	648.17	
Wavelength, Å	0.71073	
Crystal system	Triclinic	
Space group	$P\bar{1}$	
a, Å	8.4876	11.5769(4)
b, Å	13.0917	11.6650(4)
c, Å	17.15933	13.0629(5)
α, °	99.488	98.204(2)
β, °	101.5072	98.819(2)
γ, °	104.2242	99.087(2)
V, Å^3	1764.4(2)	1695.97(11)
Z, Z'	4/1[**]	4/1
ρ_{calcd}, g·cm^{-3}	*n/a*	1.269
μ, mm^{-1}	*n/a*	0.162
F(000)	*n/a*	688
θ limits, °	*n/a*	2.870 to 26.475
Limiting índices	*n/a*	$-9 \leq h \leq 14$
	n/a	$-14 \leq k \leq 13$
	n/a	$-16 \leq l \leq 16$
Reflections collected, unique	*n/a*	24904 / 6935 [R(int) = 0.0408]]
Completeness to θ, %	*n/a*	99.5 %
Data / restraints / parameters	*n/a*	6935 / 1 / 431
GOF on F^2	*n/a*	1.139
Final R indices [I>2σ(I)]	*n/a*	R_1 = 0.0518, wR_2 = 0.1512
R indices (all data)	*n/a*	R_1= 0.0737, wR_2 = 0.1612
Largest diff. peak and hole, e·Å^{-3}	*n/a*	0.620 and −0.338

* *n/a - not applicable (structure of LRC I was not determinated)*

** *- estimated based on value of measured density of LRC form I*

The dihydropyridine ring has a boat conformation and contains two carboxylate substituents. One of them, C(12)O(5)O(6), is in a *syn*-periplanar orientation relative to the ring, as indicated by the almost planar [C10-C11-C12-O6] torsion angle of −9.9(3)º; the other is also almost planar relative to the ring, with torsion angles [C9-C8-C81-O4] and [C9-C8-C81-O3] of 174.49(16) and −8.2(3)º, respectively. Some analogous compounds shown in **Figure 8**, such as felodipine (**1**) (SUROV *et al*., 2012), nifedipine (**2**) (GUNN *et al*., 2012) and efonidipine hydrochloride ethanolate (**3**) (OTSUKA *et al*., 2015), display slightly more coplanar dihydropyridine-carboxylate systems, namely 179.47–172.58º for [C10-C11-C12-O6] and, in the case of [C9-C8-C81-O4], 176.86º (felodipine, **1**) and 175.57º (nifedipine, **2**). Not unexpectedly, in efonidipine

hydrochloride ethanolate (**3**), the latter dihedral exhibits a considerable departure from planarity, –80.72º, due to the replacement of a carboxylate by a phosphate group.

Figure 8 – The structural formulas of lercanidipine hydrochloride analogous compounds: felodipine, nifedipine, and efonidipine hydrochloride ethanolate obtained by MarvinSketch 15.9.7.0

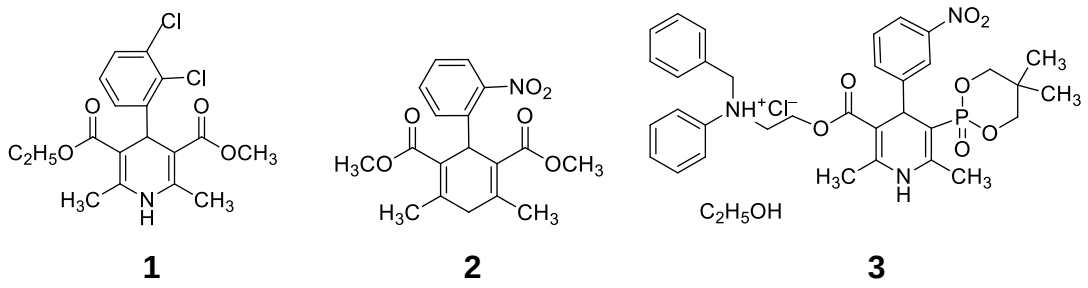

Source: Own authorship

The lercanidipine hydrochloride molecules pack as $R_4^2\ (22)$ dimeric motifs sustained by two N–H···Cl and one Cl–H···N hydrogen bonds, characterized by distances $d_{N(3)H\cdots Cl(1)}$ = 2.23(3) Å, $d_{N(2)-H\cdots Cl(1)}$ = 2.45(2) Å and $d_{C1(1)-H\cdots N(3)}$ = 2.57(13) Å, respectively demonstrated in **Figure 9**. Shown in **Figure 10**, The 3D packing emerges from a set of non-classical C–H···O hydrogen bond interactions between these dimers: $d_{C(28)H\cdots O(1)}$ = 2.66(3) Å, $d_{C(15)H\cdots O(1)}$ = 2.66(3) Å, $d_{C(6)H\cdots O(3)}$ = 2.67(3) Å, $d_{C(21)H\cdots O(5)}$ = 2.70(3) Å.

Figure 9 – The $R_4^2\ (22)$ synthon present in the crystal packing of lercanidipine hydrochloride obtained by Mercury 3.1.1

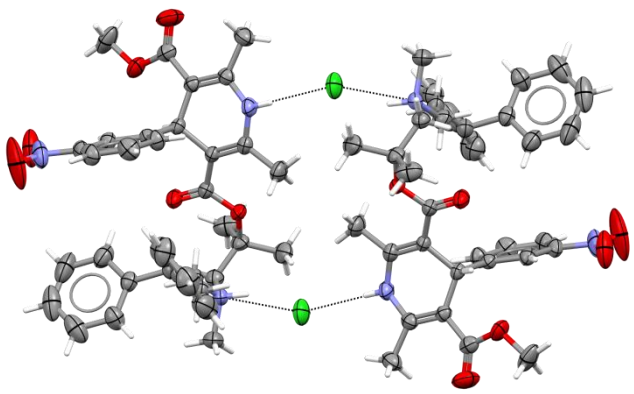

Source: Own authorship

Figure 10 – The 3D packing of lercanidipine hydrochloride obtained by Mercury 3.1.1

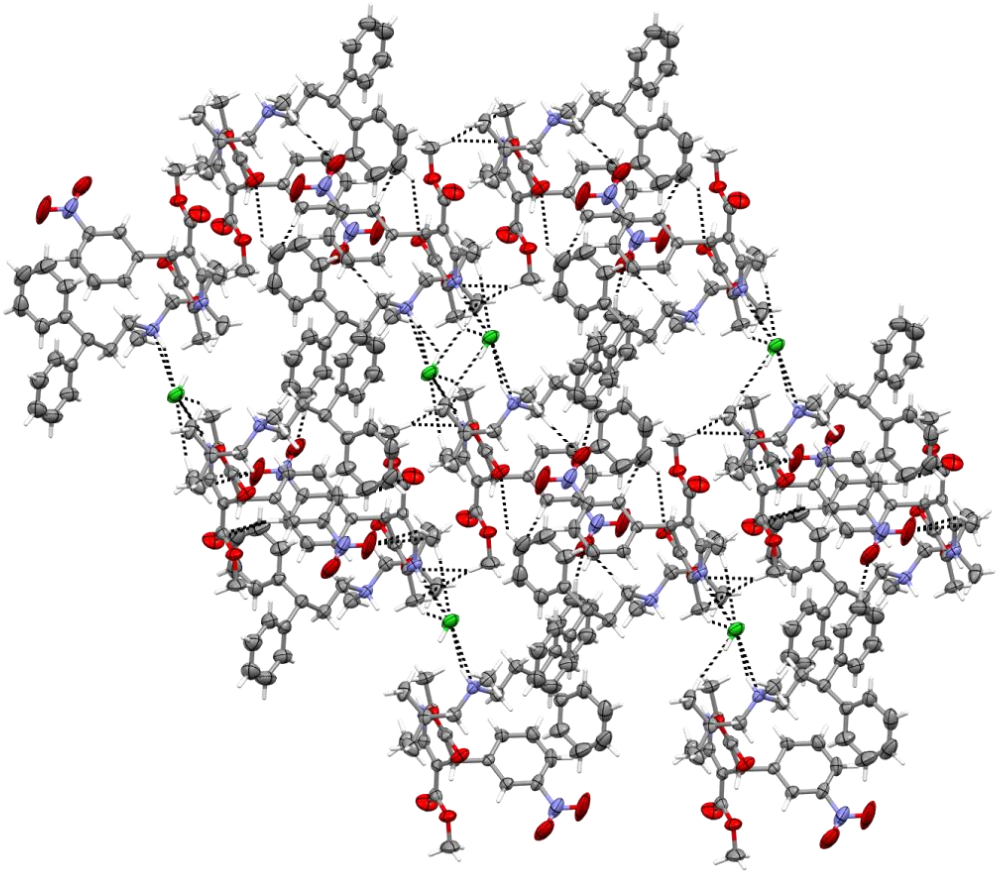

Source: Own authorship

It is worth to note that both LRC polymorphs have similar volume cell and same space group P-1; however, the cell parameters of LRC I and II are kind different, showing that LRC molecule was crystallized in two different polymorphic forms.

5.2.3 Raman results

The Raman spectra of LRC form I and II are shown in **Figure 11,** and it is in good correspondence to the data presented in the patent US 0192323 A1 (BONIFACIO *et al*., 2005).

Figure 11 – The Raman spectra of lercanidipine hydrochloride form I and II in the range from 150 to 1750 cm^{-1}

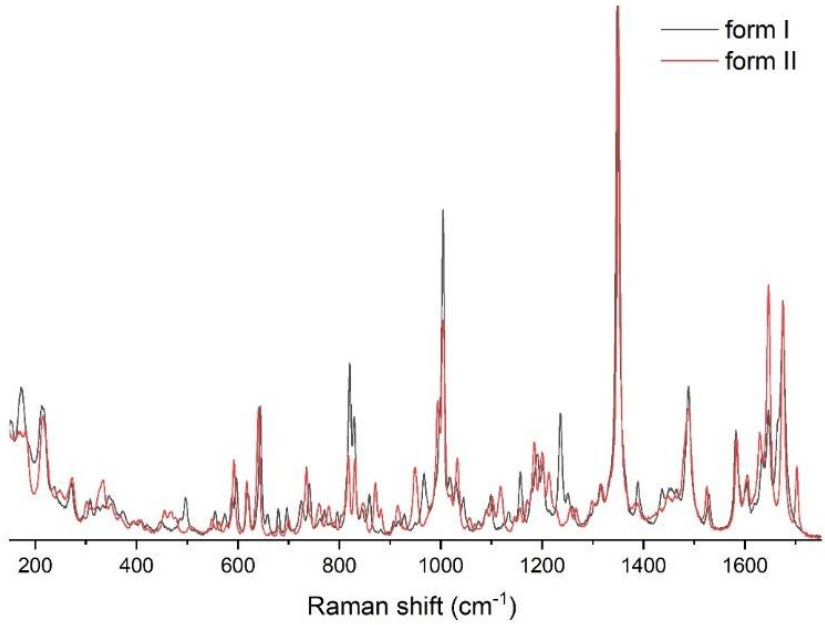

Source: Own authorship

Polymorph I of LRC shows a significant difference in its Raman spectrum in comparison with polymorph II. Form II shows peak at 1702 cm^{-1}, which is absent in the spectrum of form I, peaks at 1675, 1646 and 1633 cm^{-1} are sharper and more intense than the peaks observed in the spectrum of form I. At the region of 1580-1710 cm^{-1} both forms display similar peaks that correspond to the stretching vibration of C=O bond of both ester bonds. Two polymorphs possess an intense peak at 1348 and 1350 cm^{-1} that correlates with symmetric stretching vibration of NO2 group; both forms possess peak at 1389 cm^{-1}. However, a form I exhibits more intense one. In region 1235-1100 cm^{-1} that generally corresponds to phenyl and tertiary amine may be observed significant difference between two polymorphs form I shows peaks at 1235,

1200, 1190 and 1179, 1133 cm^{-1}, while form II at 1213, 1199, 1184, 1171 and 1117 cm^{-1} that can be explained by different arrangement of this groups in crystal unity cell.

Another intense peak corresponding to C-N-C bond of dihydropyridine ring is observed at 1003 and 1004 cm^{-1} consequently for form I and II in this case from I exhibits more intense peak some shifts between polymorphs may be observed in neighboring peaks as well. The region of 800 cm^{-1} is acknowledged mostly to N-H group of dihydropyridine and shifts between polymorphs occurred due to the difference in hydrogen bonds. Only form II shows a peak at 871 cm^{-1}, as both polymorphs have peaks at 829 and 819 cm^{-1} peaks of form I are more intense. The region from 210 to 100 cm^{-1} that corresponds to crystalline lattice vibration also shows a noticeable difference.

5.3 Physicochemical characterization results

5.3.1 Thermal behavior

According to results, only one endothermic event was observed on each DSC curves of LRC form I and II, corresponding to the melting, illustrated in **Figure 12**. Evidence of solvated or hydrated forms was neglected since no weight loss was detected in TG curves before the melting, which is followed by decomposition of samples. Additionally, the $T_{onset\ d}$ of decomposition were 200 °C and 205 °C for form I and II, respectively, indicating that the form II is slightly more thermally stable. The melting of form I occurs at $T_{onset\ m}$ of melting is 188 °C (T_{mI} = 191 °C) with ΔH_{fI} = 55.69 ± 3.47 $mJ \cdot mg^{-1}$, while the sharp endothermic peak of form II melting can be observed at a higher temperature $T_{onset\ m}$of melting is 198 °C (T_{mII} = 201 °C) with ΔH_{fII} = 73.71 ± 11.50 $mJ \cdot mg^{-1}$. According to the heat of fusion rule, the absence of phase transition together with the superior value of enthalpy of highest melting form II indicates that form II can be considered as stable one with its monotropic relation with the metastable form I (BURGER; RAMBERGER, 1979; GIRON, 1995).

Figure 12 – The DSC and TG curves of lercanidipine hydrochloride form I and II obtained under nitrogen gas flow 50 mL·min^{-1} (DSC) and 100 mL·min^{-1} (TG) with heat rate 10 ºC·min^{-1}

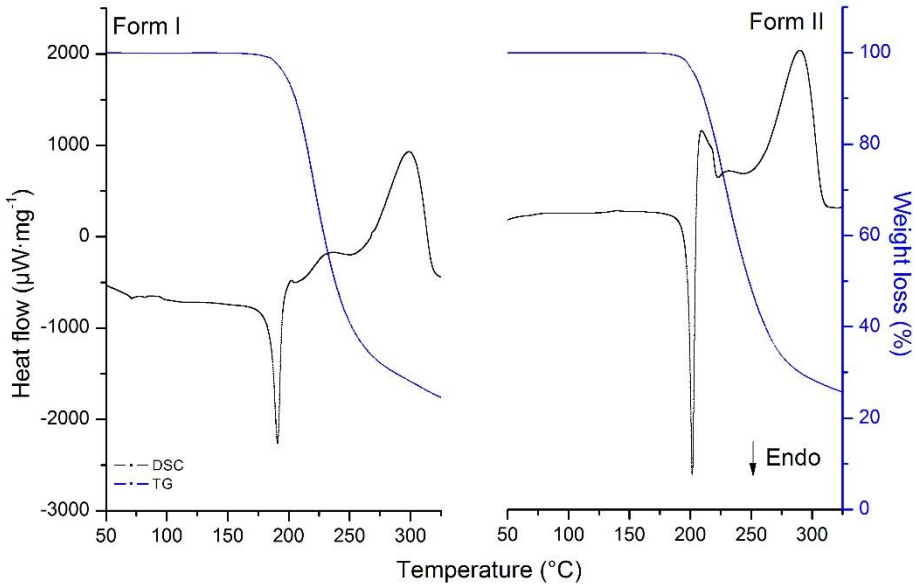

Source: Own authorship

Based on experimental data following values of the estimated transition temperature, enthalpy, entropy, and Gibbs energy were obtained by **Equations (4, 5, 6, 9)**: T_t = 514 K (241 °C), ΔH_t = – 15.71 J·g^{-1}, ΔS_t = – 30.55 mJ·g^{-1}·K, ΔG_t = – 1.18 J·g^{-1}. These thermodynamic properties of the polymorphic system are meaningful in the context of the determination of the polymorph relation. Like this, the transition enthalpy $\Delta H_t < 0$ is expected for monotropy, while $\Delta H_t > 0$ anticipated for enantiotropy, same for the transition entropy $\Delta S_t < 0$ is expected for monotropy and $\Delta S_t > 0$ for enantiotropy. The negative value of the transition Gibbs energy indicates on its spontaneous character, monotropic relation of polymorphs is also confirmed by calculated T_t, as it is higher than the melting temperature T_m of both forms. For monotrophic systems, transition temperature can be considered as a theoretical value, which can not be achieved in common experimental conditions and requires application in addition to temperature, a high pressure.

5.3.2 Particle size distribution, surface area and density measurements results

The particle size distribution and the distribution histogram are shown in **Figure 13a** (form I) and **13b** (form II).

Figure 13 – The particle size distribution and distribution histogram of lercanidipine hydrochloride form I (a) and form II (b) obtained by light scattering in wet dispersion with surfactant addition

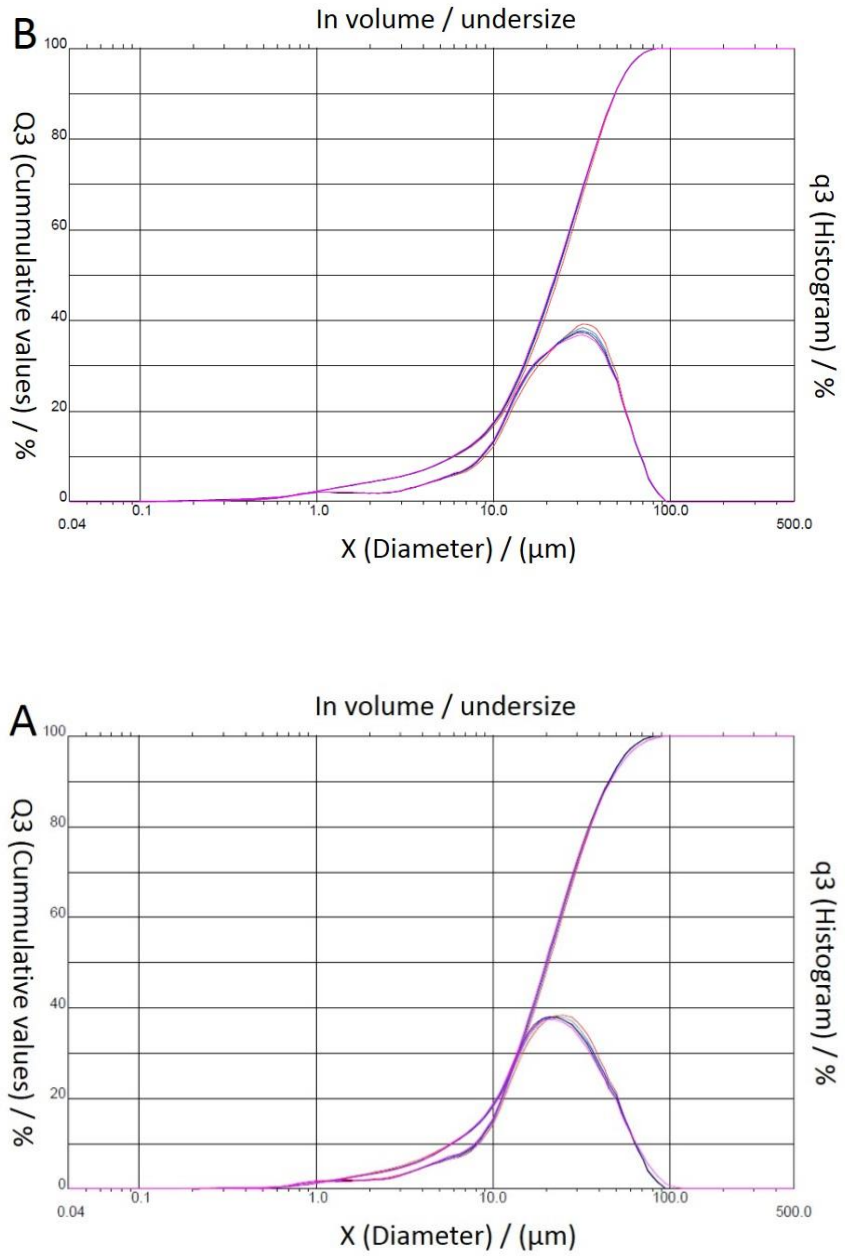

Source: Own authorship

The particle size distribution of both forms is similar; each of form exhibits monomodal distribution that means the presence of only one fraction of particles, which is located in the central part of the particle size distribution and form a sharp peak. Measured particle size distribution represented by mean diameter with polydispersity estimated by span factor, which represents the distribution width of particle size in dispersion. Span was estimated using the following **Equation (17)** (ELVERSSON *et al*., 2003):

$$Span = \frac{D_{0.9} - D_{0.1}}{D_{0.5}} \tag{17}$$

, where $D_{0.1}$, $D_{0.5}$ and $D_{0.9}$ are the size of particles below which 10%, 50% and 90% of the samples lie respectively. According to obtained results shown in **Table 7**, LRC form I possesses D_{mean} = 23.52 ± 0.22 μm with polydispersity $Span$ = 1,97 ± 0,04, while form II exhibits particles with D_{mean} = 25.53 ± 0.5 μm with polydispersity $Span$ = 1,88 ± 0,04.

Table 7 – The particle size distribution of lercanidipine hydrochloride form I and II

Run	$D_{0.1}$, μm	$D_{0.5}$, μm	$D_{0.9}$, μm	D_{mean} , μm	$Span$	Obscuration
			Form I			
1	5.75	20.76	45.64	23.75	1.92	14
2	5.87	20.37	45.58	23.58	1.95	14
3	5.92	20.15	45.49	23.45	1.96	13
4	5.84	19.89	45	23.19	1.97	13
5	5.86	19.94	46.3	23.65	2.03	12
			Form II			
1	6.01	23.45	48.96	25.95	1.83	16
2	5.98	22.86	48.57	25.55	1.86	16
3	5.93	22.65	48.46	25.46	1.88	15
4	5.88	22.48	48.72	25.39	1.91	15
5	5.83	22.28	48.8	25.3	1.93	15

The particle distribution of polymorphs matches with results of the surface area of both forms that were obtained by nitrogen sorption interpreted by Brunauer, Emmett, and Teller (BET) method (BRUNAUER; EMMETT; TELLER, 1938).

Figure 14 – The multi-point BET plot of nitrogen sorption studies of lercanidipine hydrochloride form I (a) and II (b) performed at 77 K consisted of 20 adsorption and 19 desorption points

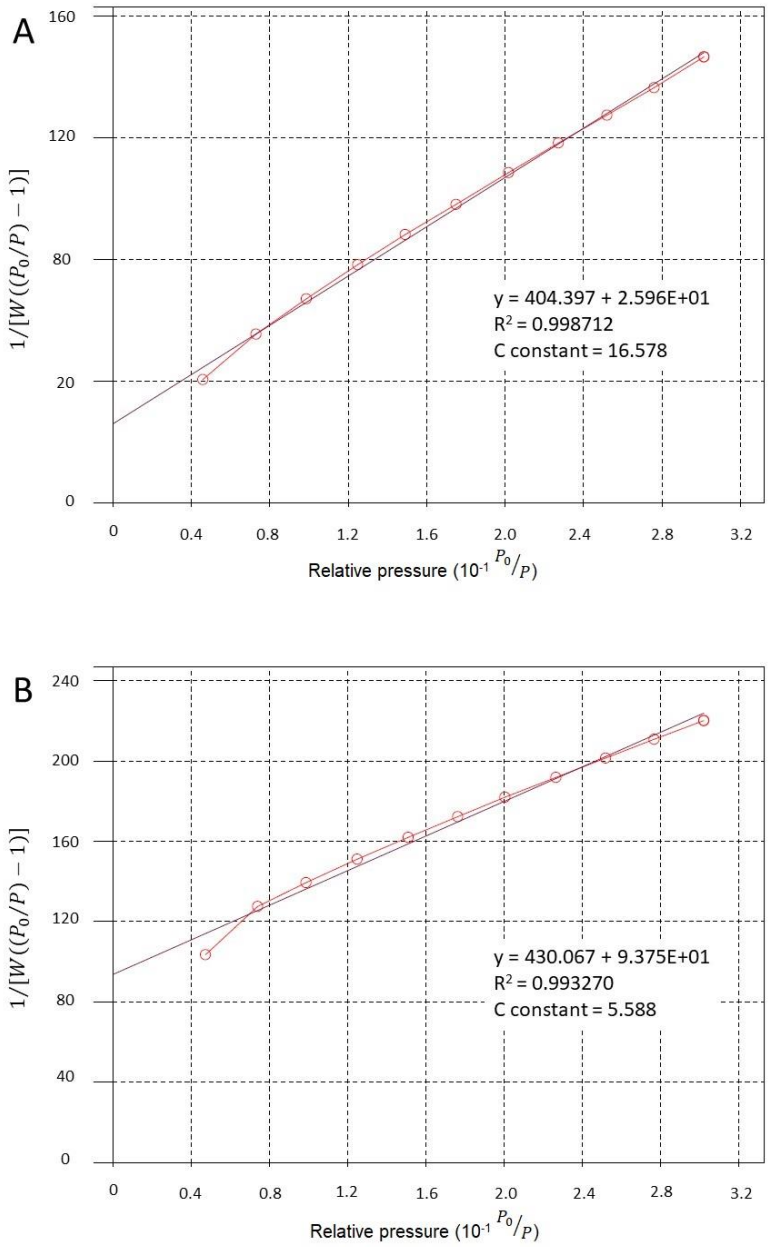

Source: Own authorship

According to results obtained by multi-point BET plot, which are shown in **Figure 14a** and **14b**, the form I possesses 8.092 $m^2 \cdot g^{-1}$ surface area that is higher than 6.648 $m^2 \cdot g^{-1}$ of form II. The measurements can be considered correct as of the value of The BET constant $C_{constant}$, which is related to the affinity of the solid with the adsorbate, is positive for both forms (AMBROZ *et al*., 2018). Surface area results intact with

particle size distribution experiments, as the form II with bigger particle size, has a smaller surface area, and with solubility studies, as it is less soluble than form I.

The measured density of stable form II equals ρ = 1280.8 ± 3.2 kg·m^{-3}, while form I density is ρ = 1391.1 ± 6.8 kg·m^{-3}; the results are in contrary to the density rule that declares more stable form to have higher density. However, exceptions are not uncommon and have been reported, and in case of monoclinic form p-hydroxyacetanilide may be explained by the large dihedral angle between the molecules and as a result quite open structure (HAISA *et al*., 1976; BURGER; RAMBERGER, 1979).

5.4 Thermodynamic characterization of the polymorphic system

5.4.1 Solubility by temperature variation method results

The results of polythermal solubility studies represented in **Table 8**.

Table 8 – Mole fraction solubility of the lercanidipine hydrochloride polymorphs in ethanol and acetonitrile as a function of temperature

LRC Form I				LRC Form II			
Ethanol		Acetonitrile		Ethanol		Acetonitrile	
T, K	$x \cdot 10^{-3}$	T, K	$x \cdot 10^{-3}$	T, K	$x \cdot 10^{-3}$	T, K	$x \cdot 10^{-3}$
288.21	1.80	309.64	1.66	310.87	1.37	330.22	1.28
300.12	2.71	319.39	2.43	317.60	1.90	336.72	1.68
307.66	3.56	326.63	3.30	323.09	2.32	341.46	2.10
313.05	4.49	331.39	4.04	326.10	2.72	345.42	2.48
315.76	5.17	335.41	4.84	330.86	3.42	346.94	2.95
320.34	6.22	337.91	5.65	331.88	3.65	350.44	3.34
289.71	1.84	308.39	1.62	310.26	1.44	329.85	1.18
301.13	2.74	320.39	2.46	316.64	1.74	337.84	1.65
308.41	3.59	326.88	3.23	322.95	2.31	341.08	2.01
312.79	4.50	330.89	4.01	326.48	2.75	344.59	2.37
317.43	5.36	336.40	4.98	329.56	3.19	348.54	2.75
320.30	6.35	337.65	5.66	332.19	3.64	350.85	3.19
289.86	1.82	311.35	1.57	310.88	1.39	330.86	1.20
301.38	2.77	320.54	2.41	317.17	1.80	338.36	1.70
308.37	3.62	326.59	3.17	323.14	2.32	341.60	2.02
313.60	4.52	330.85	3.98	326.63	2.76	345.51	2.41
317.09	5.57	334.12	4.70	329.64	3.15	348.36	2.79
319.85	6.32	336.61	5.55	332.13	3.57	352.12	3.18

Figure 15 shows data in a graphical form more accessible to interpretation, as it may be seen the solubility of both polymorphic forms of LRC showed its sensitive to temperature with the exponential character of dependence. Lesser solubility of LRC form II in both ethanol and acetonitrile allow as considering its higher stability, which is match with thermal analysis results.

Figure 15 – The mole fraction solubility of lercanidipine hydrochloride form I and II obtained in ethanol and acetonitrile as a function of temperature

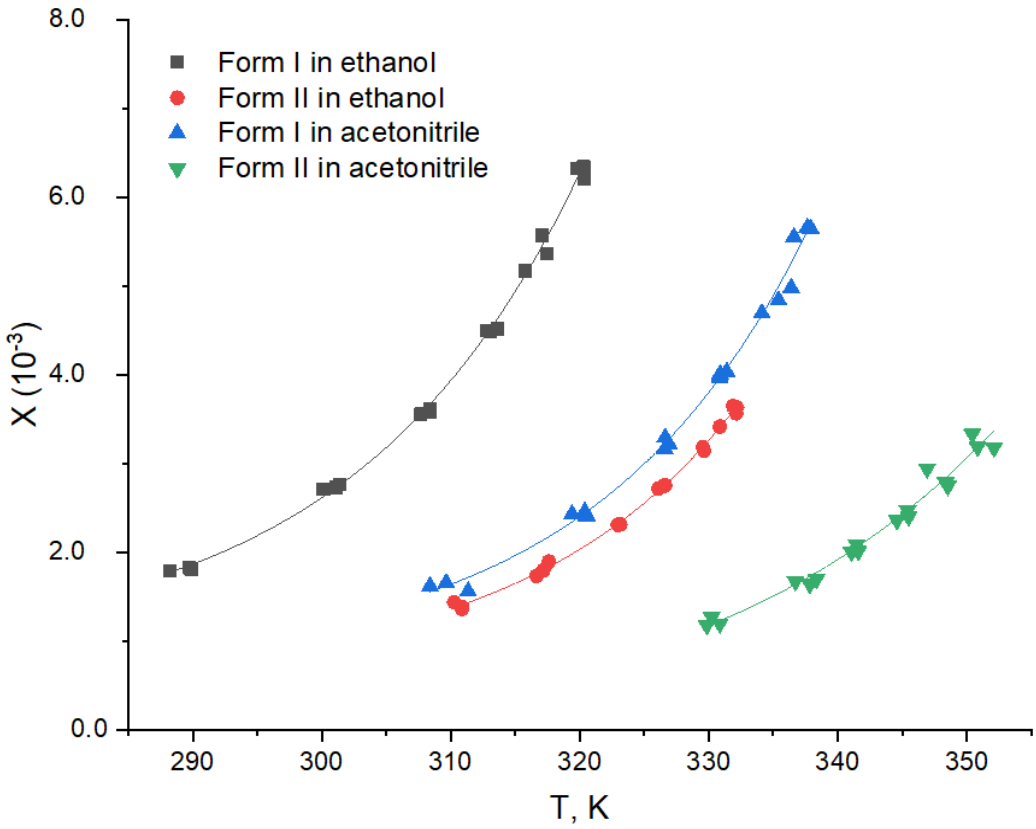

Source: Own authorship

The solubility data modified to plot into van't Hoff coordinates with further extrapolation of linear regression to the point of intersection provided us with an estimated polymorphic transition temperature T_t = 517 K (244 °C) and T_t = 624 K (351 °C) in ethanol and acetonitrile, respectively, demonstrated in **Figure 16**.

Figure 16 – The mole fraction solubility of lercanidipine hydrochloride form I and II in van't Hoff plot obtained in ethanol and acetonitrile extrapolated to the intersection point

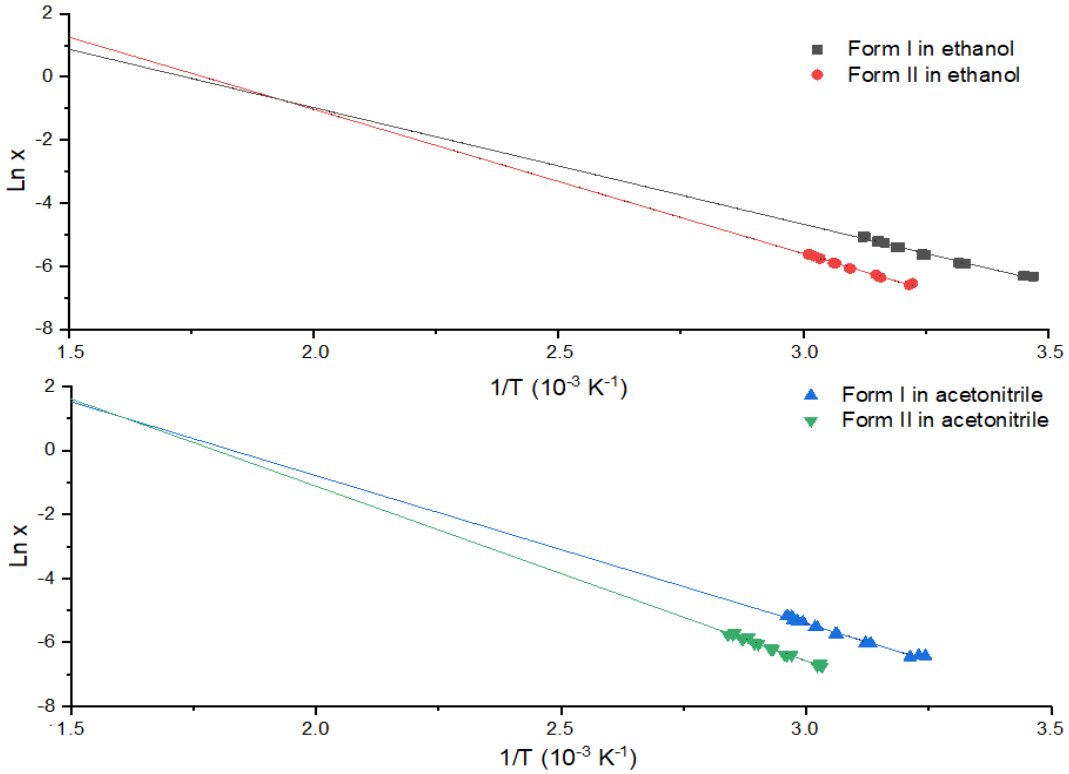

Source: Own authorship

5.4.2 Explanation in a variation of estimated Tt

Estimated transition temperature T_t vary significantly depending on the method since each method has its assumptions. Such as difference in heat capacity and its correction constant in melting method and not perfectly linear plot of Lnx versus $1/T$ and temperature and solvent dependence of heat of dissolution**.** The difference can be contributed to the calculation method; the estimation of transition temperature exhibits significant variation depending on the solvent and is not as accurate as one based on the melting data (PATEL *et al*., 2015). However, it is following expectation for monotropic pair and is higher than the melting temperature of both polymorphs.

5.4.3 Isothermal solution microcalorimetry results

Calorimetric measurements of the enthalpy of dissolution ΔH_d, of the LRC polymorphs I and II in methanol, led to the results in **Table 9**. The ΔH_d values were calculated from (ARAUJO *et al*., 2018):

$$\Delta H_d = \frac{M}{m} \cdot \varepsilon \cdot (A - A_b) \tag{18}$$

, where m and M = 648.197 g·mol^{-1} ($C_{36}H_{42}N_3O_6Cl$) denote the mass and molar mass of LRC, respectively; A is the area of the measured curve; A_b is the contribution to the measured curve area from the drop process alone; and ε is the calibration constant. The value of A_b = 0.84 ± 0.28 mV·s was determined as the mean value of eight independent experiments where an empty crucible was dropped into methanol. The calibration constant ε = 6.999 ± 0.28 V·W^{-1} was obtained from eleven electrical calibrations, where a potential difference V was applied to a glass encapsulated 60 Ω resistance immersed in the calorimetric liquid. This caused a current of intensity I to flow during a time t, leading to the dissipation of an amount of heat $Q = V \cdot I \cdot t$. The calculation of ε relied on **Equation 19** (ARAUJO *et al*., 2018):

$$\varepsilon = \frac{\sum_i V_i \cdot I_i \cdot \Delta t_i}{A_c} \tag{19}$$

, where A_c is the area of the measured curve, V_i and I_i are the ith voltage and current readings, respectively, during the overall time t of the calibration and Δt_i is the time difference between two consecutive data acquisitions.

Table 9 – The enthalpies of dissolution of lercanidipine form I and II in methanol at T = 298.15 K and P = 1 bar

m_{LRC}, mg	m_{MeOH}, mg	A, mV·s	$Q = \varepsilon(A - A_b)$, J	ΔH_d, kJ·mol^{-1}
		Form I		
8.8690	11.98728	36.909	0.252	18.418
8.7898	12.04479	39.691	0.272	20.058
8.8572	12.00963	39.272	0.269	19.686
8.7593	12.00966	39.398	0.270	19.980
8.9036	12.00577	42.181	0.289	21,040
		$\Delta H_d = 19.837 \pm 0.942$		
		Form II		
8.8947	12.0478	50.691	0.349	25.433
8.8766	12.0049	51.037	0.351	25.631
8.7359	11.9276	53.837	0.371	27.528
8.7951	12.0085	55.213	0.381	28.080
8.8589	12.0342	53.097	0.366	26.780
		$\Delta H_d = 26.690 \pm 1.156$		

Based on the enthalpy of dissolution, the enthalpy of transition can be estimated from **Equation 20** (CHADHA *et al*., 2013):

$$\Delta H_t = \Delta H_{dI} - \Delta H_{dII} \quad (20)$$

, where ΔH_{dI} is the enthalpy of dissolution of form I (low melting form) and ΔH_{dII} corresponds form II (high melting polymorph). Thus, the enthalpy of transition $\Delta H_t = -6.853$ kJ·mol^{-1} or -10.572 J·g^{-1} that matches with data estimated from thermal analysis (section 5.3.1 of the thesis).

5.4.4 Interpretation of estimated thermodynamic parameters of dissolution

The curve fitting equation corresponding to solubility data plotted in van`t Hof coordinates and estimated based on them by **Equations (14-16)** enthalpy of dissolution, entropy, and Gibbs energy is presented in **Table 10** and **11**.

Table 10 – Estimated values for the dissolution enthalpy, entropy and Gibbs free energy of LRC form I and II in ethanol

Form I in ethanol						
Curve fitting equation	$y = -3696.87 + 6.42 \cdot x$, $R^2 = 0.988$					
ΔH_d, kJ·mol^{-1}	30.74					
ΔS_d, J·mol^{-1}·K	53.42					
Run 1						
T, K	288.21	300.12	307.66	313.05	315.76	320.34
ΔG_d, kJ·mol^{-1}	15.34	14.70	14.30	14.01	13.87	13.62
Run 2						
T, K	289.71	301.13	308.41	312.79	317.43	320.3
ΔG_d, kJ·mol^{-1}	15.26	14.65	14.26	14.03	13.78	13.63
Run 3						
T, K	289.86	301.38	308.37	313.60	317.09	319.85
ΔG_d, kJ·mol^{-1}	15.25	14.64	14.26	13.98	13.80	13.65
Form II in ethanol						
Curve fitting equation	$y = -4574.08 + 8.13 \cdot x$, $R^2 = 0.992$					
ΔH_d, kJ·mol^{-1}	38.03					
ΔS_d, J·mol^{-1}·K	67.55					
Run 1						
T, K	310.87	317.6	323.09	326.10	330.86	331.88
ΔG_d, kJ·mol^{-1}	17.03	16.57	16.20	16.00	15.68	15.61
Run 2						
T, K	310.26	316.64	322.95	326.48	329.56	332.19
ΔG_d, kJ·mol^{-1}	17.06	16.64	16.21	15.97	15.77	15.59
Run 3						
T, K	310.88	317.17	323.14	326.63	329.64	332.13
ΔG_d, kJ·mol^{-1}	17.03	16.60	16.20	15.96	15.76	15.59

Table 11 – Estimated values for the dissolution enthalpy, entropy and Gibbs free energy of LRC form I and II in acetonitrile

Form I in acetonitrile						
Curve fitting equation	$y = -4625.09 + 8.47 \cdot x$, $R^2 = 0.985$					
ΔH_d, kJ·mol^{-1}	38.45					
ΔS_d, J·mol^{-1}·K	70.39					
Run 1						
T, K	309.64	319.39	326.63	331.39	335.41	337.91
ΔG_d, kJ·mol^{-1}	16.66	15.97	15.46	15.13	14.84	14.67
Run 2						
T, K	308.39	320.39	326.88	330.89	336.4	337.65
ΔG_d, kJ·mol^{-1}	16.75	15.90	15.44	15.16	14.77	14.68
Run 3						
T, K	311.35	320.54	326.59	330.85	334.12	336.61
ΔG_d, kJ·mol^{-1}	16.54	15.89	15.47	15.17	14.94	14.76
Form II in acetonitrile						
Curve fitting equation	$y = -5459.85 + 9.80 \cdot x$, $R^2 = 0.983$					
ΔH_d, kJ·mol^{-1}	45.39					
ΔS_d, J·mol^{-1}·K	81.52					
Run 1						
T, K	330.22	336.72	341.46	345.42	346.94	350.44
ΔG_d, kJ·mol^{-1}	18.48	17.95	17.56	17.24	17.11	16.83
Run 2						
T, K	329.85	337.84	341.08	344.59	348.54	350.85
ΔG_d, kJ·mol^{-1}	18.51	17.85	17.59	17.30	16.98	16.79
Run 3						
T, K	330.86	338.36	341.6	345.51	348.36	352.12
ΔG_d, kJ·mol^{-1}	18.42	17.81	17.55	17.23	17.00	16.69

The positive value of Gibbs energy ΔG_d determines the unspontaneous character of dissolution, thus estimated ΔG_d is lowest for LRC form I dissolved in ethanol followed by LRC form I in acetonitrile. Form II exhibit higher values of ΔG_d with the same sequence according to solvent, as form I with the highest value in LRC acetonitrile pair, the order of Gibbs energy is inversely proportional to the solubility of LRC in solvents. The enthalpy change of dissolution is positive ($\Delta H_d > 0$), so the heat should be applied for the dissolution to occur and the process is evident to be endothermic, this may be explained by more powerful interactions between LRC molecules and solvent molecules than those between the solvent molecules (WANG; FU; YANG, 2012). A positive value of entropy ΔS_d and enthalpy of dissolution reveal that dissolution process is the entropy-driven one and can be explained the increase of system disorder as the pure solvent is considered a highly organized system with an increase of disorder with each addition of solute and its dissolution (TAO *et al.*, 2013).

Applying **Equation 20** to the estimated enthalpy of dissolution in ethanol $\Delta H_t = -7.29$ kJ·mol^{-1} or -11.25 J·g^{-1} , while in acetonitrile $\Delta H_t = -9.94$ kJ·mol^{-1} or -15.33 J·g^{-1}, both is in a good agreement with calorimetric and thermal analysis results.

Data of mole fraction solubility x in **Table 12** was mathematically estimated based on curve fitting equation from **Tables 10, 11**. It can be further utilized to obtain ΔGt estimated values (CHADHA *et al*., 2012):

$$\Delta G_t = -RTLn\left(\frac{x_{fI}}{x_{fII}}\right) \tag{21}$$

, where x_{fI} is the mole fraction solubility of form I (low melting form) and x_{fII} corresponds form II (high melting polymorph). The negative value of calculated ΔG_t confirms not the only spontaneous character of the transition from low melting form to high melting one, but also indicates on lower Gibbs energy of this form.

Table 12 - The estimated Gibbs free energy of transition form I to form II based on mole fraction solubility data in ethanol

T, K	x_{LRC_I}	$x_{LRC_{II}}$	ΔG_t, kJ·mol^{-1}	x_{LRC_I}	$x_{LRC_{II}}$	ΔG_t, kJ·mol^{-1}
	Ethanol			Acetonitrile		
280	1.13 × 10^{-3}	2.73 × 10^{-4}	-3.53	3.20 × 10^{-4}	6.16 × 10^{-5}	-4.09
285	1.43 × 10^{-3}	3.64 × 10^{-4}	-3.39	4.27 × 10^{-4}	8.63 × 10^{-5}	-3.96
290	1.79 × 10^{-3}	4.80 × 10^{-4}	-3.26	5.65 × 10^{-4}	1.20 × 10^{-4}	-3.84
295	2.22 × 10^{-3}	6.27 × 10^{-4}	-3.13	7.40 × 10^{-4}	1.65 × 10^{-4}	-3.72
298.15	2.53 × 10^{-3}	7.38 × 10^{-4}	-3.05	8.74 × 10^{-4}	2.00 × 10^{-4}	-3.64
300	2.73 × 10^{-3}	8.11 × 10^{-4}	-3.01	9.62 × 10^{-4}	2.25 × 10^{-4}	-3.60
305	3.34 × 10^{-3}	1.04 × 10^{-3}	-2.89	1.24 × 10^{-3}	3.03 × 10^{-4}	-3.49
310	4.06 × 10^{-3}	1.32 × 10^{-3}	-2.78	1.58 × 10^{-3}	4.05 × 10^{-4}	-3.38
315	4.91 × 10^{-3}	1.68 × 10^{-3}	-2.66	2.00 × 10^{-3}	5.35 × 10^{-4}	-3.27
320	5.90 × 10^{-3}	2.10 × 10^{-3}	-2.56	2.52 × 10^{-3}	7.01 × 10^{-4}	-3.17
325	7.05 × 10^{-3}	2.62 × 10^{-3}	-2.45	3.15 × 10^{-3}	9.12 × 10^{-4}	-3.07
330	8.37 × 10^{-3}	3.24 × 10^{-3}	-2.35	3.90 × 10^{-3}	1.18 × 10^{-3}	-2.97
335	9.90 × 10^{-3}	3.99 × 10^{-3}	-2.25	4.81 × 10^{-3}	1.51 × 10^{-3}	-2.88
340	1.16 × 10^{-2}	4.88 × 10^{-3}	-2.16	5.90 × 10^{-3}	1.91 × 10^{-3}	-2.79
345	1.36 × 10^{-2}	5.93 × 10^{-3}	-2.06	7.18 × 10^{-3}	2.42 × 10^{-3}	-2.70
350	1.59 × 10^{-2}	7.16 × 10^{-3}	-1.97	8.70 × 10^{-3}	3.03 × 10^{-3}	-2.62
355	1.84 × 10^{-2}	8.61 × 10^{-3}	-1.89	1.05 × 10^{-2}	3.77 × 10^{-3}	-2.53
360	2.13 × 10^{-2}	1.03 × 10^{-2}	-1.80	1.26 × 10^{-2}	4.67 × 10^{-3}	-2.45
365	2.45 × 10^{-2}	1.22 × 10^{-2}	-1.72	1.50 × 10^{-2}	5.75 × 10^{-3}	-2.37

The Gibbs free energy of transition may also be expressed by **Equation 6** that consists of two enthalpic ΔH_t and entropic components $-T \cdot \Delta S_t$. The negative value of ΔH_t together with the approximation to zero ΔG_t with the following reversion from negative to a positive value alow as to conclude enthalpic nature of lesser stability of

form I, in other words, due to lesser lattice enthalpy in form I, it remains less stable untile with the increase of temperature the entopic factor predominates reverting stability of polymorph. It matches with calculated transition temperature as passing through it the relation of polymorph should reverse and form I become more stable one.

5.5 Solvent-mediated phase transition results

Conducted SMT slurry experiments serve as another one evidence of polymorphic relation and stability. To ensure sufficient coverage of solvents with different polarities and dielectric constants among other properties toluene, water, and ethanol were selected as test solvents in our work. The results were analyzed by XRPD and DSC tecqniques. Obtained data confirms form II as the stable one; as it was the resulting solid encountered at both temperature conditions in all solvents. As it can be observed in **Figures 17** and **18** LRC form I characteristic peak at 5.32° (2Theta) exhibits only the pattern of the initial mixture.

Figure 17 – The X-ray powder diffractograms of lercanidipine hydrochloride form I and II physical mixtures obtained from solvent-mediated phase transition study at ambient temperature

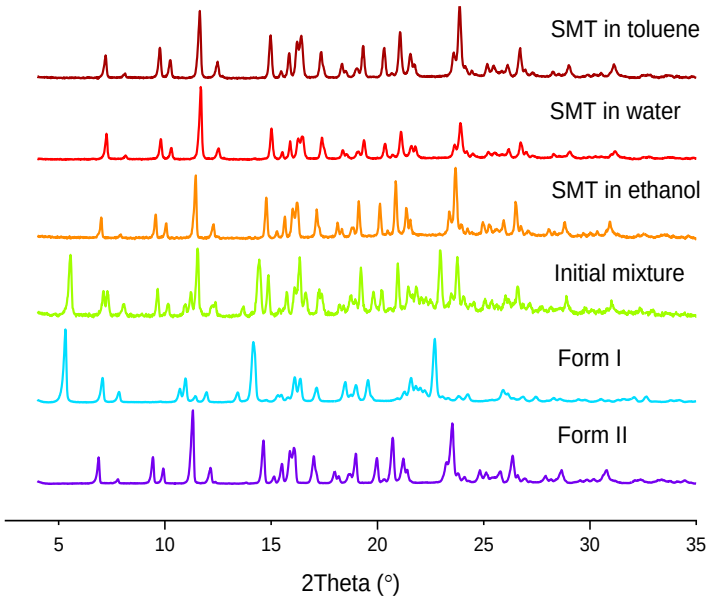

Source: Own authorship

Figure 18 – The X-ray powder diffractograms of lercanidipine hydrochloride form I and II physical mixtures obtained from solvent-mediated phase transition study at 50 °C

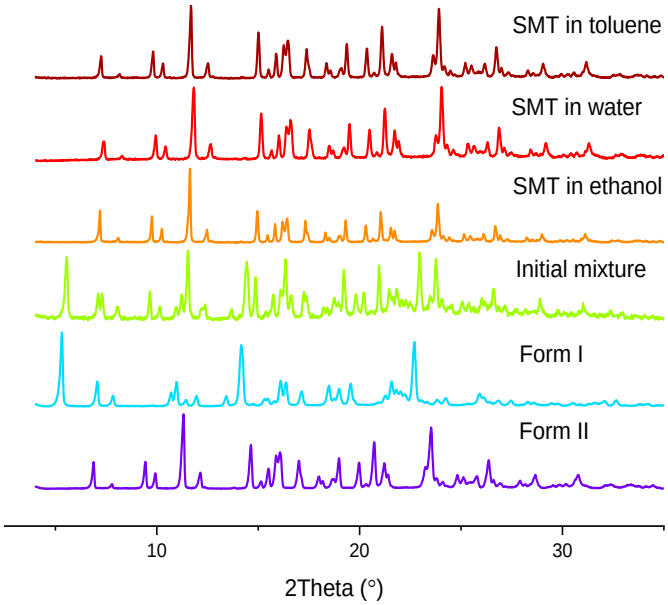

Source: Own authorship

The DSC results shown in **Figure 19 and 20** are in agreement with XRPD results. Only one endothermic event is observed in all resulting samples, peak of which lies in the temperature range that characterizes form II.

Figure 19 – The DSC curves of lercanidipine hydrochloride form I and II physical mixtures obtained from solvent-mediated phase transition study at ambient temperature

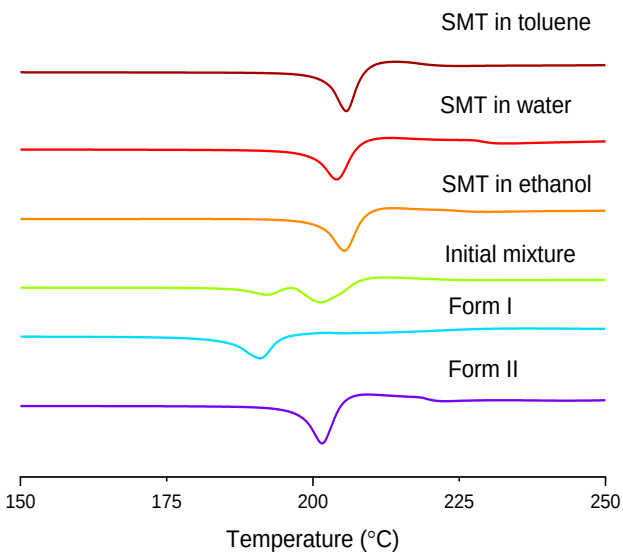

Source: Own authorship

Figure 20 – The DSC curves of lercanidipine hydrochloride form I and II physical mixtures obtained from solvent-mediated phase transition study at 50 °C

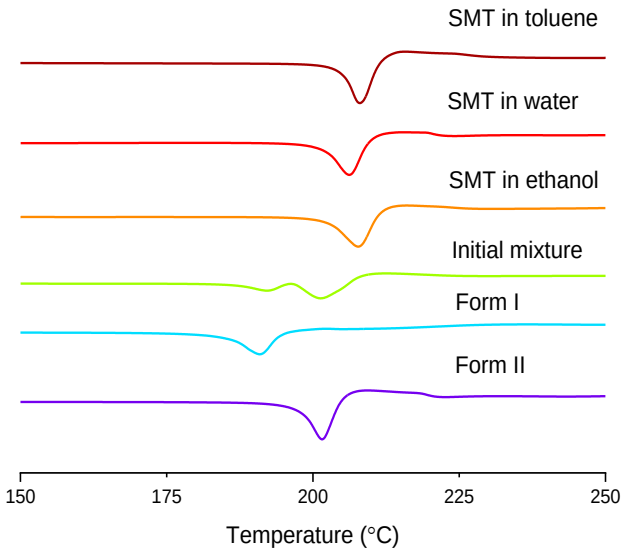

Source: Own authorship

Complete transformation into form II confirms its stable character and shows the importance of avoiding long-term solvent storage of crystalized metastable form I as it may convert into stable and less soluble form II. It is noteworthy that the LRC form I showed no evidence of polymorphic transformation throughout the solubility studies in different buffers.

5.6 Quantitative solid-state stability studies results

Samples of LRC form I and II exposed to temperature and humidity in the environmental chamber have not shown visible change or signs of degradation after the one month. Nevertheless, the metastable form I has turned out to degrade by approximately 6%, while form II remained stable in the experimental length of time. Samples exposed to light irradiation faded; however, as in the case of thermal stability, the only metastable form I showed 12% degradation as presented in **Figure 21**.

Figure 21 – The HPLC results of exposed to irradiation during 72 hours solid state samples of lercanidipine hydrochloride form I (a) and form II (b)

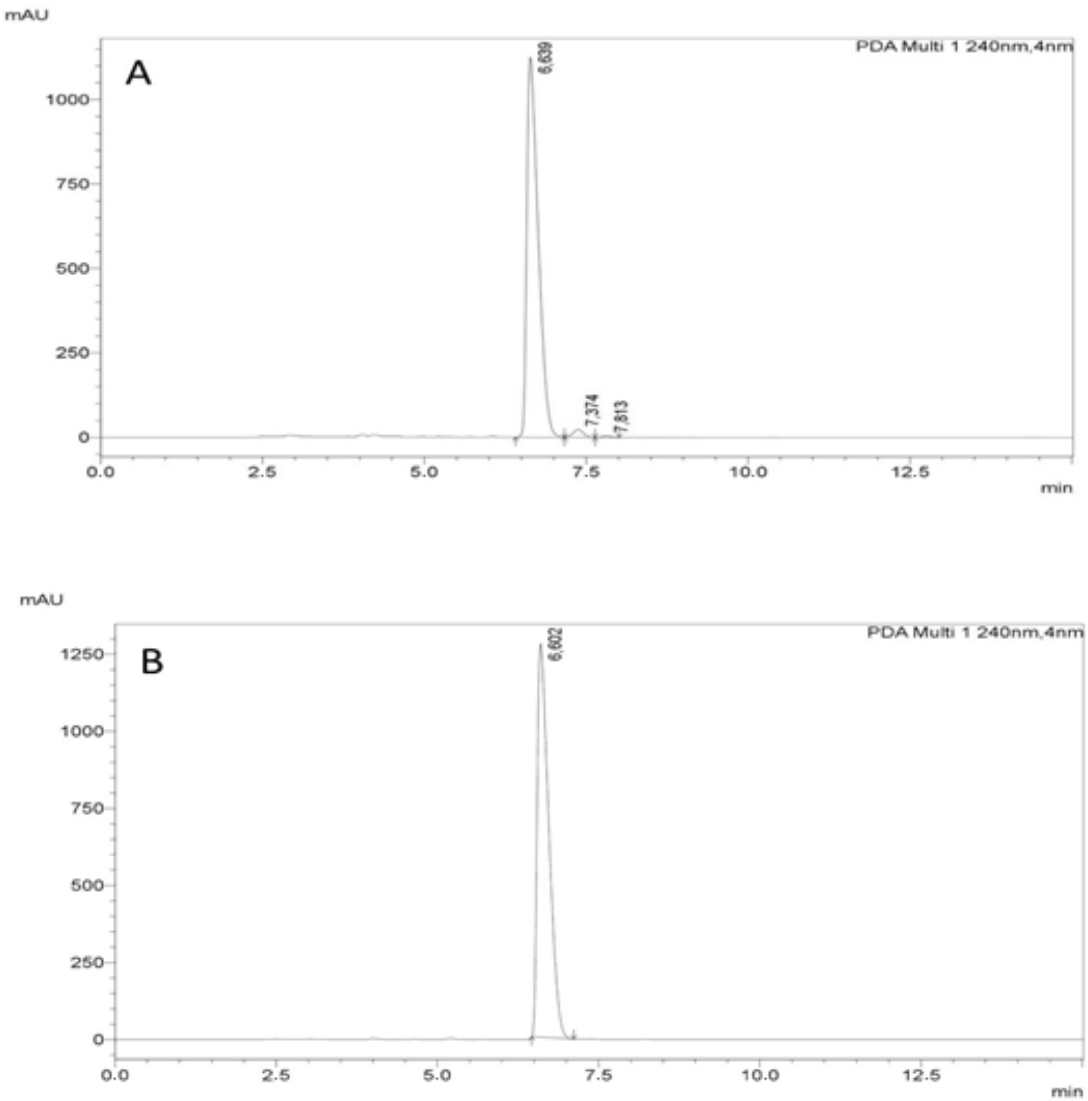

Source: Own authorship

5.7 Solubility studies results

5.7.1 Kinetic solubility determination results

To assess the effect of polymorphism on the kinetic solubility in the simulated gastric fluid medium, real-time data was acquired by using an optical fiber UV probe. The resulting solubility profile is shown in **Figure 22** and reveals that both forms dissolve and come to their equilibrium solubility plateau at approximately within the first hour of experiment, even under this unfavorable condition. The difference in solubility between polymorphs was considered significant, as metastable form I exhibits three and a half times higher solubility in the simulated gastric fluid medium than form II. The slow descending character of both curves is due to a certain degree of degradation of LRC, confirmed by HPLC analysis; the more intensive descendent curve of form I may also have the contribution of the metastability of this form, which is in congruency with solvent-mediated phase transition to form II.

Figure 22 – Kinetic solubility of lercanidipine hydrochloride form I and II obtained at pH 1.2 in a simulated gastric fluid without enzymes at 37 ± 2 °C during 24 h

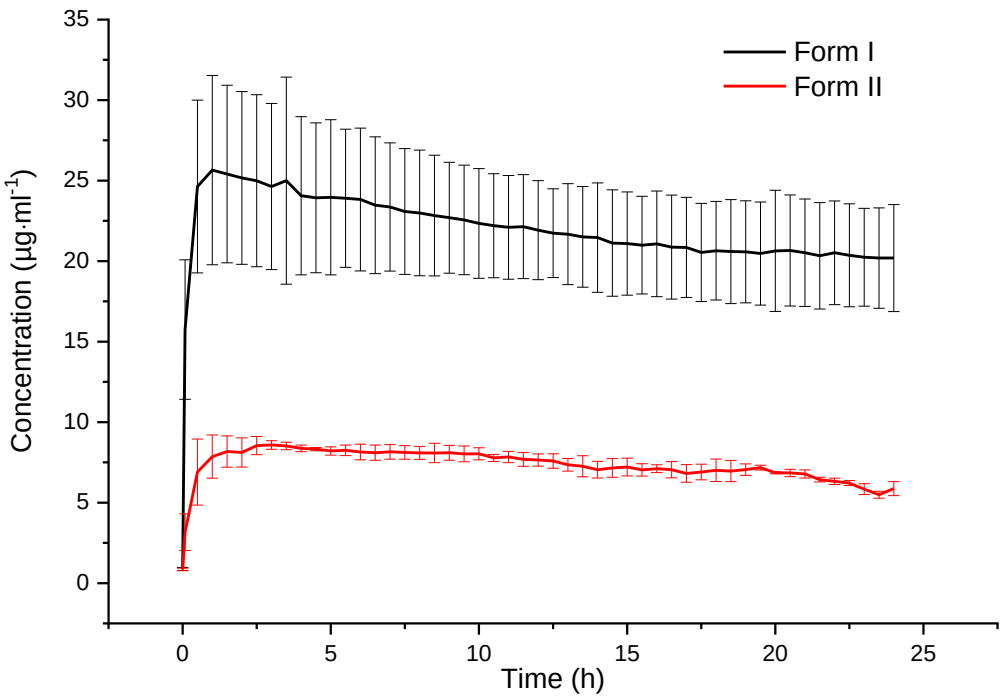

Source: Own authorship

5.7.2 Solubility by Shake-flask results

To ensure precise values of equilibrium solubility measured in each solution, the calibration of the utilized HPLC system was performed in two concentration ranges 4-200 μg·mL^{-1} and 200-1300 μg·mL^{-1}. The first curve equation shown in **Figure 23** was applied to convert results obtained in following mediums: pH 1.2 and pH 2.0 chloride, pH 3.0 phosphate 1.0M, pH 3.0 citric 1.0 M, pH 3.5 and 4.0 citric, pH 4.5 acetate. In all other cases was employed the second curve equation demonstrated in **Figure 24**.

Figure 23 – The calibration curve of HPLC applied to shake-flask solubility measurements for concentrations in scale 4-200 μg·mL^{-1}

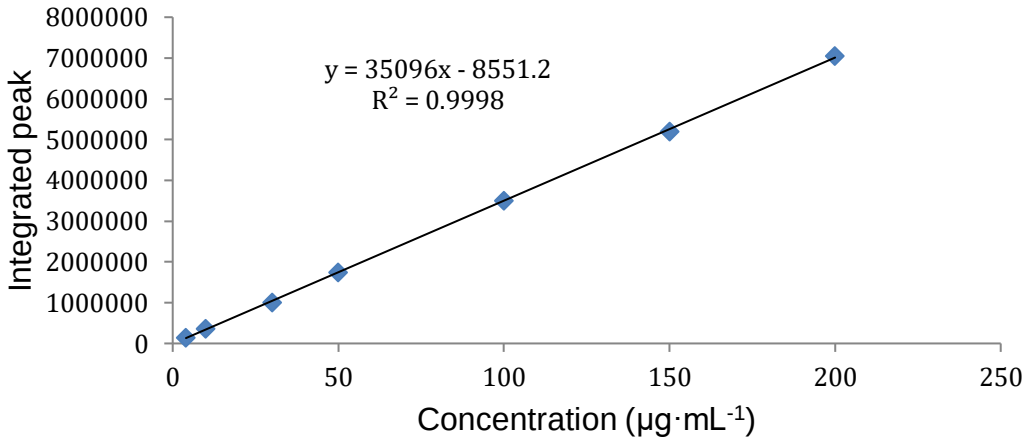

Source: Own authorship

Figure 24 – The calibration curve of HPLC applied to shake-flask solubility measurements for concentrations in scale 200-1300 μg·mL^{-1}

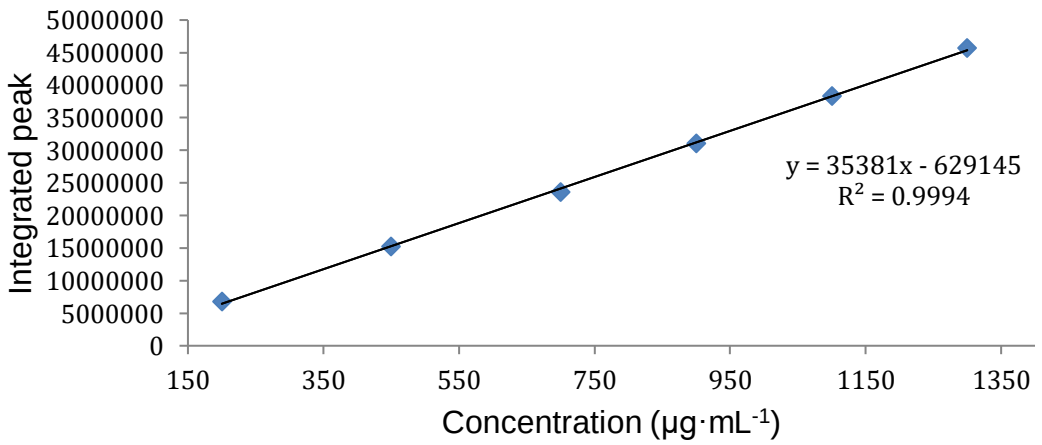

Source: Own authorship

Equilibrium solubility studies results of LRC polymorphic forms I and II are presented in **Table 13**.

Table 13 – The Dependence of equilibrium solubility of lercanidipine hydrochloride form I and II from pH medium

Buffer	Ionic strength, mol·L^{-1}	Conc. form I, µg·mL^{-1}	$DesvP$, µg·mL^{-1}	Conc. form II, µg·mL^{-1}	$DesvP$, µg·mL^{-1}	ΔGt, kJ·mol^{-1*}
pH 1.2 chloride	0.104	22.88	1.26	6.85	0.29	-3.30
pH 2.0 chloride	0.100	22.77	2.69	5.83	0.67	-3.38
pH 2.0 phosphate	0.189	655.18	4.74	558.02	33.24	-0.39
pH 2.5 phosphate	0.079	1248.95	6.75	610.46	36.39	-1.78
pH 3.0 phosphate 0.01 mol·L^{-1}	0.011	1080.90	150.21	588.73	42.82	-1.51
pH 3.0 phosphate 0.1 mol·L^{-1}	0.108	1000.78	101.78	558.09	47.15	-1.44
pH 3.0 phosphate 1.0 mol·L^{-1}	1.038	26.14	1.38	-	-	-
pH 3.0 citric 0.01 mol·L^{-1}	0.005	870.38	40.70	575.82	25.46	-1.02
pH 3.0 citric 0.1 mol·L^{-1}	0.082	250.69	25.18	269.22	66.95	-0.35
pH 3.0 citric 1.0 mol·L^{-1}	0.924	66.24	11.73	-	-	-
pH 3.5 citric	0.108	148.94	31.06	173.10	49.70	-0.37
pH 4.0 citric	0.141	88.32	3.10	65.79	5.02	-0.73
pH 4.5 acetate	0.074	22.36	1.75	24.42	0.79	-0.21

* - ΔG_t is calculated by **Equation 21**.

Independently of polymorphic form, LRC as a salt of a week base (pKa = 6.86) exhibits an expectable pH-dependent solubility profile (**Figure 25A**) and reaches higher values in the 2.5–3.0 pH range. A significant drop in solubility is observed when pH approximates to LRC´s pKa, which is assigned to a shift in the equilibrium towards the lercanidipine base formation as a result of proton neutralization. Also, a dramatic decrease in the LRC solubility at pH 1.2 was observed and can be explained by negative affection of Cl^- common ion effect. Suppression of solubility is not a rare phenomenon found in drug salts and have been reported for papaverine hydrochloride, ticlopidine hydrochloride, haloperidol hydrochloride, thus Cl^- containing opposes the positive effect of favorable to ionization in the low pH range and may overcome it (VÖLGYI *et al*., 2010).

Figure 25 – Influence of pH (a) and ionic strength of buffer medium (b) on the equilibrium solubility of lercanidipine hydrochloride form I and II

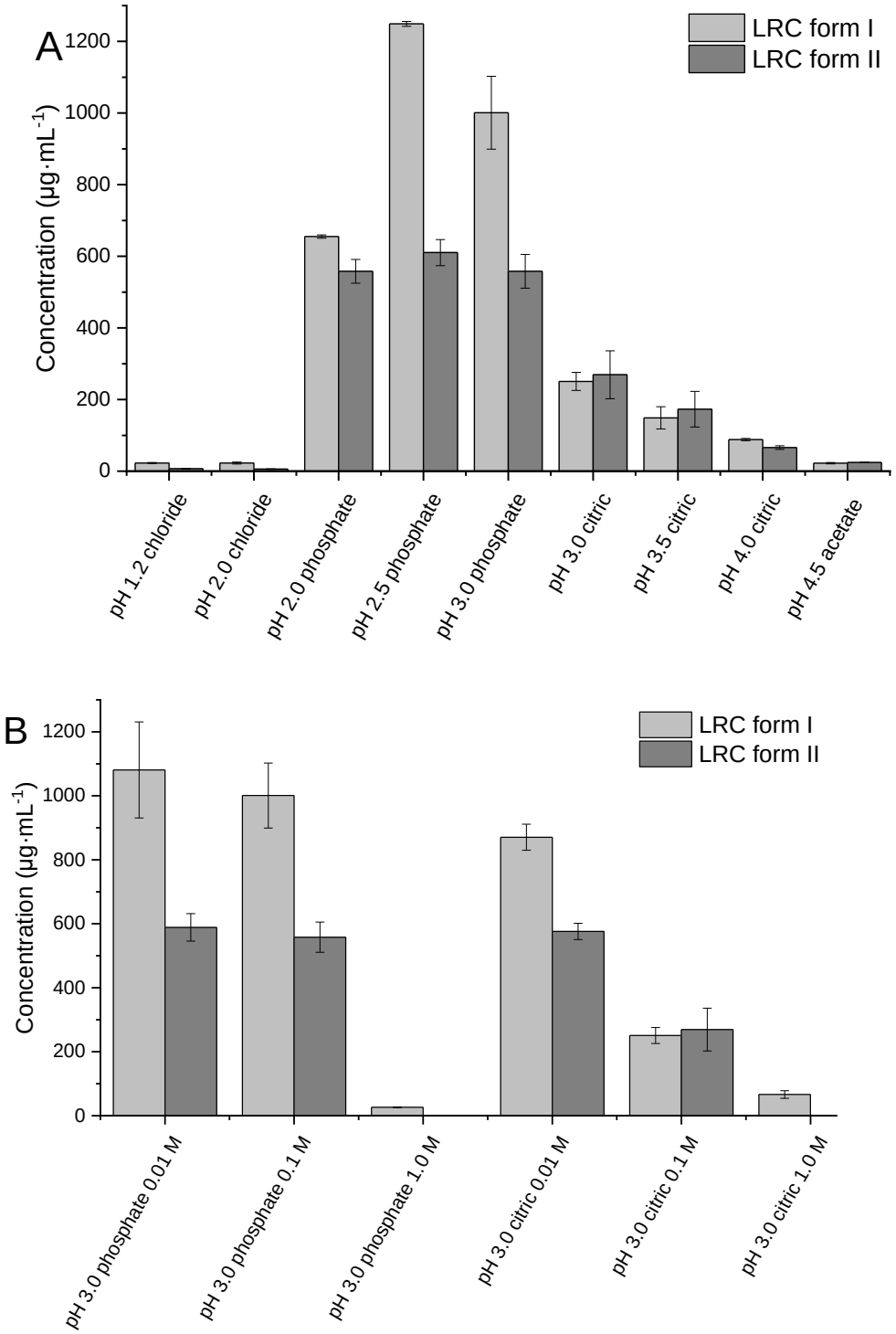

Source: Own authorship

This shift in equilibrium is an essential factor to be considered for in vitro release studies during drug development since hydrochloride salts are the most commonly used form for the enhancement of solubility of poorly soluble weak base drugs (LI *et*

al., 2005), and gastrointestinal fluids contain Cl^- ions that may affect biopharmaceutical performance.

Not only the common ion effect but also the ionic strength of the buffer medium and its ionic composition showed a significant impact on the solubility of LRC (**Figure 25B**). An excessive amount of ions present in the more concentrated buffers (e.g., ionic strength of 1 M) suppressed the solubility of LRC. The negative effect on the solubility of high ionic strength is well known and has been reported for acetaminophen, carvedilol, deferiprone, hydrochlorothiazide tablets (ASARE-ADDO *et al*., 2013; CHAHIYAN; GHARIB; FARAJTABAR, 2014; HAMED *et al*., 2016). It occurs due to salting-out process induced by an increase of the number of additional electrolytes that leads to decrease of solvating power of solute and as a result to decrease in solubility (BOROUJENI; GHARIB, 2016).

According to Streng *et al*., this direct relationship is not always valid, because solubility is also dependent on the presence and interactions of species other than those produced by the dissociation of the parent compound; when the number of additional species excesses the number of ions produced by the dissociation of the salt, suppression is observed. On the other hand, if the concentration of other species is lower than the solubility products, the addition of new species will affect only the activity coefficient, which may provide both positive or negative impact on the solubility of the parent compound depending on the nature of the ion (STRENG *et al*., 1984). For instance, Baka, John, and Takacs-Novák (BAKA; COMER; TAKÁCS-NOVÁK, 2008) reported the solubility of hydrochlorothiazide in Sörensen II buffer solution is higher than in Sörensen I despite its higher ionic strength; the authors hypothesized that the enhancement of solubility occurred due to specific interaction with citrate component medium and not by its higher ionic strength. This effect was not observed in the case of LRC as solubility in phosphate containing buffers showed a higher amount of dissolved compound.

5.7.3 Intrinsic dissolution rate results

The attempts to determine the IDR of LRC polymorphs encountered several obstacles. Initially, it was decided to perform IDR studies in pH 1.2 solution with a higher difference in solubility between two forms. However, the amount dissolved solute was so meager and lied out of detection limit by simple UV spectrophotometry that it led us to apply HPLC method of detection (**Figure 26**), which is also rested on the border of detection limit and caused high variability and doubtful results.

Figure 26 – The calibration curve HPLC system coupled with intrinsic dissolution rate studies of lercanidipine hydrochloride form I and II studies

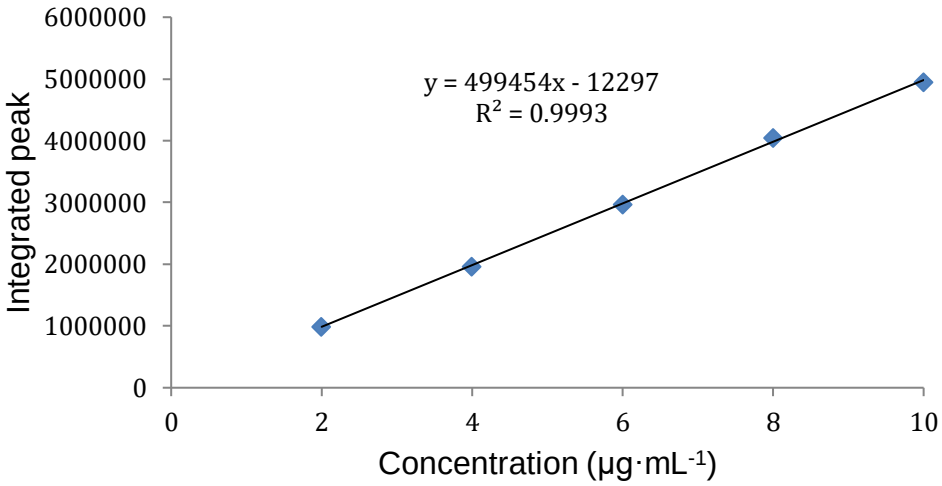

Source: Own authorship

For further studies, buffer mediums that promote high solubility of LRC were selected. Among variable experimental conditions were tested pH 3.0 phosphate and citric buffer mediums, rotation at 100 and 200 rpm, 1000 psi and 2000 psi compressing pressure. While the amount of dissolved solute increased, another obstacle was observed. The pastilles of both forms of LRC tend to break and lose the integrity of the surface area, dropping small amounts of a compressed sample into the dissolution medium.

Figure 27 – The intrinsic dissolution curve of lercanidipine hydrochloride form I and II compressed with 2000 psi and obtained in pH 3.0 citric medium at 37 °C

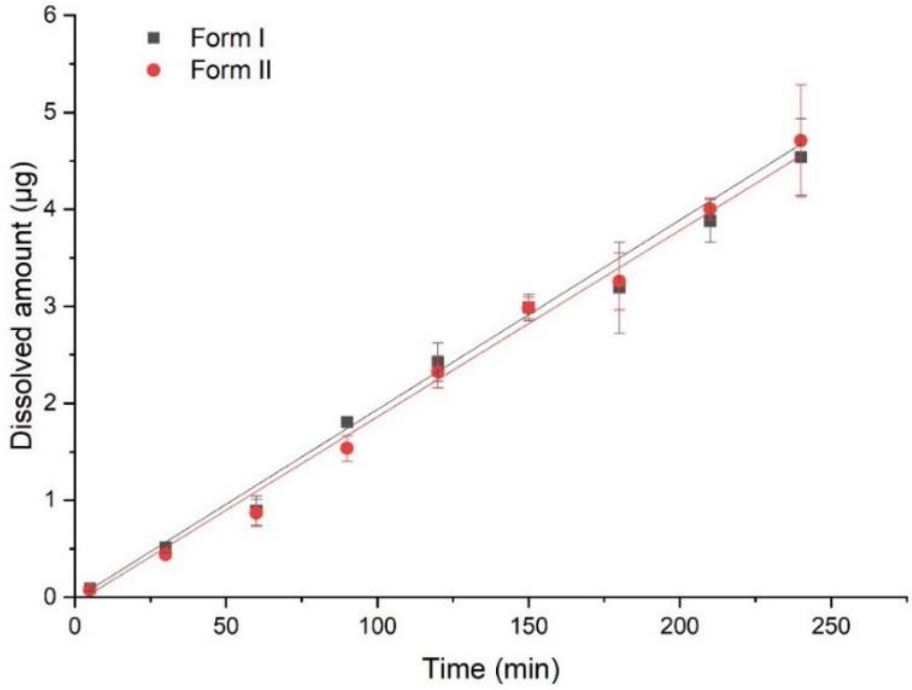

Source: Own authorship

Most reliable results were obtained in the citric buffer, pH 3.0; however, the difference in the dissolved amount of LRC form I and II was not significant in comparison with solubility measured by shake-flask in the same medium. To obtain IDR values, the dissolution curve slope, which was acquired by the plotting amount of dissolved drug against sampling time, were divided by surface area of the compressed drug (0.5 cm^2) **(Figure 27)**. The estimated IDR of LRC was 3.91×10^{-2} $\mu g \cdot cm^{-2} \cdot min^{-1}$ and 3.85×10^{-2} $\mu g \cdot cm^{-2} \cdot min^{-1}$ for form I and form II, respectively.

5.7.4 Physiologically based pharmacokinetic modeling and simulation results

PBPK simulation using GastroPlus™ was performed to access the potential impact of differences observed in solubility profiles due to polymorphism and pH variation. It is a handy tool of risk assessment to evaluate if the polymorphic forms are interchangeable, in case of accidental or intentional variability of the raw material due to changes in the manufacturing route and quality or commercial issues. The modeling was conducted by fitting clinical pharmacokinetic data and considering experimental

solubility data of form II since this form is used in the commercial product. Experimental solubility LRC form I and II data obtained by shake-flask were loaded into an optimized model to obtain *in-silico* kinetic parameters and evaluate the impact of polymorphism on them (**Table 14**).

Table 14 – The variation of the kinetic parameters of the lercanidipine hydrochloride form I and II based on experimental solubility data

Pharmacokinetics parameters	LRC form I	LRC form II	Impact, %
C_{max}, ng·mL^{-1}	5.25	3.92	133.93
t_{max}, h	1.92	2.40	80.00
AUC_t, ng·h·mL^{-1}	26.69	23.63	112.95
F_a, %	57.87	51.32	112.76
F, %	43.77	38.81	112.78

According to estimated results usage of LRC I provide an increase in bioavailability and allows achieving a slightly higher amount of dissolved drug (**Figure 28**), furthermore based on **Equations (22, 23)** and criteria of bioequivalence (RANI; PARGAL, 2004) forms were considered not bioequivalent as Cmax correlation is out of the limits, however, obtained result require *in-vivo* verification:

$$0.85 \leq \frac{C_{maxI}}{C_{maxII}} = 1.34 \leq 1.25 \tag{22}$$

$$0.85 \leq \frac{AUC_{tI}}{AUC_{tII}} = 1.13 \leq 1.25 \tag{23}$$

Figure 28 – Estimated plasmatic concentration and gastro-intestinal dissolution profile of lercanidipine hydrochloride form I and II obtained by GastroPlus™

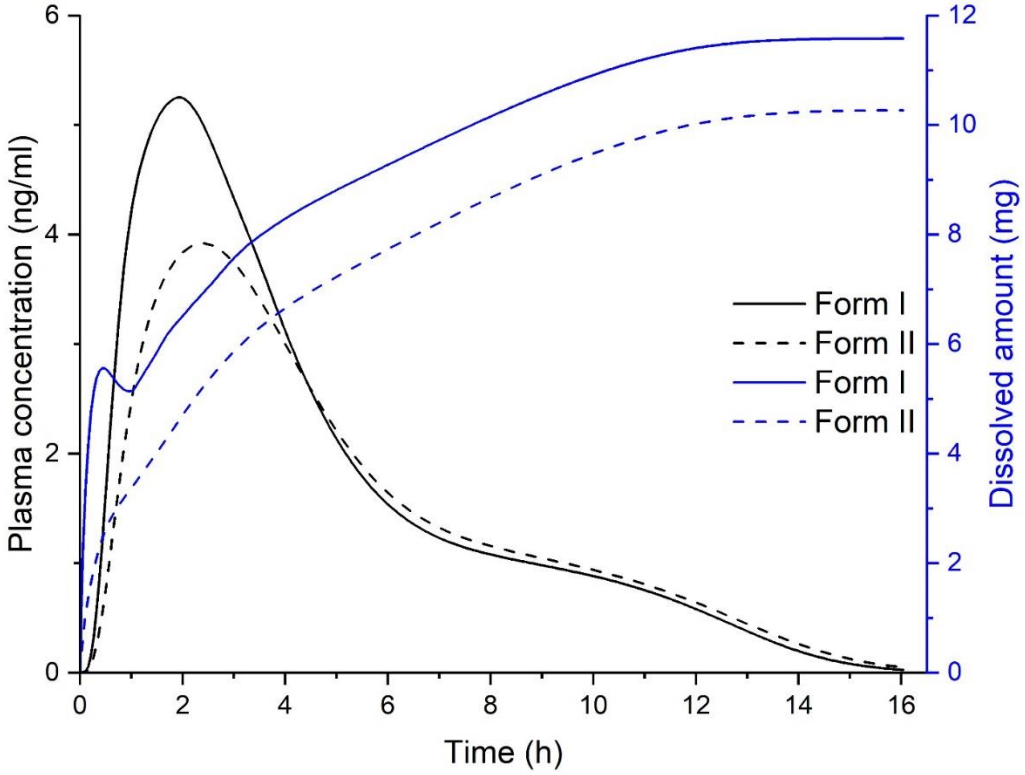

Source: Own authorship

The solubility data of LRC form I obtained in pH 3.0 phosphate and citric with different level of ionic strength were also uploaded into the model. The results, summarized in **Table 15**, indicate that both changes in ionic strength and nature of ion species of buffer medium even at same pH may lead to significant variation in the pharmacokinetic parameters and Cp profile.

Table 15 – The Variation of the kinetic parameters of lercanidipine hydrochloride form I based on the different buffer composition and ionic forces at same pH

Pharmacokinetics parameters	Phosphate 0.01 mol L^{-1}	Phosphate 1 mol L^{-1}	Impact, %	Citrate 0.1 mol L^{-1}	Citrate 1.0 mol L^{-1}	Impact, %
C_{max}, ng mL^{-1}	8.82	5.41	163.03	8.34	6.65	125.41
t_{max}, h	0.91	1.98	45.96	0.96	1.12	85.71
AUC_t, ng mL^{-1}	36.21	27.4	132.15	35.43	32.05	110.65
F_a, %	78.53	59.00	133.10	76.85	69.52	110.54
F, %	59.43	44.94	133.24	58.16	52.60	110.57

The solubility of LRC independently on a polymorphic form is significantly higher in pH 3.0 medium in compare with pH 1.2. Thus alteration of stomach pH, which is symptomatic for diseases like hypochlorhydria or even in a fed state, may lead to a significant impact on the bioavailability of the drug **Table 16**.

Table 16 – Impact on pH on pharmacokinetic parameters with lercanidipine hydrochloride form I selected as a model

Pharmacokinetics parameters	pH 1.2	pH 3.0	Impact, %
C_{max}, ng mL^{-1}$_{max, ng/ml}$	3.92	8.83	44.39
t_{max}, h$_{max, h}$	2.40	0.96	250
AUC_t, ng mL^{-1}$_{t, ng\cdot h/mL}$	23.63	37.09	63.71
F_a, %	51.32	80.43	63.81
F, %	38.81	60.87	63.76

However, it should be taken in consideration that higher solubility at pH 3.0 buffer mediums was provided not only by pH effect by itself but by the absence of Cl^- common ion, which presence is unavoidable in the human gastrointestinal tract.

CONCLUSION

In this research work, we investigated the LRC polymorphism through new crystallization routes and tested new solvent/anti-solvent pairs. For the first time, a single crystal of LRC form II and structure determination were successfully performed. Also, LRC form I indexation was carried out based on XRPD results.

Furthermore, LRC polymorphs I and II were characterized by solid-state techniques and solubility studies, allowing to establish the thermodynamic parameters and conclude a monotropic stability relationship between them, with form II being the stable one. Aqueous medium solubility measurements revealed that the influence of polymorphism on solubility is variable depending on the ionic composition and the strength of the medium, with metastable form I the most soluble form in the overall pH range investigated. The most significant impact was observed in buffers containing Cl^- within which solubility of LRC as hydrochloride salt suffers from negative affection of Cl^- common ion effect.

The SMT studies revealed that polymorphic transition of metastable form occurs only after the week period, which coincides with the absence of polymorphic transition during shake-flask experiments confirmed by XRPD allow to suppose that it is stable enough and suitable for formulation. According to results of PBPK simulation the polymorphs were not considered bioequivalent under elevated gastric pH conditions; form I was able to achieve significantly higher maximum plasmatic concentration than form II, however it should be considered the fact of its slightly worse thermal and photostability, which may require choosing appropriate package and storage conditions. As a possible solution of the observed problems may be suggested the development of new organic acid salt form or the addition of citric acid in a formulation, allowing to maintaining acidic pH microclimate during the dissolution process and protect the solute from the negative effect of Cl^- contained in gastrointestinal fluid.

REFERENCES

AALTONEN, J. *et al*. Solid form screening – a review. **European journal of pharmaceutics and biopharmaceutics**, v. 71, n. 1, p. 23–37, jan. 2009.

AGUIAR, A. J. *et al*. Effect of polymorphism on the absorption of chloramphenicol from chloramphenicol palmitate. **Journal of pharmaceutical sciences**, v. 56, n. 7, p. 847–853, 1967.

AITIPAMULA, S. *et al*. Polymorphs, salts, and cocrystals: what's in a name? **Crystal growth & design**, v. 12, n. 5, p. 2147–2152, 2012.

ALLESØ, M. *et al*. Solvent subset selection for polymorph screening. **Journal of Chemometrics: A Journal of the Chemometrics Society**, v. 22, n. 11-12, p. 621–631, 2008.

ALLESØ, M. *et al*. Towards effective solid form screening. **Journal of pharmaceutical sciences**, v. 99, n. 9, p. 3711–3718, 2010.

ALVAREZ, A. J.; SINGH, A.; MYERSON, A. S. Polymorph screening: comparing a semi-automated approach with a high throughput method. **Crystal Growth and Design**, v. 9, n. 9, p. 4181–4188, 2009.

AMBROZ, F. *et al*. Evaluation of the BET Theory for the Characterization of Meso and Microporous MOFs. **Small Methods**, v. 2, n. 11, p. 1800173, 2018.

ARAUJO, G. L. B. *et al*. A New Thermodynamically Favored Flubendazole/Maleic Acid Binary Crystal Form: Structure, Energetics, and in Silico PBPK Model-Based Investigation. **Crystal Growth & Design**, v. 18, n. 4, p. 2377–2386, 2018.

ASARE-ADDO, K. *et al*. The effect of pH and ionic strength of dissolution media on *in-vitro* release of two model drugs of different solubilities from HPMC matrices. **Colloids and Surfaces B: Biointerfaces**, v. 111, p. 384–391, 2013.

BAG, P. P.; REDDY, C. M. Screening and selective preparation of polymorphs by fast evaporation method: a case study of aspirin, anthranilic acid, and niflumic acid. **Crystal Growth & Design**, v. 12, n. 6, p. 2740–2743, 2012.

BAIRD, J. A.; VAN EERDENBRUGH, B.; TAYLOR, L. S. A classification system to assess the crystallization tendency of organic molecules from undercooled melts. **Journal of pharmaceutical sciences**, v. 99, n. 9, p. 3787–3806, 2010.

BAKA, E.; COMER, J. E. A.; TAKÁCS-NOVÁK, K. Study of equilibrium solubility measurement by saturation shake-flask method using hydrochlorothiazide as model compound. **Journal of pharmaceutical and biomedical analysis**, v. 46, n. 2, p. 335–341, 2008.

BANNIGAN, P. *et al*. Investigation into the solid and solution properties of known and novel polymorphs of the antimicrobial molecule clofazimine. **Crystal Growth & Design**, v. 16, n. 12, p. 7240–7250, 2016.

BARCHIELLI, M. *et al*. Clinical pharmacokinetics of lercanidipine. **Journal of Cardiovascular Pharmacology**, v. 29, p. S1–S15, 1997.

BENNEMA, P. *et al*. Solubility of molecular crystals: Polymorphism in the light of solubility theory. **International journal of pharmaceutics**, v. 351, n. 1–2, p. 74–91, 2008.

BERNARDES, C. E. A Program for Calorimeter Control and Data Acquisition. **FCUL** Lisbon, 2016

BIRCH, M. *et al*. Towards a PAT-based strategy for crystallization development. **Organic Process Research & Development**, v. 9, n. 3, p. 360–364, 2005.

BOBROVS, R.; SETON, L.; ACTIŅŠ, A. Solvent-mediated phase transformation between two tegafur polymorphs in several solvents. **CrystEngComm**, v. 16, n. 46, p. 10581–10591, 2014.

BOBROVS, R.; SETON, L.; DEMPSTER, N. The reluctant polymorph: investigation into the effect of self-association on the solvent mediated phase transformation and nucleation of theophylline. **CrystEngComm**, v. 17, n. 28, p. 5237–5251, 2015.

BONFILIO, R. *et al*. A discriminating dissolution method for glimepiride polymorphs. **Journal of pharmaceutical sciences**, v. 101, n. 2, p. 794–804, 2012.

BONIFACIO, F. *et al*. New York, USA. **Novel crude and crystalline forms of lercanidipine hydrochloride**. Int. Cl. A61K 31/455 US 0192323 A1. USA, out. 2005. Available at: <https://patents.google.com/patent/US20050192323A1/en>. Accessed on Jul, 2019

BOROUJENI, H. C.; GHARIB, F. Thermodynamic study on solubility of deferiprone at different ionic strengths and various temperatures. **Monatshefte für Chemie-Chemical Monthly**, v. 147, n. 7, p. 1177–1181, 2016.

BOU-CHACRA, N. *et al*. Evolution of choice of solubility and dissolution media after two decades of biopharmaceutical classification system. **The AAPS journal**, v. 19, n. 4, p. 989–1001, 2017.

BOX, K. J. *et al*. Equilibrium versus kinetic measurements of aqueous solubility, and the ability of compounds to supersaturate in solution—a validation study. **Journal of pharmaceutical sciences**, v. 95, n. 6, p. 1298–1307, 2006.

BOYLE, P. D. **Growing crystals that will make your crystallographer happy**. Available at: <http://xray.chem.uwo.ca/crystal_growing/GrowXtal.html> Accessed on Jul, 2019

BRITTAIN, H. G. Thermodynamic vs. kinetic solubility: knowing which is which. **American Pharmaceutical Review**, v. 17, n. 3, p. 10–16, 2014.

BRUKER. General profile and structure analysis software for powder diffraction data. **Bruker AXS Inc.** Karlsruhe, Germany, 2000.

BRUKER. Program for empirical absorption correction of area detector data. **Bruker AXS Inc.** Madison, Wisconsin, USA, 2004.

BRUNAUER, S.; EMMETT, P. H.; TELLER, E. Adsorption of gases in multimolecular layers. **Journal of the American chemical society**, v. 60, n. 2, p. 309–319, 1938.

BURGER, A.; RAMBERGER, R. On the polymorphism of pharmaceuticals and other molecular crystals. II. **Microchimica Acta**, v. 72, n. 3–4, p. 273–316, 1979.

CENSI, R.; DI MARTINO, P. Polymorph impact on the bioavailability and stability of poorly soluble drugs. **Molecules**, v. 20, n. 10, p. 18759–18776, 2015.

CHADHA, R. *et al*. An insight into thermodynamic relationship between polymorphic forms of efavirenz. **Journal of Pharmacy & Pharmaceutical Sciences**, v. 15, n. 2, p. 234–251, 2012.

CHADHA, R. *et al*. Thermoanalytical and spectroscopic studies on different crystal forms of nevirapine. **Journal of thermal analysis and calorimetry**, v. 111, n. 3, p. 2133–2142, 2013.

CHAHIYAN, H.; GHARIB, F.; FARAJTABAR, A. Thermodynamic studies on solubility and protonation constant of acetaminophen at different ionic strengths and various temperatures. **Journal of Molecular Liquids**, v. 199, p. 137–142, 2014.

CHANG, R. *et al*. A new polymorphic form and polymorphic transformation of loratadine. **RSC Advances**, v. 6, n. 88, p. 85063–85073, 2016.

CHEN, J. *et al*. Pharmaceutical crystallization. **Crystal growth & design**, v. 11, n. 4, p. 887–895, 2011.

CHIENG, N.; RADES, T.; AALTONEN, J. An overview of recent studies on the analysis of pharmaceutical polymorphs. **Journal of pharmaceutical and biomedical analysis**, v. 55, n. 4, p. 618–644, 2011.

CHOQUESILLO-LAZARTE, D.; GARCÍA-RUIZ, J. M. Poly (ethylene) oxide for small-molecule crystal growth in gelled organic solvents. **Journal of applied crystallography**, v. 44, n. 1, p. 172–176, 2011.

COELHO, A. A. Whole-profile structure solution from powder diffraction data using simulated annealing. **Journal of Applied Crystallography**, v. 33, n. 3, p. 899–908, 2000.

COELHO, A. A. Indexing of powder diffraction patterns by iterative use of singular value decomposition. **Journal of Applied Crystallography**, v. 36, n. 1, p. 86–95, 2003.

COUNCIL OF EUROPE. European Directorate for the Quality of Medicines & HealthCare. European Pharmacopoeia Commission. **European Pharmacopoeia**. 7th ed. Strasbourg. 2011, v. 1, cp. 4, p. 489-494

COVACI, O. I. *et al*. Bringing new life into old drugs: a case study on nifuroxazide polymorphism. **CrystEngComm**, v. 19, n. 26, p. 3584–3591, 2017.

CRUZ-CABEZA, A. J.; REUTZEL-EDENS, S. M.; BERNSTEIN, J. Facts and fictions about polymorphism. **Chemical Society Reviews**, v. 44, n. 23, p. 8619–8635, 2015.

DETRICH, Á. *et al*. Polymorphic forms of bisoprolol fumarate. **Journal of Thermal Analysis and Calorimetry**, v. 135, n. 6, p. 3043–3055, 2019.

DOMINGOS, S. *et al*. New forms of old drugs: improving without changing. **Journal of Pharmacy and Pharmacology**, v. 67, n. 6, p. 830–846, 2015.

ELLIS, K. J.; MORRISON, J. F. Buffers of constant ionic strength for studying pH-dependent processes. **Methods in Enzymology**, v.87, p. 405–426, 1982.

ELVERSSON, J. *et al*. Droplet and particle size relationship and shell thickness of inhalable lactose particles during spray drying. **Journal of Pharmaceutical Sciences**, v. 92, n. 4, p. 900–910, 2003.

FARRUGIA, L. J. WinGX suite for small-molecule single-crystal crystallography. **Journal of Applied Crystallography**, v. 32, n. 4, p. 837–838, 1999.

FOOD AND DRUG ADMINISTRATION. **Guidance for Industry ANDAs: Pharmaceutical Solid Polymorphism Chemistry, Manufacturing, and Controls Information**. 2007. Available at: <https://www.fda.gov/media/71375/download> Accessed on Jul, 2019

FOOD AND DRUG ADMINISTRATION. **Waiver of In Vivo Bioavailability and Bioequivalence Studies for Immediate-Release Solid Oral Dosage Forms Based on a Biopharmaceutics Classification System Guidance for Industry**. 2015. Available at: <https://www.fda.gov/media/70963/download> Accessed on Jul, 2019

GARDNER, C. R. *et al*. Application of high throughput technologies to drug substance and drug product development. **Computers and Chemical Engineering**, v. 28, p. 943–953, 2004.

GE, Y.; LI, T.; CHENG, J. Crystal type I of Azilsartan polymorphs: preparation and analysis. **Journal of Crystallization Process and Technology**, v. 6, n. 01, p. 1, 2016.

GIRON, D. Thermal analysis and calorimetric methods in the characterisation of polymorphs and solvates. **Thermochimica acta**, v. 248, p. 1–59, 1995.

GOYAL, P.; RANI, D.; CHADHA, R. Exploring Structural Aspects of Nateglinide Polymorphs Using Powder X-Ray Diffraction. **International Journal of Pharmacy and Pharmaceutical Sciences**, v. 9, n. 10 SE-Original Article(s), 2017.

GU, C.-H. *et al*. Grouping solvents by statistical analysis of solvent property parameters: implication to polymorph screening. **International journal of pharmaceutics**, v. 283, n. 1–2, p. 117–125, 2004.

GUNN, E. *et al*. Polymorphism of nifedipine: crystal structure and reversible transition of the metastable β polymorph. **Crystal Growth & Design**, v. 12, n. 4, p. 2037–2043, 2012.

HAISA, M. *et al*. The monoclinic form of p-hydroxyacetanilide. **Acta Crystallographica Section B: Structural Crystallography and Crystal Chemistry**, v. 32, n. 4, p. 1283–1285, 1976.

HAMED, R. *et al*. pH-dependent solubility and dissolution behavior of carvedilol—case example of a weakly basic BCS class II drug. **AAPS PharmSciTech**, v. 17, n. 2, p. 418–426, 2016.

HANEEF, J. *et al*. Novel polymorph of ambrisentan: Characterization and stability. **Journal of pharmaceutical and biomedical analysis**, v. 153, p. 102–109, 2018.

HILFIKER, R.; BLATTER, F; MARKUS, V. O. N. Relevance of Solid-state Properties for Pharmaceutical Products. In: HILFIKER, R. (Ed.) **Polymorphism in the pharmaceutical industry**. 2nd ed. Weinheim: Wiley-Vch, 2006, cp. 1, p. 1-17.

HONORATO, S. B. *et al*. Novel polymorphs of the anti-Trypanosoma cruzi drug benznidazole. **Spectrochimica Acta Part A: Molecular and Biomolecular Spectroscopy**, v. 118, p. 389–394, 2014.

HULLIGER, J. Chemistry and crystal growth. **Angewandte Chemie International Edition in English**, v. 33, n. 2, p. 143–162, 1994.

JIA, L. *et al*. Polymorphs of daidzein and intermolecular interaction effect on solution crystallization. **CrystEngComm**, v. 19, n. 47, p. 7146–7153, 2017.

JIANG, H.; KLOC, C. Single-crystal growth of organic semiconductors. **MRS bulletin**, v. 38, n. 1, p. 28–33, 2013.

JIN, M. R.; SOHN, Y. T. Crystal Form of Celecoxib: Preparation, Characterization and Dissolution. **Journal of the Korean Chemical Society**, v. 62, n. 5, p. 352–357, 2018.

JONES, P. G. Crystal growing. **Chemistry in Britain**, v. 17, n. 5, p. 222–225, 1981.

JOSEPH, A. *et al*. Tautomer selection through solvate formation: the case of 5-hydroxynicotinic acid. **CrystEngComm**, 2019.

KAVANAGH, A. *et al*. Developing Amorphous Pharmaceuticals: Opportunity and Necessity. **American pharmaceutical review**, v. 15, n. 5, p. 10, 2012.

KRIVANKOVA, I.; MARCISINOVA, M.; SOHNEL, O. Solubility of itaconic and kojic acids. **Journal of Chemical and Engineering Data**, v. 37, n. 1, p. 23–24, 1992.

ŁASZCZ, M. *et al*. Structural and physicochemical studies of olopatadine hydrochloride conformational polymorphs. **Journal of pharmaceutical sciences**, v. 105, n. 8, p. 2419–2426, 2016.

LEE, A. Y.; ERDEMIR, D.; MYERSON, A. S. Crystal polymorphism in chemical process development. **Annual review of chemical and biomolecular engineering**, v. 2, p. 259–280, 2011.

LEE, E. H. A practical guide to pharmaceutical polymorph screening & selection. **Asian Journal of Pharmaceutical Sciences**, v. 9, n. 4, p. 163–175, 2014.

LI, J. *et al*. Polymorphism of the antitubercular isoxyl. **Crystal Growth & Design**, v. 11, n. 11, p. 4950–4957, 2011.

LI, S. *et al*. Investigation of solubility and dissolution of a free base and two different salt forms as a function of pH. **Pharmaceutical research**, v. 22, n. 4, p. 628–635, 2005.

MACRAE, C. F. *et al*. Mercury CSD 2.0–new features for the visualization and investigation of crystal structures. **Journal of Applied Crystallography**, v. 41, n. 2, p. 466–470, 2008.

MAHLIN, D.; BERGSTRÖM, C. A. S. Early drug development predictions of glass-forming ability and physical stability of drugs. **European Journal of Pharmaceutical Sciences**, v. 49, n. 2, p. 323–332, 2013.

MAUGER, J. W. Physicochemical properties of buffers used in simulated biological fluids with potential application for in vitro dissolution testing: a mini-review. **Dissolution Technologies**, v. 24, n. 3, p. 38–51, 2017.

MCCRONE, W. C. Polymorphism. In: FOX, D., LABES, M.M., and WEISSBERGER, A. (Eds.) **Physics and chemistry of the organic solid state**. New York: Wiley-Interscience, 1965, v. 2, cp. 8, p. 725–767.

MIHALJICA, S.; RADULOVIĆ, D.; TRBOJEVIĆ, J. Determination of lercanidipine hydrochloride and its impurities in tablets. **Chromatographia**, v. 61, n. 1–2, p. 25–29, 2005.

MORENO, A.; MENDOZA, M. E. Crystallization in Gels. In NISHINAGA, T; RUDOLPH, P. (Eds.) **Handbook of Crystal Growth**. Amsterdam: Elsevier, 2015, v. 2, p. 1277–1315.

MORISSETTE, S. L. *et al*. High-throughput crystallization: polymorphs, salts, co-crystals and solvates of pharmaceutical solids. **Advanced drug delivery reviews**, v. 56, n. 3, p. 275–300, 2004.

MUKHERJEE, A. Building upon supramolecular synthons: some aspects of crystal engineering. **Crystal Growth & Design**, v. 15, n. 6, p. 3076–3085, 2015.

MUNROE, A. *et al*. Solution-mediated polymorphic transformation of FV sulphathiazole. **Crystal Growth & Design**, v. 14, n. 7, p. 3466–3471, 2014.

NANGIA, A. Conformational polymorphism in organic crystals. **Accounts of chemical research**, v. 41, n. 5, p. 595–604, 2008.

NATIONAL CENTER FOR BIOTECHNOLOGY INFORMATION. PubChem Database. **Lercanidipine hydrochloride**, CID=157917. Available at: <https://pubchem.ncbi.nlm.nih.gov/compound/Lercanidipine-hydrochloride>. Accessed on Jul, 2019.

NEGLUR, R. *et al*. Water and the relationship to the crystal structure stability of azithromycin. **Journal of Thermal Analysis and Calorimetry**, v. 132, n. 1, p. 373–384, 2018.

NEWMAN, A. Specialized solid form screening techniques. **Organic Process Research & Development**, v. 17, n. 3, p. 457–471, 2012.

NEWMAN, A. W.; BYRN, S. R. Solid-state analysis of the active pharmaceutical ingredient in drug products. **Drug discovery today**, v. 8, n. 19, p. 898–905, 2003.

NOONAN, T. J. *et al*. Polymorphism of the antiviral agent clevudine. **CrystEngComm**, v. 18, n. 42, p. 8172–8181, 2016.

OMAR, M.; MAKARY, P.; WLODARSKI, M. A review of polymorphism and the amorphous state in the formulation strategy of medicines and marketed drugs. **UK Journal of Pharmaceutical and Biosciences**, v. 3, n. 60, 2015.

OTSUKA, M. *et al*. Developmental considerations for ethanolates with regard to stability and physicochemical characterization of efonidipine hydrochloride ethanolate. **CrystEngComm**, v. 17, n. 38, p. 7430–7436, 2015.

PATEL, J. *et al*. Characterization and thermodynamic relationship of three polymorphs of a xanthine oxidase inhibitor, Febuxostat. **Journal of pharmaceutical sciences**, v. 104, n. 11, p. 3722–3730, 2015.

PAWLEY, G. S. Unit-cell refinement from powder diffraction scans. **Journal of Applied Crystallography**, v. 14, n. 6, p. 357–361, 1981.

PUDIPEDDI, M.; SERAJUDDIN, A. T. M. Trends in solubility of polymorphs. **Journal of pharmaceutical sciences**, v. 94, n. 5, p. 929–939, 2005.

QI, M.-H. *et al*. Estimating thermodynamic stability relationship of polymorphs of sofosbuvir. **Crystal Growth & Design**, v. 15, n. 10, p. 5062–5067, 2015.

RANI, S.; PARGAL, A. Bioequivalence: An overview of statistical concepts. **Indian Journal of Pharmacology**, v. 36, p. 209–216, 2004.

RENUKA, S. S. K. *et al*. Polymorph control: success so far and future expectations. **Int J PharmTech Res**, v. 9, p. 144–165, 2016.

RIEKES, M. *et al*. Development and validation of an intrinsic dissolution method for nimodipine polymorphs. **Open Chemistry**, v. 12, n. 5, p. 549–556, 2014.

RODRÍGUEZ-SPONG, B. *et al*. General principles of pharmaceutical solid polymorphism: a supramolecular perspective. **Advanced drug delivery reviews**, v. 56, n. 3, p. 241–274, 2004.

SAINI, A. *et al*. New conformational polymorph of hydrochlorothiazide with improved solubility. **Pharmaceutical development and technology**, v. 21, n. 5, p. 611–618, 2016.

SAINT, M. Area-Detector Integration Software.(version 7.23) Brukee AXS Inc. **Madison, WI**, 2004.

SHELDRICK, G. M. A short history of SHELX. **Acta Crystallographica Section A: Foundations of Crystallography**, v. 64, n. 1, p. 112–122, 2008.

SHELDRICK, G. M. Crystal structure refinement with SHELXL. **Acta Crystallographica Section C: Structural Chemistry**, v. 71, n. 1, p. 3–8, 2015.

SINGH, P.; CHADHA, R. A new polymorph of ciprofloxacin saccharinate: Structural characterization and pharmaceutical profile. **Journal of pharmaceutical and biomedical analysis**, v. 146, p. 7–14, 2017.

SOUZA, J. B. *et al*. Evaluation of the losartan solubility in the biowaiver context by shake-flask method and intrinsic dissolution. **Pharmaceutical development and technology**, v. 24, n. 3, p. 283–292, 2019.

SPEK, A. L. Structure validation in chemical crystallography. **Acta Crystallographica Section D: Biological Crystallography**, v. 65, n. 2, p. 148–155, 2009.

SPINGLER, B. *et al*. Some thoughts about the single crystal growth of small molecules. **CrystEngComm**, v. 14, n. 3, p. 751–757, 2012.

STOREY, R. A “roadmap” to solid form selection. In: STOREY, R. A.; YMEN, I., (Eds.) **Solid State Characterization of Pharmaceuticals**. Chichester, UK: John Wiley & Sons, 2011, p-473-491.

STRENG, W. H. *et al*. General treatment of pH–solubility profiles of weak acids and bases and the effects of different acids on the solubility of a weak base. **Journal of pharmaceutical sciences**, v. 73, n. 12, p. 1679–1684, 1984.

SUBRAMANIAN, L. *et al*. Preparation, Characteristic Evaluation and Dissolution Enhancement of Amlodipine Besylate by Polymorphism Technique. v. 6, n. 10, p. 1456–1465, 2017.

SUN, Y. *et al*. Stability of amorphous pharmaceutical solids: crystal growth mechanisms and effect of polymer additives. **The AAPS journal**, v. 14, n. 3, p. 380–388, 2012.

SUN, Z. *et al*. Thermodynamic properties of form A and form B of florfenicol. **Industrial & Engineering Chemistry Research**, v. 53, n. 34, p. 13506–13512, 2014.

SURESH, K. *et al*. Polymorphism, isostructurality and physicochemical properties of glibenclamide salts. **CrystEngComm**, v. 19, n. 6, p. 918–929, 2017.

SUROV, A. O. *et al*. Crystallization and polymorphism of felodipine. **Crystal Growth & Design**, v. 12, n. 8, p. 4022–4030, 2012.

TAO, M. *et al*. Determination of the solubility, dissolution enthalpy, and entropy of pioglitazone hydrochloride (form II) in different pure solvents. **Industrial & Engineering Chemistry Research**, v. 52, n. 8, p. 3036–3041, 2013.

TATUM, N. **Crystallographic Studies for Structure-Based Drug Design**. 2012. Thesis (Master of Science) - School of Biological and Biomedical Sciences, Durham University, Durham

THABET, Y.; KLINGMANN, V.; BREITKREUTZ, J. Drug formulations: Standards and novel strategies for drug administration in pediatrics. **The Journal of Clinical Pharmacology**, v. 58, p. S26–S35, 2018.

VAN DER SLUIS, P.; HEZEMANS, A. M. F.; KROON, J. Crystallization of low-molecular-weight organic compounds for X-ray crystallography. **Journal of applied crystallography**, v. 22, n. 4, p. 340–344, 1989.

VARIANKAVAL, N. *et al*. High-Throughput Screening to Enable Salt and Polymorph Screening. In: MOLANDER, G. A. (ed.) **Comprehensive Organic Synthesis II**. 2nd ed. Amsterdam: Elsevier, 2014. p. 207-233.

VEGA, D. R. *et al*. A New, More Stable Polymorphic Form of Otilonium Bromide: Solubility, Crystal Structure, and Phase Transformation. **Journal of Pharmaceutical Sciences**, v. 105, n. 10, p. 3013–3020, 2016.

VISHWESHWAR, P. *et al*. Pharmaceutical co-crystals. **Journal of pharmaceutical sciences**, v. 95, n. 3, p. 499–516, 2006.

VÖLGYI, G. *et al*. Study of pH-dependent solubility of organic bases. Revisit of Henderson-Hasselbalch relationship. **Analytica chimica acta**, v. 673, n. 1, p. 40–46, 2010.

WANG, C. *et al*. Solubilities of 3-chlorophthalic anhydride and 4-chlorophthalic anhydride in different pure solvents. **Journal of Chemical & Engineering Data**, v. 60, n. 10, p. 3053–3061, 2015.

WANG, N.; FU, Q.; YANG, G. Determination of the solubility, dissolution enthalpy and entropy of icariin in water, ethanol, and methanol. **Fluid Phase Equilibria**, v. 324, p. 41–43, 2012.

XIONG, X. *et al*. Solvates and polymorphs of rebamipide: preparation, characterization, and physicochemical analysis. **RSC Advances**, v. 7, n. 38, p. 23279–23286, 2017.

XU, D.; REDMAN-FUREY, N. Statistical cluster analysis of pharmaceutical solvents. **International journal of pharmaceutics**, v. 339, n. 1–2, p. 175–188, 2007.

XU, K. *et al*. A new polymorph of glipizide with enhanced properties obtained using environmentally friendly methods. **CrystEngComm**, v. 18, n. 24, p. 4508–4512, 2016.

XU, L. *et al*. Preparation and characterization of a novel polymorph of indiplon, Form α. **Bioorganic & medicinal chemistry letters**, v. 22, n. 2, p. 963–968, 2012.

YU, L. Inferring thermodynamic stability relationship of polymorphs from melting data. **Journal of pharmaceutical sciences**, v. 84, n. 8, p. 966–974, 1995.

YU, L.; REUTZEL-EDENS, S. M.; MITCHELL, C. A. Crystallization and polymorphism of conformationally flexible molecules: Problems, patterns, and strategies. **Organic Process Research & Development**, v. 4, n. 5, p. 396–402, 2000.

ZANOLLA, D. *et al*. A new soluble and bioactive polymorph of praziquantel. **European Journal of Pharmaceutics and Biopharmaceutics**, v. 127, p. 19–28, 2018.

ZEIDAN, T. A. *et al*. Structural Diversity of Brexpiprazole and Related Analogues: Impact on Solubility and Drug Delivery. **Crystal Growth & Design**, v. 18, n. 4, p. 2326–2334, 2018.

ZHANG, J. *et al*. Characterization of two polymorphs of lornoxicam. **Journal of Pharmacy and Pharmacology**, v. 65, n. 1, p. 44–52, 2013.

ZHANG, P. *et al*. Measurement and Correlation of the Solubility of Florfenicol Form A in Several Pure and Binary Solvents. **Journal of Chemical & Engineering Data**, v. 63, n. 6, p. 2046–2055, 2018a.

ZHANG, T. *et al*. Confirmation of More Stable Polymorphic Form of Etoricoxib at Room Temperature. **Journal of pharmaceutical sciences**, v. 107, n. 7, p. 1903–1910, 2018b.

ZHANG, W.-P.; CHEN, D.-Y. Crystal structures and physicochemical properties of amisulpride polymorphs. **Journal of pharmaceutical and biomedical analysis**, v. 140, p. 252–257, 2017.

ZHOU, M. *et al*. A new polymorphic form of metoprolol succinate. **Pharmaceutical development and technology**, v. 22, n. 1, p. 58–62, 2017.

ZHOU, X. *et al*. Polymorphism of flucloxacillin sodium. **Die Pharmazie-An International Journal of Pharmaceutical Sciences**, v. 66, n. 12, p. 933–935, 2011.

ZHU, B.; WANG, J.-R.; MEI, X. Insight into the phase transformation among various solid forms of baicalein. **Crystal Growth & Design**, v. 15, n. 10, p. 4959–4968, 2015.

ATTACHMENTS

Attachment A. pH buffer solution preparation for shake-flask solubility (COUNCIL OF EUROPE, 2011)

pH 1.2 chloride buffer solution

0.4 g sodium chloride was dissolved in 150 mL ultra-purified osmotic water; consistently, 1.2 mL hydrochloric acid was added. The pH was adjusted by addition of 0.5 mL with molarity 0.2 M sodium hydroxide and diluted with water up to 200 mL.

pH 2.0 chloride buffer solution

1.31 g potassium chloride was dissolved in 150 mL ultra-purified osmotic water; consistently 23.8 mL with molarity 0.1 M hydrochloric acid was added. The pH was adjusted by addition of 0.5 mL with molarity 0.2 M hydrochloric acid and diluted with water up to 200 mL.

pH 2.0 phosphate buffer solution

1.79 g disodium hydrogen phosphate and 0.68 g potassium dihydrogen phosphate were dissolved in 150 mL ultra-purified osmotic water. The pH was adjusted by addition of 3 mL o-phosphoric acid and diluted with water up to 200 mL.

pH 2.5 phosphate buffer solution

1.56 g sodium dihydrogen phosphate was dissolved in 150 mL ultra-purified osmotic water. The pH was adjusted by addition of 0.4 mL o-phosphoric acid and diluted with water up to 200 mL.

pH 3.0 phosphate buffer solution 0.1 M

2.40 g sodium dihydrogen phosphate was dissolved in 150 mL ultra-purified osmotic water. The pH was adjusted by addition of 0.2 mL o-phosphoric acid and diluted with water up to 200 mL.

pH 3.0 phosphate buffer solution 1.0 M

12 g sodium dihydrogen phosphate was dissolved in 80 mL ultra-purified osmotic water. The pH was adjusted by addition of 0.7 mL o-phosphoric acid and diluted with water up to 100 mL.

pH 3.0 phosphate buffer solution 0.01 M

0.6 g sodium dihydrogen phosphate was dissolved in 450 mL ultra-purified osmotic water. The pH was adjusted by addition of 0.04 mL o-phosphoric acid and diluted with water up to 50 mL.

pH 3.0 citric buffer solution 0.1 M

0.543 g sodium citrate and 3.487 g citric acid were dissolved in 150 mL ultra-purified osmotic water. The pH was adjusted by addition of 35 mL with molarity 0.2 M sodium hydroxide and diluted with water up to 200 mL.

pH 3.0 citric buffer solution 1.0 M

2.71 g sodium citrate and 17.44 g citric acid were dissolved in 50 mL ultra-purified osmotic water. The pH was adjusted by addition of 45 mL with molarity 1.0 M sodium hydroxide and diluted with water up to 100 mL.

pH 3.0 citric buffer solution 0.01 M

0.136 g sodium citrate and 0.872 g citric acid were dissolved in 450 mL ultra-purified osmotic water. The pH was adjusted by addition of 3 mL with molarity 0.2 M sodium hydroxide and diluted with water up to 500 mL.

pH 3.5 citric buffer solution

1.255 g sodium citrate and 3.022 g citric acid were dissolved in 150 mL ultra-purified osmotic water. pH was adjusted by addition of 24 mL with molarity 0.2 M sodium hydroxide and diluted with water up to 200 mL.

pH 4.0 citric buffer solution

1.969 g sodium citrate and 2.556 g citric acid were dissolved in 150 mL ultra-purified osmotic water. The pH was adjusted by addition of 21 mL with molarity 0.2 M sodium hydroxide and diluted with water up to 200 mL.

pH 4.5 acetate buffer solution

0.738 g sodium acetate was dissolved in 150 mL ultra-purified osmotic water; consistently 0.63 mL (0.66 g) glacial acetic acid was added. The Adjustment of pH was not necessary, and the solution was diluted with water up to 200 mL.

Attacment B Crystallization results

Table 17 – The cooling crystallization results

Solvent	Concentration $mg \cdot mL^{-1}$	Observation	Form
Methanol	1000	Clear solution after cooling	n/a
Toluene	2	Have not dissolved (antisolvent candidate)	n/a
Ethyl acetate	3	Clear solution after cooling (antisolvent candidate)	n/a
Acetone	25	Clear solution after cooling	n/a
THF	7	Clear solution after cooling	n/a
2-Propanol	40	Clear solution after cooling	n/a
Ethanol	115	Clear solution after cooling	n/a
Benzyl alcohol	500	Clear solution after cooling	n/a
Isobutanol	150	Clear solution after cooling	n/a
Diethyl ether	2	Have not dissolved antisolvent candidate	n/a
1,4-Dioxane	3	Clear solution after cooling, antisolvent candidate	n/a
MEK	15	Clear solution after cooling	n/a
Chloroform	250	Clear solution after cooling	n/a
Dichloromethane	200	Clear solution after cooling	n/a
1,2-Dichloroethane	250	Clear solution after cooling	n/a
Hexane	2	Have not dissolved antisolvent candidate	n/a
Dimethylformamide	500	Clear solution after cooling	n/a
Dimethyl Sulfoxide	500	Clear solution after cooling	n/a
Acetonitrile	150	Clear solution after cooling	n/a
Anisole	2	Clear solution after cooling, antisolvent candidate	n/a
Pyridine	300	Clear solution after cooling	n/a

Table 18 – The evaporation crystallization results

Solvent	**Concentration mg·mL^{-1}**	**Observation**	**Form**
		Evaporation from single solvent	
Methanol	200	Viscous amorphous mass	n/a
Acetone	25	Viscous amorphous mass	n/a
2-Propanol	40	Crystals obtained on the walls and bottom of vial	
Ethanol	100	Viscous amorphous mass	n/a
Isobutanol	150	Viscous amorphous mass	n/a
MEK	15	Crystals obtained on the walls and bottom of vial	
Dichloromethane	150	Crystals obtained in volume of solution	I
1,2-Dichloroethane	250	Crystals obtained in volume of solution	I
Acetonitrile	100	Viscous amorphous mass	n/a
Acetone	25	Viscousus amorphous mass	n/a
		Evaporation from solvent mixture	
Dichloromethane/Dioxane (v/v=1/5)	40	Crystals obtained in volume of solution	I
Dichloromethane/Anisole (v/v=1/5)	40	Crystals obtained in volume of solution	I
Dichloromethane/THF (v/v=1/5)	40	Crystals obtained in volume of solution	I
Methanol/THF (v/v=1/5)	40	Viscous amorphous mass	n/a
Methanol/Dioxane (v/v=1/5)	40	Viscous amorphous mass	n/a
Methanol/MEK (v/v=1/5)	40	Viscous amorphous mass	n/a
Methanol/Anisole (v/v=1/5)	40	Viscous amorphous mass	n/a

Table 19 – The antisolvent crystallization results

Solvent	**Concentration mg·mL^{-1}**	**Observation**	**Form**
Dichloromethane /Toluene	150	Crystals obtained in volume of solution	I
Methanol/Ethyl Acetate	100	Crystals obtained in volume of solution	II
Ethanol/Water	125	Crystals obtained in volume of solution	II
2-Propanol/Water	150	Crystals obtained in volume of solution	II
Methanol/Water	200	Crystals obtained in volume of solution	II
Dichloroethane /Toluene	200	Crystals obtained in volume of solution	I
Dichloromethane/Hexane	150	Crystals obtained in volume of solution	amorf
Dichloroethane / Hexane	200	Crystals obtained in volume of solution	I
Dichloromethane /Toluene	150	Crystals obtained in volume of solution	I
Methanol/Anisole	27	Crystals obtained in volume of solution	I
Chloroform/Anisole	27	Crystals obtained in volume of solution	I
Chloroform/THF	27	Crystals obtained in volume of solution	I
Chloroform/Dioxane	27	Crystals obtained in volume of solution	I
Methanol/N-buthyl acetate	90	Crystals obtained in volume of solution	II
Methanol /Dioxane	90	Crystals obtained in volume of solution	I
Benzyl alcohol/Diethyl ether	90	Crystals obtained in volume of solution	I
MEK/ Hexane	15	Crystals obtained in volume of solution	amorf
Benzyl alcohol/Dioxane	90	Crystals obtained in volume of solution	I
Benzyl alcohol/Diethyl Ether	90	Crystals obtained in volume of solution	I
Benzyl alcohol/N-buthyl acetate	90	Crystals obtained in volume of solution	I
Dimethylformamide (DMF)/Dioxane	90	Crystals obtained in volume of solution	I
DMF/N-buthyl acetate	90	Crystals obtained in volume of solution	I
DMA/Dioxane	90	Crystals obtained in volume of solution	II
DMA/N-buthyl acetate	90	Crystals obtained in volume of solution	II
Pyridine/Dioxane	90	Crystals obtained in volume of solution	I
Pyridine/Anisole	90	Crystals obtained in volume of solution	I
Chloroform/Dioxane	90	Crystals obtained in volume of solution	I
Chloroform/Anisole	90	Crystals obtained in volume of solution	I
Chloroform / N-buthyl acetate	90	Crystals obtained in volume of solution	I

Attacment C Certificate of participation

UNIVERSIDADE DE SÃO PAULO
Faculdade de Ciências Farmacêuticas

LIII SUPFAI

XXIII SEMANA FARMACÊUTICA DE CIÊNCIA E TECNOLOGIA
LIII Semana Universitária Paulista de Farmácia e Bioquímica
X Simpósio Anual de Pesquisas em Ciências Farmacêuticas
XVIII Campanha de Diabetes

CERTIFICADO

Certificamos que **ILIA ALEKSEEVICH REPIN** apresentou o trabalho "POLYMORPH SCREENING AND SOLUBILITY CHARACTERISATION OF LERCANIDIPINE HCL", de autoria de ILIA ALEKSEEVICH REPIN (M)*, HUMBERTO GOMES FERRAZ*, SELMA GUTIERREZ ANTONIO**, GABRIEL LIMA BARROS DE ARAUJO, em forma de pôster, durante a XXIII Semana Farmacêutica de Ciência e Tecnologia, realizada no período de 22 a 31 de outubro de 2018.

São Paulo, 26 de outubro de 2018.

Profa. Dra. Jeanine Giarolla Vargas
Presidente da Comissão de Avaliação de Pôsteres

Prof. Dr. Joilson de Oliveira Martins
Presidente da Comissão Organizadora

Attacment D Ficha de aluno

Janus - Sistema Administrativo da Pós-Graduação

Universidade de São Paulo
Faculdade de Ciências Farmacêuticas
Documento sem validade oficial
FICHA DO ALUNO

9139 - 10121202/1 - Ilia Alekseevich Repin

Email:	repinily@usp.br
Data de Nascimento:	22/07/1986
Cédula de Identidade:	RNE - G131721-S - DF
Local de Nascimento:	Rússia
Nacionalidade:	Russa
Graduação:	Engenheiro - Saint Petersburg State Institute of Technology - Rússia - 2009

Curso:	Mestrado
Programa:	Fármaco e Medicamentos
Área:	Produção e Controle Farmacêuticos
Data de Matrícula:	06/02/2017
Início da Contagem de Prazo:	06/02/2017
Data Limite para o Depósito:	06/08/2019
Orientador:	Prof(a). Dr(a). Humberto Gomes Ferraz - 06/02/2017 até 06/03/2018. Email: sferraz@usp.br
Orientador:	Prof(a). Dr(a). Gabriel Lima Barros de Araujo - 07/03/2018 até o presente. Email: gabriel.araujo@usp.br
Proficiência em Línguas:	Inglês, Aprovado em 06/02/2017 Português, Aprovado em 25/04/2018
Data de Aprovação no Exame de Qualificação:	Aprovado em 22/03/2018
Data do Depósito do Trabalho:	
Título do Trabalho:	
Data Máxima para Aprovação da Banca:	
Data de Aprovação da Banca:	
Data Máxima para Defesa:	
Data da Defesa:	
Resultado da Defesa:	
Histórico de Ocorrências:	Primeira Matrícula em 06/02/2017

Janus - Sistema Administrativo da Pós-Graduação

Universidade de São Paulo
Faculdade de Ciências Farmacêuticas
Documento sem validade oficial
FICHA DO ALUNO

9139 - 10121202/1 - Ilia Alekseevich Repin

Sigla	Nome da Disciplina	Início	Término	Carga Horária	Cred.	Freq.	Conc.	Exc.	Situação
FBF5704-6/5	Análise Espectrométrica de Fármacos	06/03/2017	18/06/2017	150	10	100	A	N	Concluída
FBF5751-8/1	Introdução aos Métodos Termoanalíticos	29/08/2017	09/11/2017	150	10	90	A	N	Concluída
FBF5805-2/5	Delineamento de Experimentos e Ferramentas Estatísticas Aplicadas às Ciências Farmacêuticas	06/02/2018	16/04/2018	90	6	100	A	N	Concluída
FBF5800-2/2	Patentes em Fármaco e Medicamentos	15/03/2018	16/05/2018	45	3	100	A	N	Concluída
FBA5728-4/6	Aprimoramento Pedagógico	03/04/2018	30/04/2018	60	0	-	-	N	Pré-matrícula indeferida
FBF5777-4/1	Tópicos Gerais de Fármacos e Medicamentos	02/08/2018	14/11/2018	45	3	77	B	N	Concluída
QFL5925-6/6	Prática de Ensino de Química (Instituto de Química - Universidade de São Paulo)	21/08/2018	03/12/2018	45	0	-	-	N	Matrícula cancelada
FBF5821-1/4	Tópicos Avançados em Fármaco e Medicamentos (Avanços e Desafios no Desenvolvimento de Sistemas Nanoestruturados para a Liberação Modificada de Fármacos)	03/09/2018	16/09/2018	30	2	100	A	N	Concluída
FBA5728-4/7	Aprimoramento Pedagógico	02/10/2018	29/10/2018	60	4	100	A	N	Concluída
FBF5837-1/1	Tecnologia do estado-sólido na indústria farmacêutica	31/01/2019	06/02/2019	30	2	100	A	N	Concluída

	Créditos mínimos exigidos		Créditos obtidos
	Para exame de qualificação	Para depósito da dissertação	
Disciplinas:	0	25	40
Estágios:			
Total:	0	25	40

Créditos Atribuídos à Dissertação: 71

Conceito a partir de 02/01/1997:

A - Excelente, com direito a crédito; B - Bom, com direito a crédito; C - Regular, com direito a crédito; R - Reprovado; T - Transferência.

Um(1) crédito equivale a 15 horas de atividade programada.

Janus - Sistema Administrativo da Pós-Graduação

Universidade de São Paulo
Faculdade de Ciências Farmacêuticas
Documento sem validade oficial
FICHA DO ALUNO

9139 - 10121202/1 - Ilia Alekseevich Repin

Comissão julgadora da dissertação de mestrado:

NUSP	Nome	Vínculo	Função
3127038	Gabriel Lima Barros de Araujo	FCF - USP	Presidente

Attacment E - Copyrights for reproduction

Copyright Clearance Center RightsLink®

Home Create Account Help LIVE CHAT

ACS Publications Most Trusted. Most Cited. Most Read.

Title: Conformational Polymorphism in Organic Crystals
Author: Ashwini Nangia
Publication: Accounts of Chemical Research
Publisher: American Chemical Society
Date: May 1, 2008

LOGIN

If you're a copyright.com user, you can login to RightsLink using your copyright.com credentials.

Already **a RightsLink user** or want to learn more?

PERMISSION/LICENSE IS GRANTED FOR YOUR ORDER AT NO CHARGE

This type of permission/license, instead of the standard Terms & Conditions, is sent to you because no fee is being charged for your order. Please note the following:

- Permission is granted for your request in both print and electronic formats, and translations.
- If figures and/or tables were requested, they may be adapted or used in part.
- Please print this page for your records and send a copy of it to your publisher/graduate school.
- Appropriate credit for the requested material should be given as follows: "Reprinted (adapted) with permission from (COMPLETE REFERENCE CITATION). Copyright (YEAR) American Chemical Society." Insert appropriate information in place of the capitalized words.
- One-time permission is granted only for the use specified in your request. No additional uses are granted (such as derivative works or other editions). For any other uses, please submit a new request.

If credit is given to another source for the material you requested, permission must be obtained from that source.

BACK CLOSE WINDOW

ACS Publications
Most Trusted. Most Cited. Most Read.

Title: Polymorphs, Salts, and Cocrystals: What's in a Name?
Author: Srinivasulu Aitipamula, Rahul Banerjee, Arvind K. Bansal, et al
Publication: Crystal Growth and Design
Publisher: American Chemical Society
Date: May 1, 2012

PERMISSION/LICENSE IS GRANTED FOR YOUR ORDER AT NO CHARGE

This type of permission/license, instead of the standard Terms & Conditions, is sent to you because no fee is being charged for your order. Please note the following:

- Permission is granted for your request in both print and electronic formats, and translations.
- If figures and/or tables were requested, they may be adapted or used in part.
- Please print this page for your records and send a copy of it to your publisher/graduate school.
- Appropriate credit for the requested material should be given as follows: "Reprinted (adapted) with permission from (COMPLETE REFERENCE CITATION). Copyright (YEAR) American Chemical Society." Insert appropriate information in place of the capitalized words.
- One-time permission is granted only for the use specified in your request. No additional uses are granted (such as derivative works or other editions). For any other uses, please submit a new request.

If credit is given to another source for the material you requested, permission must be obtained from that source.

BACK CLOSE WINDOW

ELSEVIER LICENSE
TERMS AND CONDITIONS

Jul 09, 2019

This Agreement between Mr. ILIA REPIN ("You") and Elsevier ("Elsevier") consists of your license details and the terms and conditions provided by Elsevier and Copyright Clearance Center.

License Number	4624891258916
License date	Jul 09, 2019
Licensed Content Publisher	Elsevier
Licensed Content Publication	European Journal of Pharmaceutics and Biopharmaceutics
Licensed Content Title	Solid form screening – A review
Licensed Content Author	Jaakko Aaltonen,Morten Allesø,Sabiruddin Mirza,Vishal Koradia,Keith C. Gordon,Jukka Rantanen
Licensed Content Date	Jan 1, 2009
Licensed Content Volume	71
Licensed Content Issue	1
Licensed Content Pages	15
Start Page	23
End Page	37
Type of Use	reuse in a thesis/dissertation
Portion	figures/tables/illustrations
Number of figures/tables/illustrations	1
Format	both print and electronic
Are you the author of this Elsevier article?	No
Will you be translating?	No
Original figure numbers	Table 1
Title of your thesis/dissertation	Polymorph screening and solubility characterisation of lercanidipine HCl
Expected completion date	Aug 2019
Estimated size (number of pages)	100
Requestor Location	Mr. ILIA REPIN Avenida General Valdomiro de Lima, 642 São Paulo, São Paulo 04344-070 Brazil Attn: Mr. ILIA REPIN
Publisher Tax ID	GB 494 6272 12
Total	0.00 USD
Terms and Conditions	

INTRODUCTION

1. The publisher for this copyrighted material is Elsevier. By clicking "accept" in connection with completing this licensing transaction, you agree that the following terms and conditions apply to this transaction (along with the Billing and Payment terms and conditions

Copyright Clearance Center

Confirmation Number: 11830349
Order Date: 07/09/2019

Customer Information

Customer: ILIA REPIN
Account Number: 3001481341
Organization: ILIA REPIN
Email: repinily@usp.br
Phone: +55 (11)942698020
Payment Method: Invoice

This is not an invoice

Order Details

Chemical Society reviews

Billing Status: **N/A**

Order detail ID:	71941243
ISSN:	1460-4744
Publication Type:	e-Journal
Volume:	
Issue:	
Start page:	
Publisher:	ROYAL SOCIETY OF CHEMISTRY
Author/Editor:	Royal Society of Chemistry (Great Britain)

Permission Status: **Granted**

Permission type: Republish or display content
Type of use: Thesis/Dissertation
Order License Id: 4624900997987

Requestor type	Not-for-profit entity
Format	Print, Electronic
Portion	chart/graph/table/figure
Number of charts/graphs/tables/figures	5
The requesting person/organization	Ilia Alekseevih Repin
Title or numeric reference of the portion(s)	Figure 5
Title of the article or chapter the portion is from	Facts and fictions about polymorphism
Editor of portion(s)	N/A
Author of portion(s)	N/A
Volume of serial or monograph	N/A
Page range of portion	8619-8635
Publication date of portion	2015
Rights for	Main product
Duration of use	Current edition and up to 5 years
Creation of copies for the disabled	no
With minor editing privileges	yes
For distribution to	Worldwide
In the following language(s)	Original language of publication
With incidental promotional use	no
Lifetime unit quantity of new product	Up to 499
Title	Polymorph screening and solubility characterisation

ELSEVIER LICENSE
TERMS AND CONDITIONS

Jul 09, 2019

This Agreement between Mr. ILIA REPIN ("You") and Elsevier ("Elsevier") consists of your license details and the terms and conditions provided by Elsevier and Copyright Clearance Center.

License Number	4625000123981
License date	Jul 09, 2019
Licensed Content Publisher	Elsevier
Licensed Content Publication	Advanced Drug Delivery Reviews
Licensed Content Title	High-throughput crystallization: polymorphs, salts, co-crystals and solvates of pharmaceutical solids
Licensed Content Author	Sherry L. Morissette,Örn Almarsson,Matthew L. Peterson,Julius F. Remenar,Michael J. Read,Anthony V. Lemmo,Steve Ellis,Michael J. Cima,Colin R. Gardner
Licensed Content Date	Feb 23, 2004
Licensed Content Volume	56
Licensed Content Issue	3
Licensed Content Pages	26
Start Page	275
End Page	300
Type of Use	reuse in a thesis/dissertation
Intended publisher of new work	other
Portion	figures/tables/illustrations
Number of figures/tables/illustrations	1
Format	both print and electronic
Are you the author of this Elsevier article?	No
Will you be translating?	No
Original figure numbers	Table 1. Crystallization composition and processing variables
Title of your thesis/dissertation	Polymorph screening and solubility characterisation of lercanidipine HCl
Expected completion date	Aug 2019
Estimated size (number of pages)	100
Requestor Location	Mr. ILIA REPIN Avenida General Valdomiro de Lima, 642 São Paulo, São Paulo 04344-070 Brazil Attn: Mr. ILIA REPIN
Publisher Tax ID	GB 494 6272 12
Total	0.00 USD
Terms and Conditions	

ELSEVIER LICENSE
TERMS AND CONDITIONS

Jul 09, 2019

This Agreement between Mr. ILIA REPIN ("You") and Elsevier ("Elsevier") consists of your license details and the terms and conditions provided by Elsevier and Copyright Clearance Center.

License Number	4625000849139
License date	Jul 09, 2019
Licensed Content Publisher	Elsevier
Licensed Content Publication	Journal of Pharmaceutical and Biomedical Analysis
Licensed Content Title	An overview of recent studies on the analysis of pharmaceutical polymorphs
Licensed Content Author	Norman Chieng,Thomas Rades,Jaakko Aaltonen
Licensed Content Date	Jun 25, 2011
Licensed Content Volume	55
Licensed Content Issue	4
Licensed Content Pages	27
Start Page	618
End Page	644
Type of Use	reuse in a thesis/dissertation
Intended publisher of new work	other
Portion	figures/tables/illustrations
Number of figures/tables/illustrations	1
Format	both print and electronic
Are you the author of this Elsevier article?	No
Will you be translating?	No
Original figure numbers	Table 1 Analytical techniques commonly used for solid-state characterization of drugs
Title of your thesis/dissertation	Polymorph screening and solubility characterisation of lercanidipine HCl
Expected completion date	Aug 2019
Estimated size (number of pages)	100
Requestor Location	Mr. ILIA REPIN Avenida General Valdomiro de Lima, 642 São Paulo, São Paulo 04344-070 Brazil Attn: Mr. ILIA REPIN
Publisher Tax ID	GB 494 6272 12
Total	0.00 USD
Terms and Conditions	

INTRODUCTION

ELSEVIER LICENSE
TERMS AND CONDITIONS

Jul 09, 2019

This Agreement between Mr. ILIA REPIN ("You") and Elsevier ("Elsevier") consists of your license details and the terms and conditions provided by Elsevier and Copyright Clearance Center.

License Number	4625001107082
License date	Jul 09, 2019
Licensed Content Publisher	Elsevier
Licensed Content Publication	Drug Discovery Today
Licensed Content Title	Solid-state analysis of the active pharmaceutical ingredient in drug products
Licensed Content Author	Ann W. Newman,Stephen R. Byrn
Licensed Content Date	Oct 1, 2003
Licensed Content Volume	8
Licensed Content Issue	19
Licensed Content Pages	8
Start Page	898
End Page	905
Type of Use	reuse in a thesis/dissertation
Intended publisher of new work	other
Portion	full article
Circulation	5
Format	both print and electronic
Are you the author of this Elsevier article?	No
Will you be translating?	No
Title of your thesis/dissertation	Polymorph screening and solubility characterisation of lercanidipine HCl
Expected completion date	Aug 2019
Estimated size (number of pages)	100
Requestor Location	Mr. ILIA REPIN Avenida General Valdomiro de Lima, 642 São Paulo, São Paulo 04344-070 Brazil Attn: Mr. ILIA REPIN
Publisher Tax ID	GB 494 6272 12
Total	0.00 USD
Terms and Conditions	

INTRODUCTION

1. The publisher for this copyrighted material is Elsevier. By clicking "accept" in connection with completing this licensing transaction, you agree that the following terms and conditions apply to this transaction (along with the Billing and Payment terms and conditions